

MONOS: Multiplicity Of Northern O-type Spectroscopic systems.

I. Project description and spectral classifications and visual multiplicity of previously known objects.

J. Maíz Apellániz¹, E. Trigueros Páez^{1,2}, I. Negueruela², R. H. Barbá³, S. Simón-Díaz^{4,5}, J. Lorenzo², A. Sota⁶, R. C. Gamen⁷, C. Fariña^{4,8}, J. Salas⁹, J. A. Caballero¹, N. I. Morrell¹⁰, A. Pellerin¹¹, E. J. Alfaro⁶, A. Herrero^{4,5}, J. I. Arias³, and A. Marco¹²

- ¹ Centro de Astrobiología, CSIC-INTA. Campus ESAC. Camino bajo del castillo s/n. E-28 692 Vill. de la Cañada, Madrid, Spain
e-mail: jmaiz@cab.inta-csic.es
- ² Departamento de Física Aplicada. Universidad de Alicante. Ctra. S. Vicente del Raspeig. E-03 690 S. Vicente del Raspeig, Spain
- ³ Departamento de Física y Astronomía. Universidad de La Serena. Av. cisternas 1200 norte. La Serena, Chile.
- ⁴ Instituto de Astrofísica de Canarias. E-38 200 La Laguna, Tenerife, Spain
- ⁵ Departamento de Astrofísica. Universidad de La Laguna. E-38 205 La Laguna, Tenerife, Spain
- ⁶ Instituto de Astrofísica de Andalucía-CSIC. Glorieta de la astronomía s/n. E-18 008 Granada, Spain
- ⁷ Instituto de Astrofísica de La Plata (CONICET, UNLP). Paseo del bosque s/n. 1900 La Plata, Argentina
- ⁸ Isaac Newton Group of Telescopes. Apartado de correos 321. E-38 700 Santa Cruz de La Palma, La Palma, Spain
- ⁹ Agrupación Astronómica de Huesca. Parque Tecnológico Walqa, parcela 13. E-22 197 Huesca, Spain
- ¹⁰ Las Campanas Observatory. Carnegie Observatories. Casilla 601. La Serena, Chile
- ¹¹ Department of Physics and Astronomy. State University of New York at Geneseo. 1 College Circle. Geneseo, NY 14 454, U.S.A.
- ¹² Departamento de Física, Ingeniería de Sistemas y Teoría de la Señal. Universidad de Alicante. Ctra. S. Vicente del Raspeig. E-03 690 S. Vicente del Raspeig, Spain

Received 25 Feb 2019 / Accepted 25 April 2019

ABSTRACT

Context. Multiplicity in massive stars is a key element to understand the chemical and dynamical evolution of galaxies. Among massive stars, those of O type play a crucial role due to their high masses and short lifetimes.

Aims. MONOS (Multiplicity Of Northern O-type Spectroscopic systems) is a project designed to collect information and study O-type spectroscopic binaries with $\delta > -20^\circ$. In this first paper we describe the sample and provide spectral classifications and additional information for objects with previous spectroscopic and/or eclipsing binary orbits. In future papers we will test the validity of previous solutions and calculate new spectroscopic orbits.

Methods. The spectra in this paper have two sources: the Galactic O-Star Spectroscopic Survey (GOSSS), a project that is obtaining blue-violet $R \sim 2500$ spectroscopy of thousands of massive stars, and LiLiMaRlin, a library of libraries of high-resolution spectroscopy of massive stars obtained from four different surveys (CAFÉ-BEANS, OWN, IACOB, and NoMaDS) and additional data from our own observing programs and public archives. We also use lucky images obtained with AstraLux.

Results. We present homogeneous spectral classifications for 92 O-type spectroscopic multiple systems and ten optical companions, many of them original. We discuss the visual multiplicity of each system with the support of AstraLux images and additional sources. For eleven O-type objects and for six B-type objects we present their first GOSSS spectral classifications. For two known eclipsing binaries we detect double absorption lines (SB2) or a single moving line (SB1) for the first time, to which we add a third system already reported by us recently. For two previous SB1 systems we detect their SB2 nature for the first time and give their first separate spectral classifications, something we also do for a third object just recently identified as a SB2. We also detect nine new astrometric companions and provide updated information on several others. We emphasize the results for two stars: for σ Ori AaAbB we provide spectral classifications for the three components with a single observation for the first time thanks to a lucky spectroscopy observation obtained close to the Aa,Ab periastron and for θ^1 Ori CaCb we add it to the class of Galactic Of?p stars, raising the number of its members to six. Our sample of O-type spectroscopic binaries contains more triple- or higher-order systems than double systems.

Key words. stars: kinematics and dynamics — stars: early-type — binaries: general

1. Introduction

Massive stars are key components of galaxies and one of the most important factors that determine their chemical and dynamical evolution. However our knowledge of them is still quite incomplete. Among massive stars multiplicity (both visual and spectroscopic) is very high (Duchêne & Kraus 2013; Sota et al. 2014). This effect may be related to their formation mechanisms (Zinnecker & Yorke 2007) and is not fully studied since there are

many hidden or poorly studied systems (Mason et al. 1998, from now on M98, Mason et al. 2009). As a large fraction of them are part of short-period systems (Sana & Evans 2011), an accurate knowledge of their binary properties is crucial to understand the role of massive stars as a population (Langer et al. 2008). This strong preference for close systems with short periods implies that almost a third of the systems will interact while both components are still on the main sequence and nearly 70% of

all massive stars will exchange mass with the companion (Sana et al. 2012).

We have started an ambitious project that aims to bring homogeneity to the extensive but diverse literature data on Galactic O-type spectroscopic binaries. The logical division into two hemispheres produced by the samples available from different observatories prompted us to do two subprojects, one for the south and one for the north. In the southern hemisphere the OWN subproject (Barbá et al. 2010, 2017) is obtaining spectroscopic orbits for a large number of Galactic O-type (plus WN) systems to do a systematic analysis of their multiplicity for periods in the range from ~ 1 day to a few years. The northern equivalent, MONOS (Multiplicity Of Northern O-type Spectroscopic systems) is presented in this paper, with the division between the two established at $\delta = -20^\circ$ (e.g. we include the Orion and the M16 stars in the northern sample) to leave similar numbers of Galactic O stars in each subproject. The main data basis for MONOS is LiLiMaRlin (Maíz Apellániz et al. 2019), a **Library of Libraries of Massive-Star High-Resolution Spectra** built by collecting data from four different surveys (CAFÉ-BEANS, Negueruela et al. 2015; IACOB, Simón-Díaz et al. 2015b; NoMaDS, Maíz Apellániz et al. 2012; and OWN itself) plus additional spectra from other programs led by us and from public archives. Currently LiLiMaRlin has 18 077 epochs for 1665 stars, of which 549 are O stars.

In this first MONOS paper we select as our sample spectroscopic and/or eclipsing O+OBcc binaries (by OBcc we mean a star of spectral type O or B or a compact object) with previously published orbits and $\delta > -20^\circ$. We specifically exclude systems that have been tentatively identified as spectroscopic binaries but that have no published orbits, see below for the case of some OWN targets. We present spectral classifications following the Galactic O-Star Spectroscopic Survey (GOSSS, Maíz Apellániz et al. 2011) methodology and spectrograms for the systems that had not appeared or had different spectral classifications in previous GOSSS papers. For each system we discuss its visual multiplicity, in some cases with the help of AstraLux lucky images. We have also compiled literature spectral classifications for those SB2/SB3 (double-lined/triple-lined spectroscopic systems) targets that had been previously separated into kinematic components, and for some targets we give new spectral classifications based on LiLiMaRlin spectra. In paper II we will start presenting our compilation of literature orbits and compare our LiLiMaRlin radial velocity measurements with their predictions. In subsequent MONOS papers we will publish new spectroscopic orbits.

Our plans for OWN include three papers in the near future. Two of them will be similar to MONOS-I (spectral classification and multiplicity) and MONOS-II (a compilation of published orbital solutions) but for targets with $\delta < -20^\circ$. The third paper will present a large number of new orbits, many of them for systems that currently have none, and will be referred to here as the OWN orbit paper. A few of the MONOS-I targets in the equatorial region have orbits from that future OWN paper.

2. Methods

2.1. Building the sample

To collect the sample, we started with the Galactic O-Star Catalog (GOSC, Maíz Apellániz et al. 2004, 2012, 2017a; Sota et al. 2008, <http://gosc.cab.inta-csic.es>), which is a repository of data for massive stars compiled from different projects, most notably GOSSS. GOSC has a public version that

includes the previously published GOSSS spectral types and a private version that adds those targets that we have already classified as being of O type using GOSSS data but that we have not published yet. We have used the current private version of GOSC to select O-type systems with $\delta > -20^\circ$ and we have found 520 of them. For those targets we have thoroughly searched the literature for spectroscopic or eclipsing orbits where the companion is an O star, a B star, or an unseen object (that is, we exclude cases where the companion may be a non-OB supergiant or a Wolf-Rayet star such as WR 113, WR 127, WR 133, WR 139, WR 140, WR 151, or WR 153ab) and found 92 systems. Of those, five have only eclipsing orbits published but the references have no information on the radial velocity amplitudes (so there are no published spectroscopic orbits). One of the sources we have used is SB9, the ninth catalog of spectroscopic binary orbits (Pourbaix et al. 2004), but we note that there is a significant number of orbits missing there. We do not include in our sample systems where only an indication of variability in radial velocity (as opposed to a full published orbit) is available, as other mechanisms such as pulsations can masquerade as spectroscopic binaries, especially when only a few epochs are available and no clear period is observed (Simón-Díaz et al. 2017). Indeed, some of the objects presented here have published orbits but we have strong suspicions that they are not really spectroscopic binaries but are instead misidentifications in the literature. We have left those cases in the sample for completeness but in MONOS-II we will present a table with the published orbits, compare their predictions with our data, and discuss which targets should be removed from the list.

2.2. GOSSS data

GOSSS is obtaining $R \sim 2500$ blue-violet spectroscopy with a high signal-to-noise ratio (S/N) of all optically accessible Galactic O stars. To this date, three survey papers (Sota et al. 2011, 2014; Maíz Apellániz et al. 2016, from now on, GOSSS I+II+III) have been published and along with other recent papers (Maíz Apellániz et al. 2018a,b) GOSSS has produced spectral types for a total of 594 O-type, 24 non-O early-type, and 11 late-type systems. The GOSSS spectra are being gathered with six facilities: the 1.5 m Telescope at the Observatorio de Sierra Nevada (OSN), the 2.5 m du Pont Telescope at Las Campanas Observatory (LCO), the 3.5 m Telescope at the Observatorio de Calar Alto (CAHA), and the 2.0 m Liverpool Telescope (LT), the 4.2 m William Herschel Telescope (WHT), and the 10.4 m Gran Telescopio Canarias (GTC) at the Observatorio del Roque de los Muchachos (ORM). Additionally, several hundreds of O stars and several thousands of B- and later-type stars have been observed, and their data will be published in the near future. The reduction of the GOSSS data is explained in the three survey papers above. The spectral classification is performed with MGB and the GOSSS spectral classification grid OB2500 v3.0 (Maíz Apellániz et al. 2012, 2015a). MGB is used in this paper for the spectral classification of SB2 systems because the software allows for the generation of synthetic linear combinations of standards with different spectral classifications, radial velocity separations, magnitude differences, and rotation indices. The GOSSS spectra and spectral types can be accessed through the GOSC web site.

The GOSSS spectrograms and spectral types for the 92 systems (as well as for ten optical companions) described in the previous subsection are the main scientific content of this paper. The new spectrograms are shown in Fig. 1 and in Table 3 we give the names, GOSC IDs, coordinates, and spectral types for

the objects in our sample sorted by GOSC ID (or, equivalently, by Galactic longitude). In the rest of this subsection we describe some general information about the GOSSS data in that table and in the next section we analyze it star by star.

We have been recently successful (Maíz Apellániz et al. 2018a) in applying a new technique, lucky spectroscopy, to spatially separate close visual components in GOSSS data, which is used for five of the systems in this paper (MY Cam A+B, LY Aur A+B, δ Ori Aa+Ab, ζ Ori AaAb+B, and σ Ori AaAb+B). The first two of those systems did not appear in Maíz Apellániz et al. (2018a) and for the last one we have repeated the observations and obtained new data. LY Aur A and MY Cam A are fainter targets than the other three and that led us to observe them with a different setup. Instead of using EEV12, the standard CCD for the ISIS spectrograph at the WHT, we selected the alternative CCD, QUCAM3. QUCAM3 has the advantage of having a much faster readout time than EEV12, allowing us to obtain a spectrum per second with little dead time between exposures, as opposed to EEV12, for which the one-exposure cycle lasts for ~ 15 seconds. On the other hand, QUCAM3 spans a significantly lower wavelength range than EEV12 at the same spectral resolution, so we had to do three different central wavelengths per star to cover the whole GOSSS spectral range. Also, QUCAM3 does not allow to do 0.1 s exposures, as EEV12 does. Therefore, we used QUCAM3 for faint stars and EEV12 for bright ones.

Regarding the components included in the name of the star, we follow the general strategy for GOSSS, namely, we always try to spatially deconvolve visual components and give the spectral classification for the brightest visual star (or combination of if no deconvolving of all of them is possible). In those cases where the number of components in the GOSSS spectrum is different from the number in the high-resolution aperture, we indicate it (see section on spectroscopic nomenclature below). If more than one visual component is left in the final spectrum we only name those that can significantly alter the spectral classification, for which we establish a dividing criterion at a ΔB of 2 magnitudes. For example, the A and B components in HD 193443 are separated by $0''.1$ and have a ΔB of 0.3 (too close even for lucky spectroscopy), so we cannot resolve them and both have a significant effect on the (combined) spectral type and we leave “AB” in the name. On the other hand, ι Ori also has two visual components (Aa and Ab) separated by $0''.1$ but in that case ΔB is larger than 3 magnitudes, so the secondary does not contribute significantly to the spectral classification and its name is left out (note that for ι Ori there are two additional dim B and C components located further away). Whenever possible we follow the Washington Double Star Catalog (WDS, Mason et al. 2001) component nomenclature and we use our AstraLux lucky images, both previously published (Maíz Apellániz 2010) and newly presented here, to add information about visual companions.

The GOSSS spectral classifications in Table 3 can be divided in four categories:

- Spectral classifications of spectroscopic binaries previously published and not modified here. There are 58 of them and in each case the reference is given. Note that in those cases we do not show the spectrograms in Fig. 1, as they are available in the previous references.
- Objects that had previously appeared in GOSSS papers but for which we provide a new classification. That can be because we have obtained a new epoch in which we have caught the two spectroscopic components with a large

enough radial velocity separation to provide separate classifications or because we have been able to reclassify an old epoch with new standards. They are marked as “mod” (for modified) and there are 17 of them.

- Spectroscopic binaries that had no previous GOSSS spectral classification. They are marked as “new” and there are 17 of them.
- Visual companions to spectroscopic binaries that were observed by placing them on the GOSSS slit at the same time as the primary target. They are marked as “vis” (for visual companion) and there are ten of them.

2.3. Alternate spectral classifications

In addition to the spectral types derived from GOSSS data, Table 3 gives spectral classifications from two other types of sources. First, the literature provides separate spectral types for part of the sample, as some of the papers that publish orbits also publish the spectral types of each component. Most of those types are generated using spectral disentangling techniques (González & Levato 2006), which allow for the decomposition of the individual spectra of a multiple object by using the information in a large number of high-S/N high-spectral-resolution spectrograms. Spectral disentangling allows for the separation of multiple components whose presence is not immediately apparent in single exposures. When done properly, it is a highly efficient technique but one has to be careful with data selection and parameter tuning to avoid the generation of artificial structures in the output.

The second source of spectral types is the LiLiMarlin data (Maíz Apellániz et al. 2019) that will be used for future MONOS papers, which consists of high-resolution spectra obtained with seven different telescopes: HET 9.2 m, NOT 2.56 m, CAHA 2.2 m, MPG-ESO 2.2 m, OHP 1.93 m, Mercator 1.2 m, and Stella 1.2 m. Here we use the high-resolution spectra for some targets for which we do not have GOSSS epochs at large radial velocity separations. In future papers we will use disentangling techniques but for now we simply select the epoch with the best radial velocity separation between components, apply a smoothing algorithm to degrade the resolution to 2500, and use MGB with the GOSSS standards to derive the spectral classifications. The LiLiMarlin spectra processed in that way used to derive new spectral classifications are shown in Fig. 2.

The alternate spectral types are also listed in Table 3, indicating either the reference (for literature values) or “new” (for LiLiMarlin data). Most of the literature and all of the LiLiMarlin spectra were obtained with echelle spectrographs using circular apertures with diameters of $1''$ - $3''$. Therefore, their spatial resolution is significantly worse than that of GOSSS spectra and may include different components. In the next two subsections we explain how we deal with this.

We repeat here a comment about spectral classifications we have done in the past but that is important to keep in mind. Why do we present different spectral classifications and keep updating them? There are three reasons.

- Spectral classification is a process by which the spectrogram of a star is compared to those of a grid of standards. Since we published our first OSTAR grid in GOSSS I we have updated it regularly with data of better quality, filled some gaps in the grid, and defined new subtypes. For example, some stars in the original grid have turned out to be SB2 and we have replaced them with others. Therefore, some of our own spectral

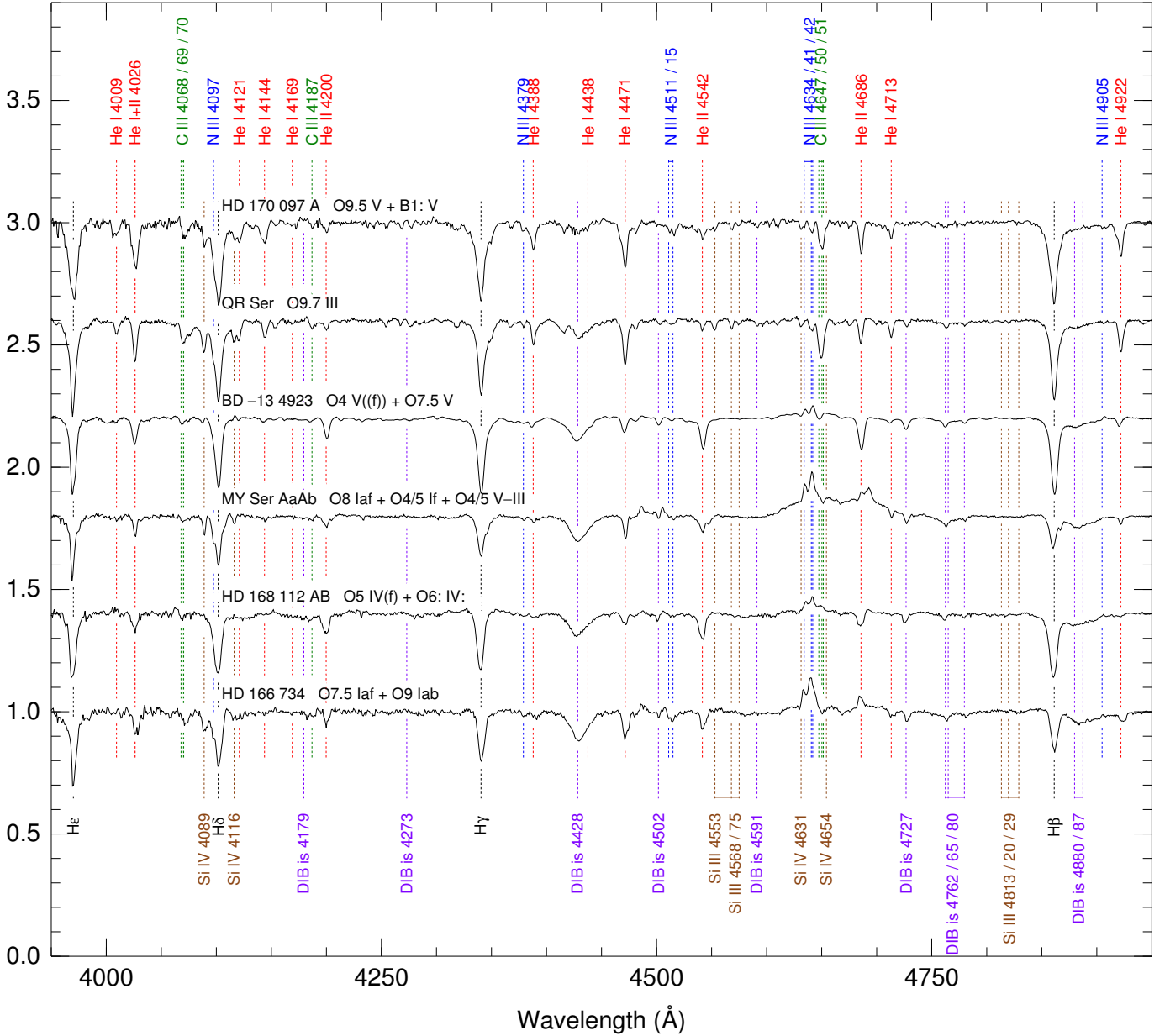


Fig. 1. New GOSSS spectrograms. The targets are sorted by Galactic O-Star (GOS) ID.

types need to be revised over time and literature types need to be analyzed to see how they were obtained.

- We are obtaining new data not only for the standards but also for stars that were previously observed. This can be because the spectra had poor S/N, the spatial resolution could be improved to spatially separate visual components, or the phase at which a SB2 system had been observed was not optimal for the kinematic separation of components.
- Finally, the spectral types of the stars themselves can change over time. The observed cases with secular evolution are rare (but they exist, see Walborn et al. 2017) but more frequent are those that vary periodically or quasi-periodically, such as magnetic stars (Walborn et al. 2010), Oe/Be stars (Porter & Rivinius 2003), and spectroscopic binaries. For that reason, it is important to differentiate between “star X has spectral

type Y” (which implies that it is constant or nearly so) and “star X shows a spectral type Y at moment Z” (which does not). For example, Oe/Be stars can lose their disks (to regain them later) so one can say that an Oe/Be star has a non-Oe/Be spectral type at a given moment.

It is for the reasons above that we present new and alternate spectral classifications in this paper. SB2 systems are especially subject to these issues, mostly due to the need of a large radial velocity difference to easily separate components. For close systems, the apparent spectral types of each star throughout the orbit can change as [a] high rotational velocities induce temperature differences between equator and poles, [b] ellipsoidal deformations vary the effective stellar areas as a function of orbital phase, [c] the regions of each star directly exposed to the radiation of the companion are overheated, and [d] different parts of each

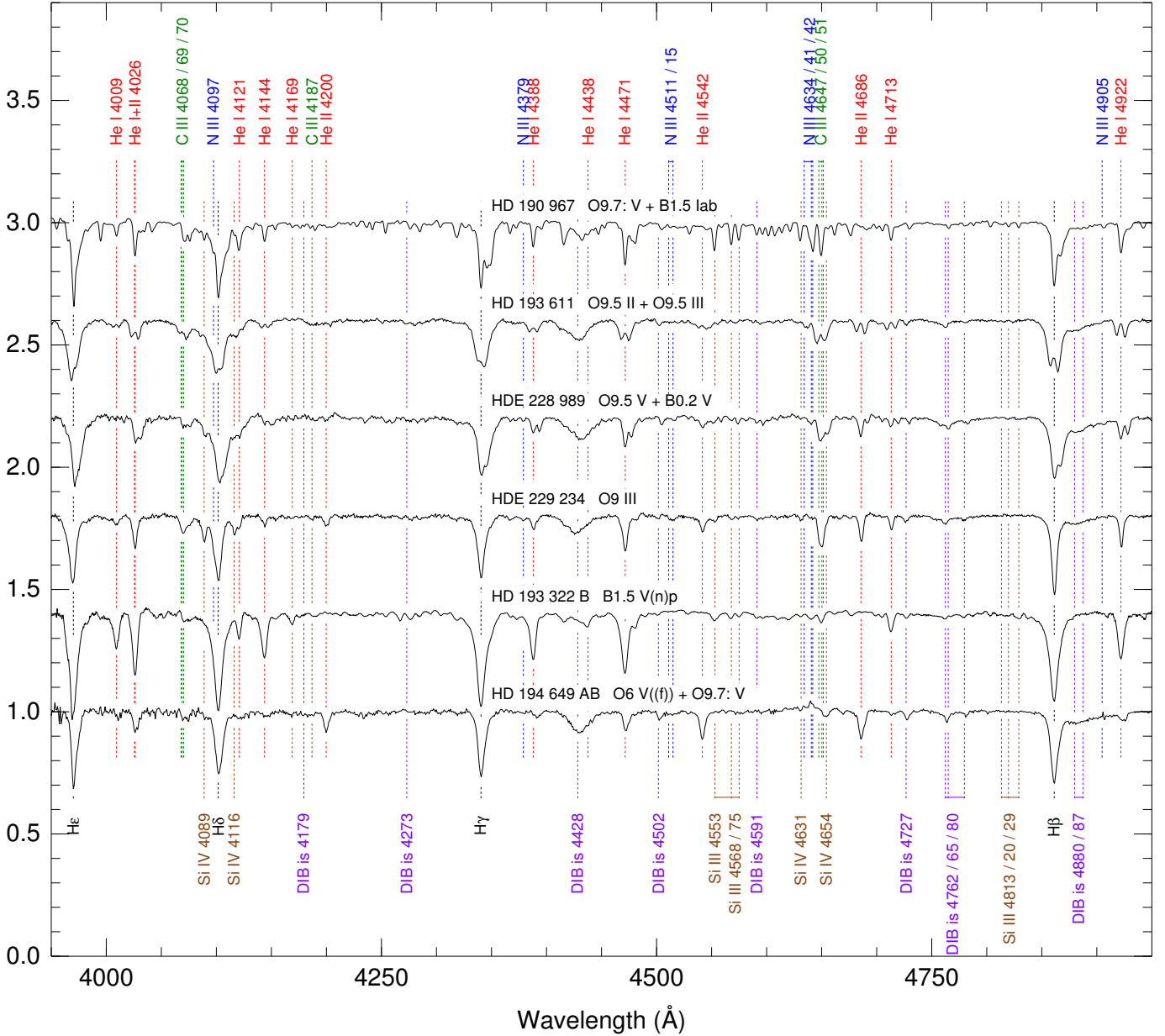


Fig. 1. (continued).

component are visible or blocked by eclipses (in extreme cases this also applies to the emission lines generated in interacting regions close to the stars).

We also warn about the confusion that exists in some papers about real measurements and estimates of spectral types. It is possible to read in the literature expressions like “no signature of the companion is seen in the spectrum and the non-detection of the X line implies that the companion must be of spectral type Y to Z” or “given the Δm between the visual A and B components, we deduce that B has to have a spectral type X”. Those comments can be (more or less) reasonable estimates of the spectral type but they are not real measurements, as they do not follow the criteria for spectral classifications. It is important to label them as such in order not to propagate errors in papers that cite the original works.

2.4. Visual multiplicity and AstraLux images

Even though the main goal of MONOS is to study spectroscopic multiplicity, that is, stellar components detected through radial velocity differences, we find it necessary to also discuss the visual multiplicity of our sample, that is, stellar components detected through imaging or interferometric means. There are several reasons for this:

- The most important one is that to obtain a complete picture of the dynamics of massive star systems and their formation it is necessary to explore the different scales involved, from contact or near-contact systems separated by distances measured in stellar radii to weakly bound systems separated by distances of a fraction of a pc.

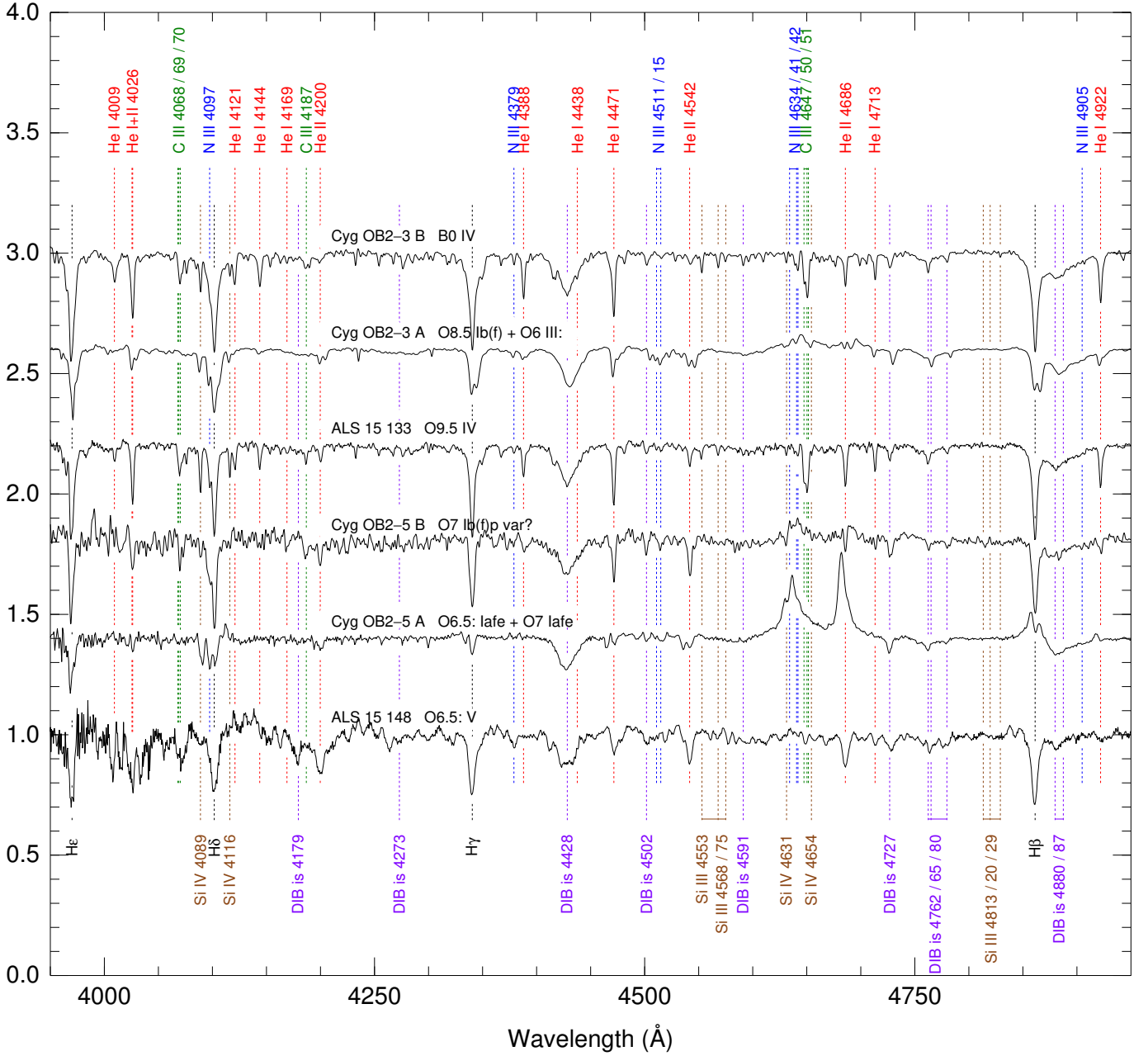


Fig. 1. (continued).

- It has become clear in recent years that many multiple systems are triples or of a higher order (Sota et al. 2014). These are typically composed of an inner (spectroscopic) pair orbited at a larger distance by a visual companion. Therefore, many multiple systems have both visual and spectroscopic components.
- The line between visual and spectroscopic components has become blurred in the last decade, with an increasing number of cases where a pair is detected through both means (Simón-Díaz et al. 2015a; Aldoretta et al. 2015; Le Bouquin et al. 2017; Maíz Apellániz et al. 2017b). This provides an excellent opportunity to derive the stellar parameters of each component with even better precision.
- As a result of the two previous reasons, it is possible to have confusing circumstances where it is not clear whether a newly discovered visual corresponds to a previously known spectroscopic one (or viceversa). Therefore, it is a good idea to have all the information accessible in one place, following the pioneering work of M98 in this respect.

Our main source of information for visual multiplicity is the WDS catalog. In addition, we present new lucky images obtained with AstraLux at the 2.2 m Calar Alto Telescope, a technique that allows the obtention of images close to the diffraction limit in the z and i bands. The reader is referred to Maíz Apellániz (2010), where we present a first set of observations with that setup. Since that paper was published, we have obtained further images of many of the systems there. Here we

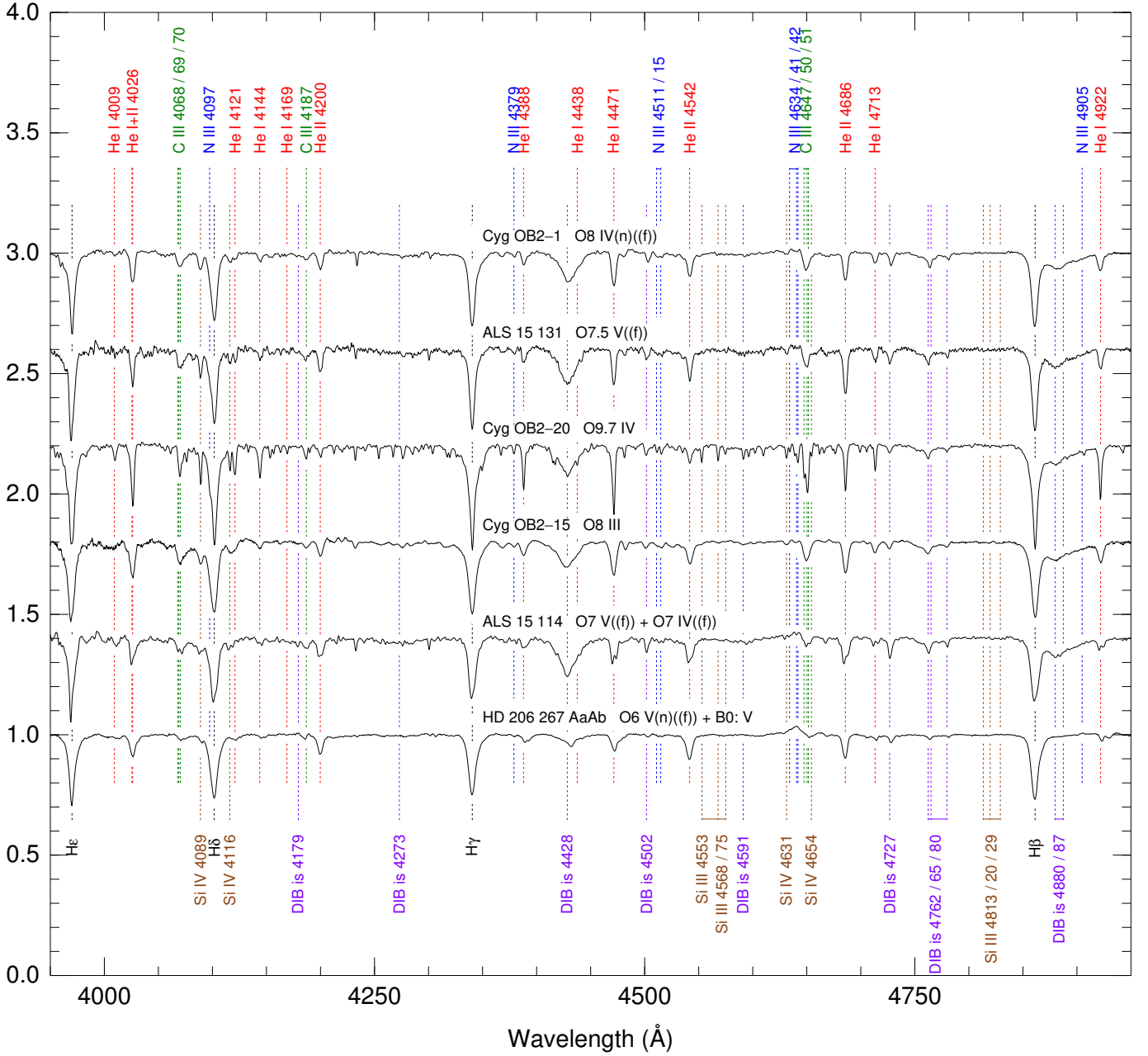


Fig. 1. (continued).

present some images (Figs. 3, 4, and 5) and results (Table 1) which we will expand in future papers. The values for the separations (ρ), position angles (θ), and magnitude differences (Δm) were obtained using a custom-made PSF fitting code written in IDL, an optimized version of the one used in Simón-Díaz et al. (2015a). Some of the results presented here are a reanalysis of the ones in Maíz Apellániz (2010) with the new code and represent a significant improvement due to the use of more accurate PSFs for fitting and of Gaia DR2 positions and proper motions for the calibration of the astrometric fields.

2.5. Spectroscopic/eclipsing multiplicity nomenclature

The previous subsections indicate that studying multiplicity in massive stars is complicated by the different possible orbital configurations and what is detected through imaging/interferometry (visual systems), long-slit spectroscopy (GOSSS), and high-resolution spectroscopy (LiLiMaRlin and others). To clarify the status of each of the spectroscopic systems in this paper, we have devised a spectroscopic binarity status (SBS) nomenclature that expands on the traditional notation and a series of diagrams (Fig. 6) to accompany it. We use this nomenclature to classify each system based on the characteristics of the components that fall within the high-resolution spectroscopic aperture.

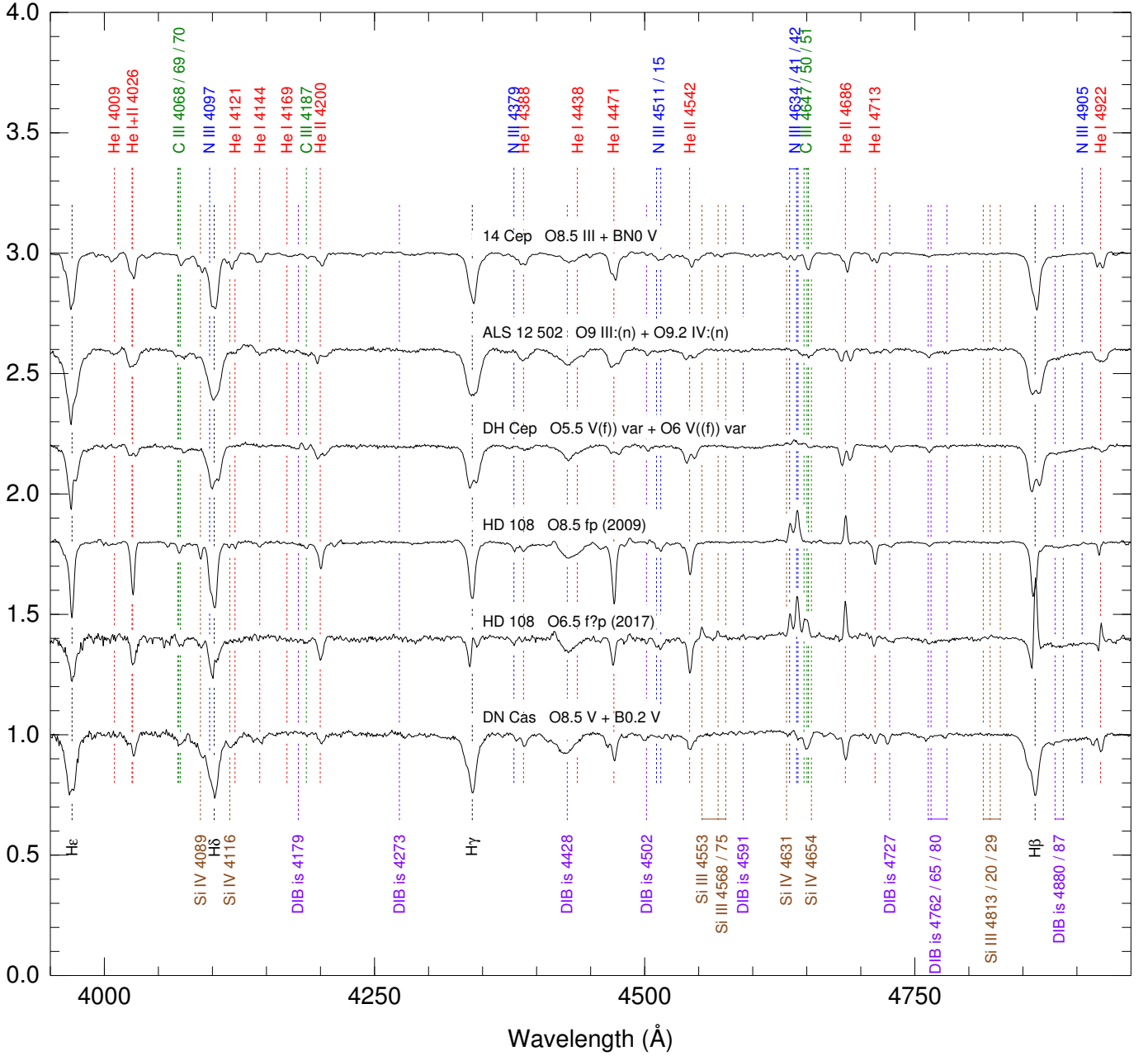


Fig. 1. (continued).

- We start with the traditional notation for systems with two components: **SB1** for single-lined spectroscopic binaries and **SB2** for double-lined ones. An **E** is used for eclipsing binaries or added to SB1/SB2 if the system is also spectroscopic.
- If the two components of the pair are spatially separated with imaging/interferometry, we add an **a** (astrometric or visual) to the SBS as in the SB2a case in Fig. 6.
- If a third component in an orbit around the inner pair falls within the high-resolution spectroscopic aperture, we add it after a plus sign. There are three possibilities: **C** (constant) indicates that the third component is detected in the spectrum but is too distant to induce significant radial velocity

- variations in the inner pair (or viceversa)¹, **S** (spectroscopic) is used when such radial velocity variations are detected but the third component appears to be single itself, and **SB1/SB2** are used if a short-period orbit is detected for the third component itself (implying a fourth component). The nomenclature can get more complicated if three spectroscopic orbits are detected but that does not happen for the sample here, at least at this point.
- If the third component is spatially separated with imaging/interferometry, we add an **a** to the SBS as we did for the inner-orbit components.

¹ We include here the cases where the motion of the outer orbit can be detected but only through astrometry or light-time effects.

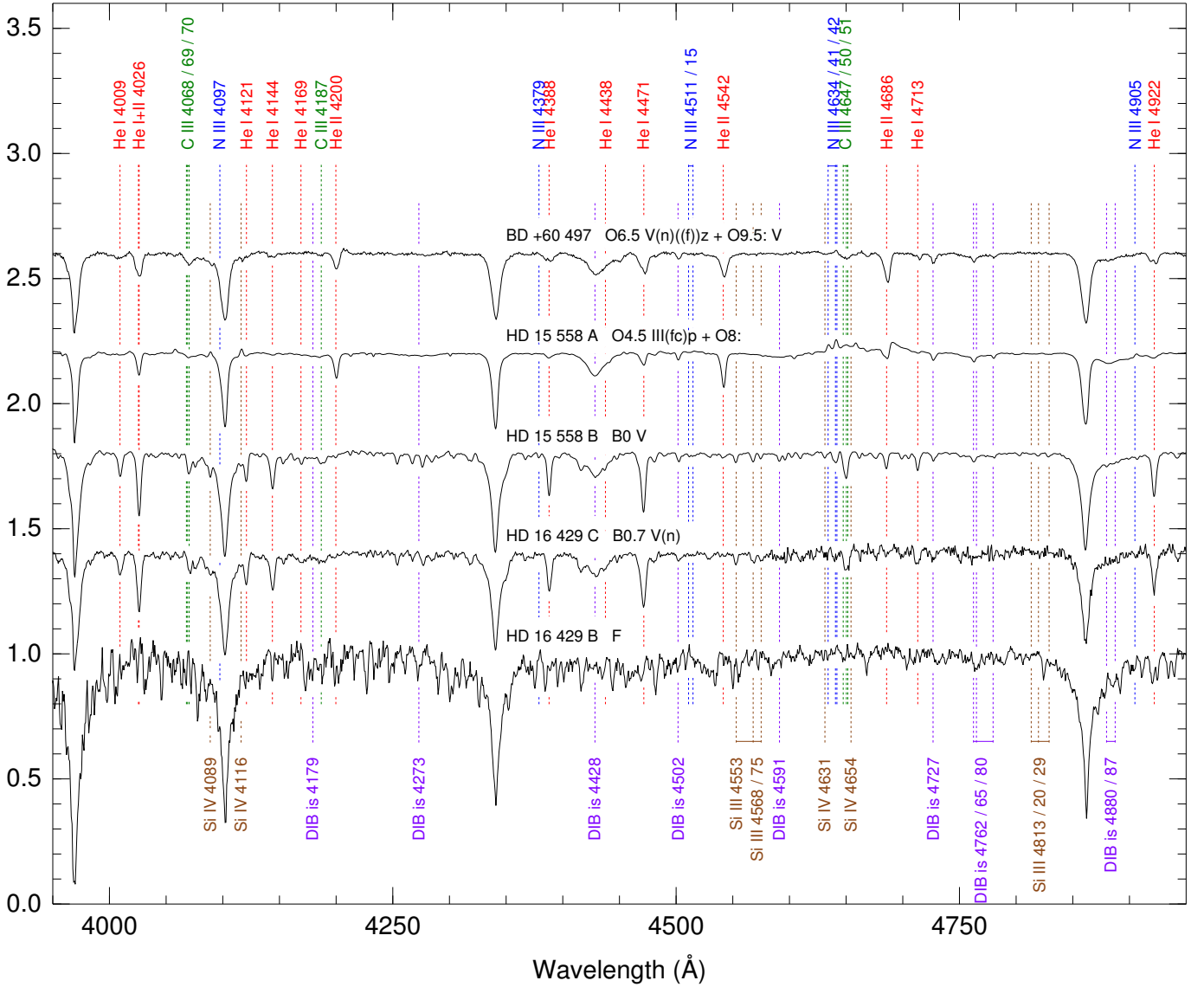


Fig. 1. (continued).

– Finally, if the third component is spatially separated in GOSSS data, we add an s to the SBS.

We identify 17 different SBS configurations in the 92 targets in our sample, as shown in the diagrams and listings in Fig. 6. See the caption there for the meanings of the different symbols and lines used. When discussing each individual system below, we first indicate its current SBS.

3. Individual systems

In this section we discuss the spectral classification, multiplicity, and special characteristics of each system. The stars are sorted by Galactic longitude and grouped in regions of the sky. Each system has one paragraph that starts with the most common names used in the literature and its spectroscopic/eclipsing multiplicity status. If the status changes as a result of this paper, we indicate it in parenthesis.

3.1. Sagittarius-Sagitta

HD 164 438 = BD -19 4800 = ALS 4567. **SB1.** Mayer et al. (2017) identified this system as a SB1, which was classified as O9.2 IV in GOSSS II. HD 164 438 has no WDS entry. M98 detected a possible companion with a $0''.05$ separation indicating that confirmation was needed but Sana et al. (2014) did not detect it. It also appears single in our AstraLux data, hence the SB1 typing.

HD 167 771 = BD -18 4886 = ALS 4874. **SB2.** Morrison & Conti (1978) classified this system as O7 III((f)) + O9 III and was detected as a SB2 in GOSSS I and in GOSSS II we classified it as O7 III((f)) + O8 III. A LiLiMaRlin epoch yields the same spectral classification. The WDS catalog lists two visual components (Aa and Ab) with a small Δm and a separation of $0''.1$. However, we have not included the components in the name because of the uncertain nature of that visual binary: there is only a single detection from 1923 and the modern attempts by Turner

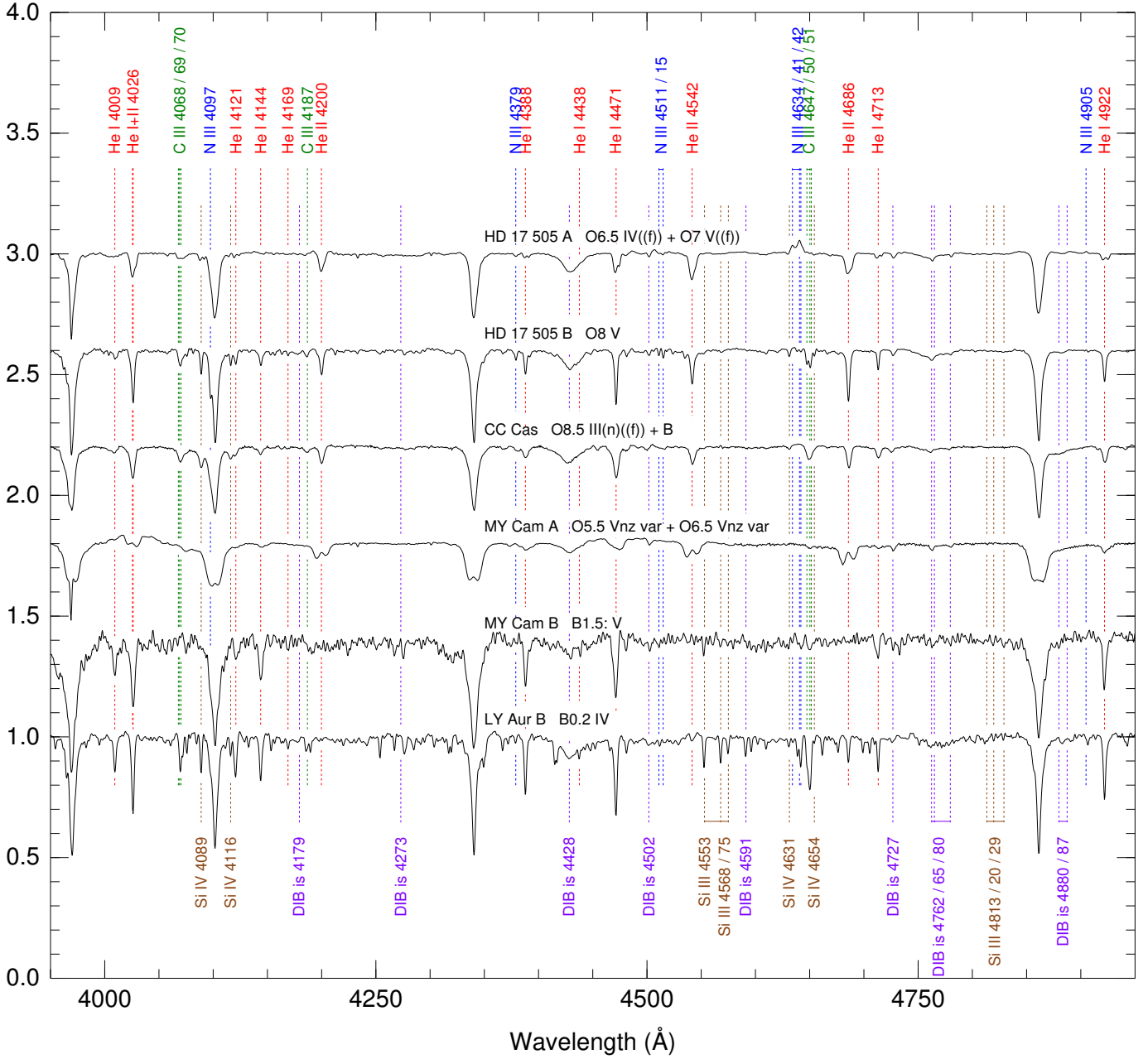


Fig. 1. (continued).

et al. (2008) and Maíz Apellániz (2010) did not detect the alleged Ab companion (but the second paper detected the distant dim B companion).

BD -16 4826 = ALS 4944. **SB2 (previously SB1)**. The most recent multi-epoch study for this target by Williams et al. (2013) gave a SB1 orbital solution for this member of the NGC 6618 cluster. They only had a small number of epochs and covered a short period of time (less than an orbital period), making its orbital parameters only preliminary. The object was analyzed in GOSSS III, where we gave it a spectral type of O5.5 V((f))z and noted that the lines were asymmetric, indicating the possibility of assigning a SB2 character with better data. In some of

the LiLiMaRlin data we see double lines and we use one of the epochs to give the first ever SB2 spectral classification for this object as O5 V((f))z + O9/B0 V. The object has no entry in the WDS catalog.

HD 170 097 A = V2349 Sgr = ALS 5061 = BD -16 4888 A. **SB2E (previously E)**. This object was known to be an eclipsing binary (Dvorak 2004) but had only received previous spectral classifications as a B star. It had not been previously observed by GOSSS and the spectrogram shown on Fig. 1 yields a SB2 spectral classification of O9.5 V + B1: V, with the uncertainty in the secondary classification caused by the small radial velocity difference and large Δm between the two spectro-

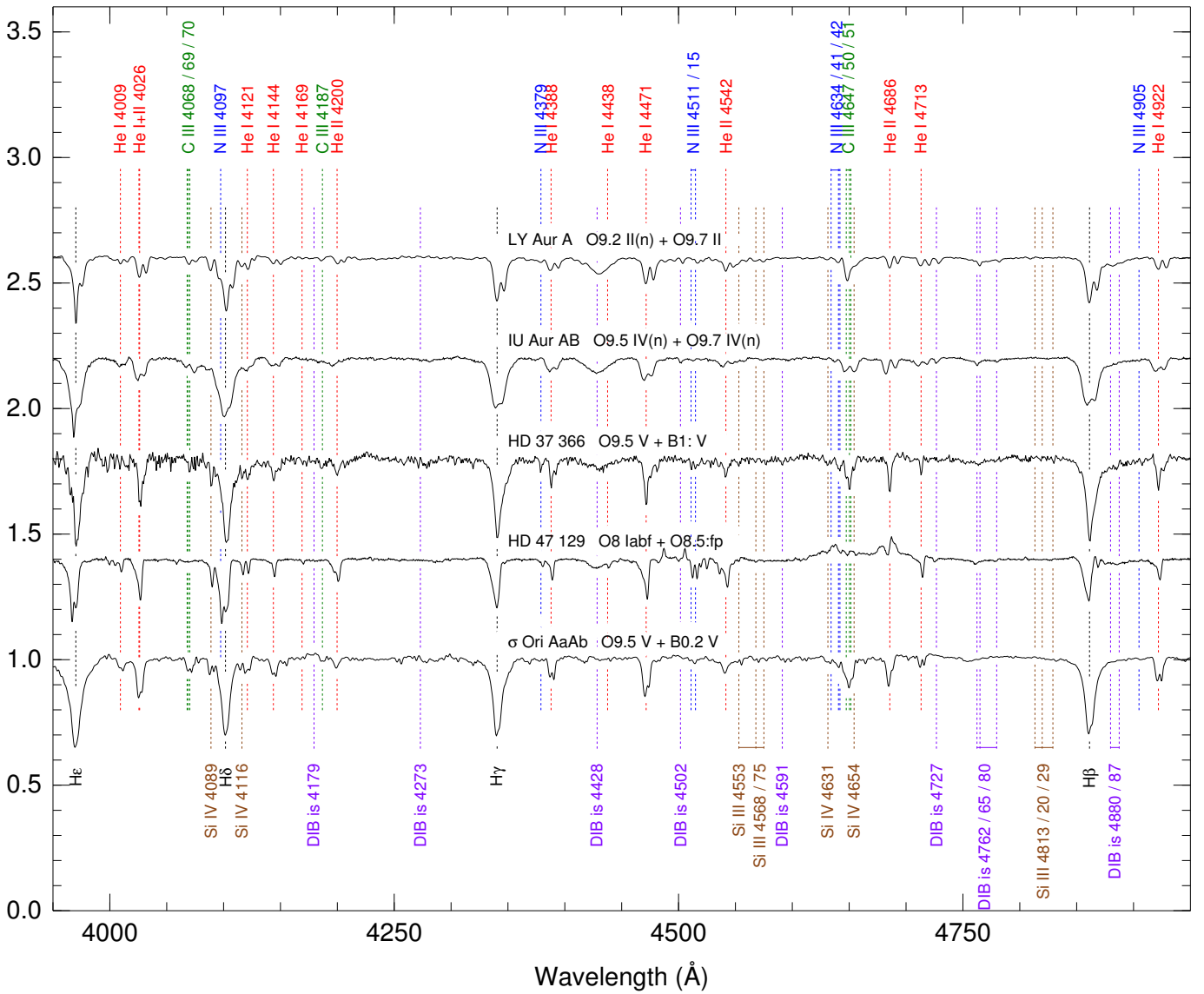


Fig. 1. (continued).

scopic components. HD 170 097 A also appears as SB2 in some LiLiMaRlin epochs and we derive the same spectral types from them. Unpublished OWN data suggests the possible existence of a third spectroscopic component. There is a bright visual companion $17''.2$ away (HD 170 097 B) with its own ALS number (ALS 5060) but the system has no entry in the WDS catalog.

QR Ser = HD 168 183 = BD -14 4991 = ALS 4916. **SB2E**. This object was classified by Sana et al. (2009) as O9.5 III + B, with the secondary having an uncertain spectral subtype (likely mid-B) based on a weak detection of He I $\lambda 5876$. It has not previously appeared in a GOSSS paper. We cannot detect the weak B-type companion in our spectra and we assign it a composite spectral type of O9.7 III. QR Ser has no entry in the WDS catalog.

V479 Sct = ALS 5039. **SB1**. McSwain et al. (2004) determined the SB1 orbit of this γ -ray binary, which is also a runaway star

(Maíz Apellániz et al. 2018b). We classified it as ON6 V((f))z in GOSSS III. V479 Sct has no WDS entry.

HD 168 075 = BD -13 4925 = ALS 4907. **SB2**. This spectroscopic binary has a long period of 43.627 d and has been previously classified as O6.5 V((f)) + B0-1 V (Sana et al. 2009; Barbá et al. 2010). In GOSSS-III we obtained the same spectral type for the primary but we were unable to detect the secondary. The WDS catalog lists several components but caution should be used when assigning names, as the WDS entry 18186-1348 also includes another O-type system (HD 168 076) in M16 at a distance of $26''$ away with its own BD and ALS entries. WDS 18186-1348 A corresponds to HD 168 076 A (with a bright B component unresolved in most observations $0''.1$ away) while WDS 18186-1348 H corresponds to HD 168 075 A. The WDS catalog lists an unresolved companion to HD 168 075 A (Ab or WDS 18186-1348 Hb) but with a Δm larger than 3 mag (Sana et al. 2014), making it too faint to contribute to the com-

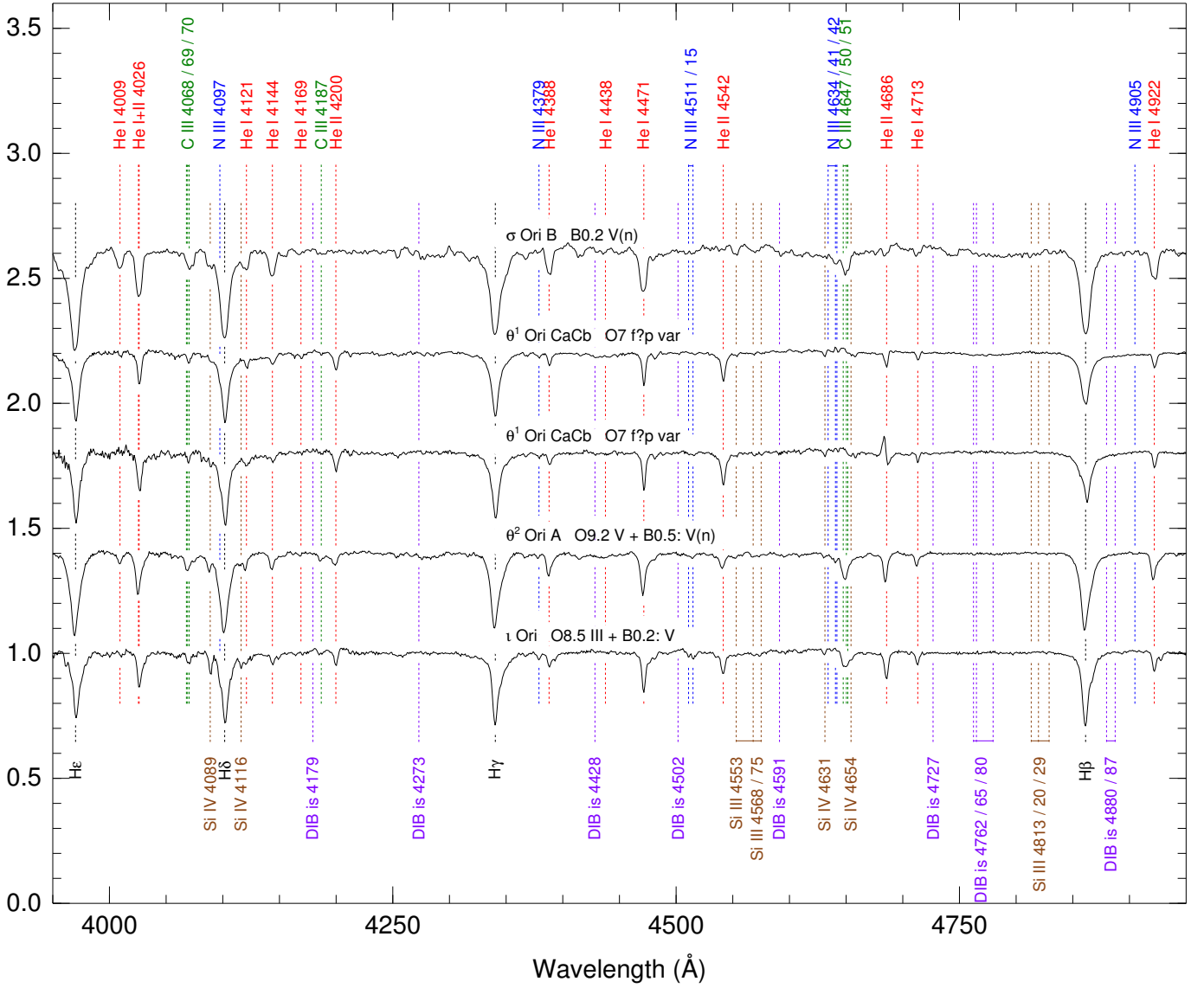


Fig. 1. (continued).

binned spectrum. There are also three additional faint components within $6''$ of HD 168 075 A.

HD 168 137 AaAb = BD -13 4932 AaAb = ALS 4915 AaAb. **SB2a**. Sana et al. (2009) gave a spectral classification of O7 V + O8 V for this SB2 system. In GOSSS-III we could not detect the two components and derived a combined spectral type of O8 Vz. Using LiLiMaRlin data we derive new spectral types of O7.5 Vz + O8.5 V. The WDS catalog lists a bright Ab component at a short distance (hence the designation AaAb for the system) which is likely the same component detected by Le Bouquin et al. (2017) with VLTI. It is likely that this visual Ab component is also the spectroscopic component detected by Sana et al. (2009), given the extreme eccentricity of 0.9 of the preliminary orbit.

BD -13 4923 = ALS 4905. **SB2**. Sana et al. (2009) gave a spectral classification of O4 V(f) + O7.5 V for this object.

BD -13 4923 had not been previously included in GOSSS and here we present a spectrogram that yields the same spectral type as those authors. We have also found a LiLiMaRlin epoch appropriate for spectral classification with MGB and found again the same spectral type. The WDS catalog lists a third component $0.7''$ away with a Δm larger than 3 magnitudes which we also see in AstraLux images.

MY Ser AaAb = HD 167 971 AaAb = BD -12 4980 AaAb = ALS 4894 AaAb. **SB2E+Sa**. Leitherer et al. (1987) derived spectral types of O8 If for the primary star and O5-8 for each of the secondary and tertiary components of this SB3 system. The latter two are an eclipsing binary. This complex system was also studied by Ibanoglu et al. (2013), who found periods of 3.321 616 d and 21.2 a for the inner and outer orbits, respectively, and a large eccentricity of 0.53 for the outer orbit. They also derive spectral types of O9.5-B0 IIII + O7.5 III + O9.5 III. In GOSSS-I we separated two of the kinematic components into O8 Iaf(n) and O4/5. With new GOSSS spectra and a re-

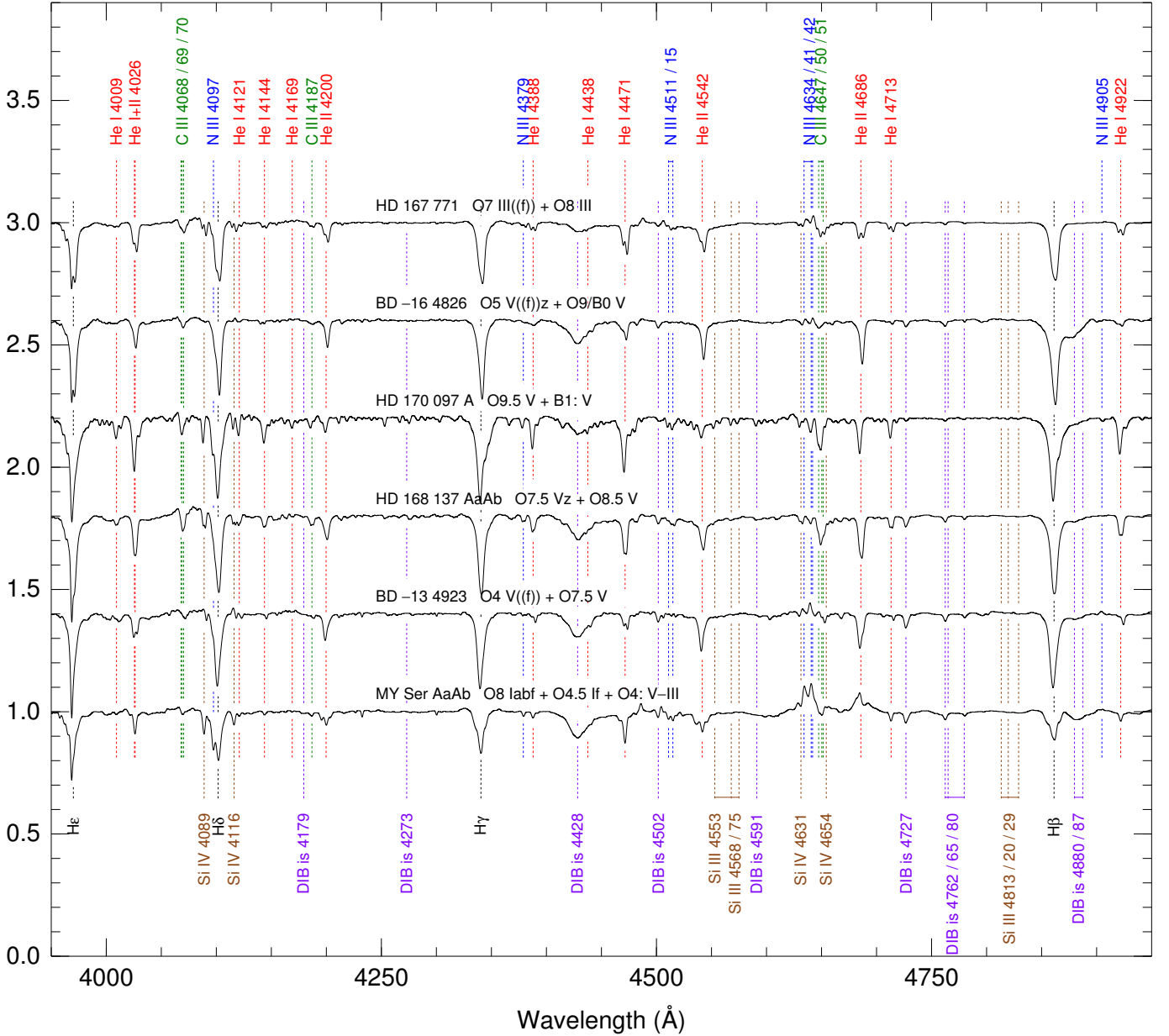


Fig. 2. New LiLiMaRlin spectrograms degraded to $R = 2500$. The targets are sorted by GOS ID. The Cyg OB2-9 spectrogram does not include the 4710-4760 Å region

analysis of the old spectrograms we are now able to resolve the three components as O8 Iaf + O4/5 If + O4/5 V-III. With LiLiMaRlin data we obtain a similar spectral classification of O8 Iabf + O4.5 If + O4: V-III. The spectral type of the primary is relatively well established but those of the secondary and tertiary are more uncertain. The secondary has strong He II $\lambda 4686$ emission, hence the supergiant luminosity class (even though it is not clear if the emission arises on a typical supergiant wind or is the result of the interaction between the two close components). Our classifications are incompatible with the previous one of Ibanoglu et al. (2013), as both the secondary and tertiary have He II $\lambda 4542$ stronger than He I $\lambda 4471$ and, hence, they have to be earlier (not later) than O7. On the other hand, the earlier (and more imprecise) classifications of Leitherer et al. (1987)

are closer to ours. Sana et al. (2014) detect two astrometric components (Aa and Ab) with a small magnitude difference and a separation of 17 mas. These are likely to be the spectroscopic primary on the one hand and the combination of secondary and tertiary spectroscopic components on the other hand, as the Δm derived from the spectral fitting is also close to zero. The latter work of Le Bouquin et al. (2017) elaborate on this idea and present an astrometric outer orbit based on a yet incomplete arc (note that the previous outer orbit by Ibanoglu et al. (2013) was based on eclipse timings). Our LiLiMaRlin spectra span 9 a (from 2006 to 2015) and show small radial velocities differences, hence we type this system as SB2E+Sa instead of SB2E+Ca. The WDS catalog also lists a large number of dim companions, some of them possibly bound but the rest likely members of the

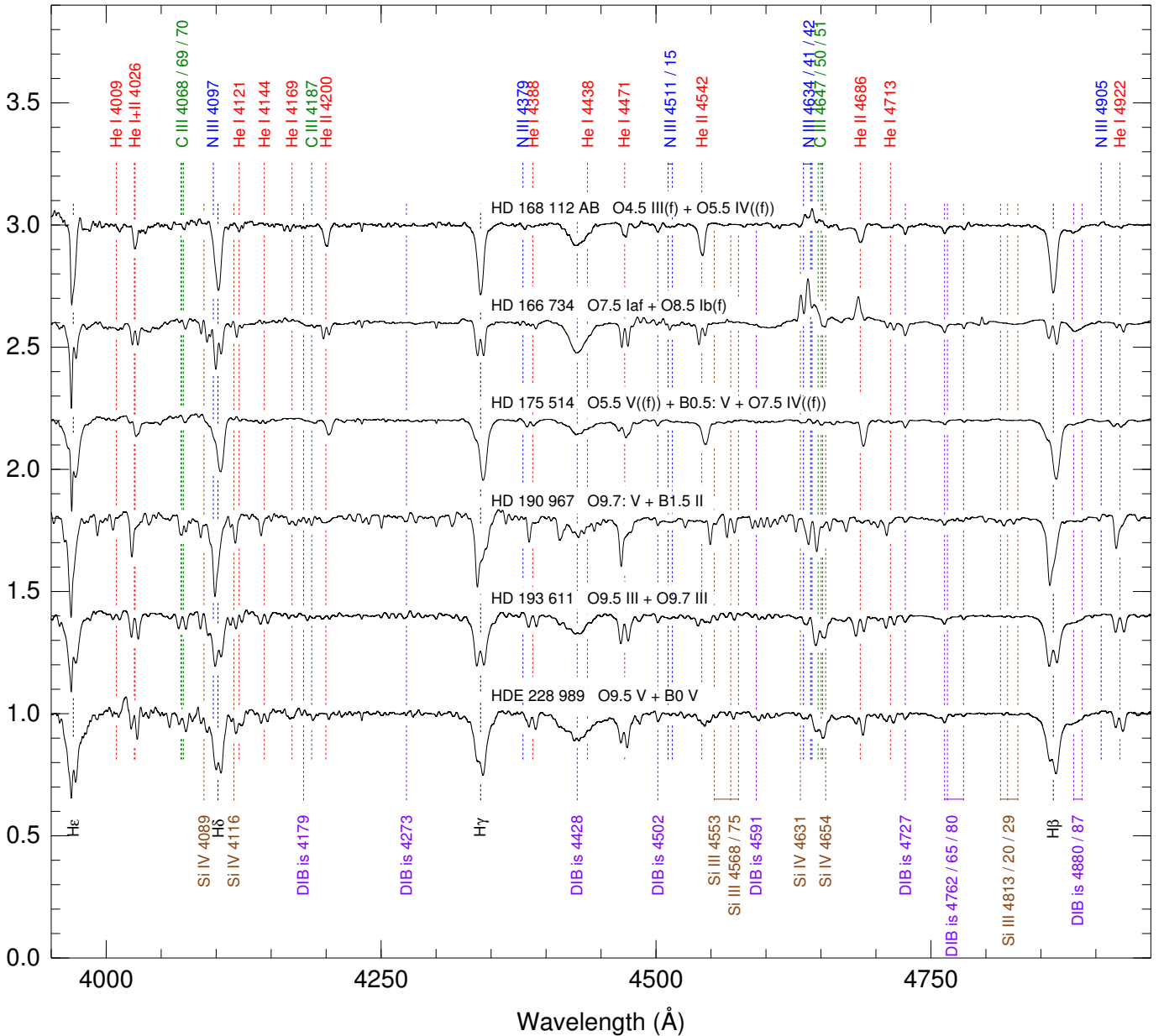


Fig. 2. (continued).

NGC 6604 cluster, of which the MY Ser system is the brightest member.

HD 168 112 AB = BD -12 4988 = ALS 4912 AB. **SB2a.** The first orbital solution for this system is given in the OWN orbit paper. HD 168 112 AB was classified as a single star in GOSSS I and III and had no previous separate spectral classifications but a new GOSSS spectrogram yields the two spectral types O5 IV(f) + O6: IV:. Alternatively, with LiLiMaRlin data we obtain O4.5 III(f) + O5.5 IV((f)). Sana et al. (2014) detected two components (A and B) with a small Δm and a separation of just over 3 mas. Given the long spectroscopic period of the system it is likely that the A and B visual components are also the spectroscopic ones. Sana et al. (2014) also detected two more distant and faint C and D companions (note that the current ver-

sion of the WDS catalog follows a different component convention for this system).

HD 166 734 = V411 Ser = BD -10 4625 = ALS 9405. **SB2E.** Walborn (1973) classified this eccentric system as O7 Ib(f) + O8-9 I. In GOSSS I we derived a combined spectral type of O7.5 Iaf + O8.5 Ib(f). This target has no entry in the WDS catalog and no significant companion is detected in our AstraLux images or by Sana et al. (2014).

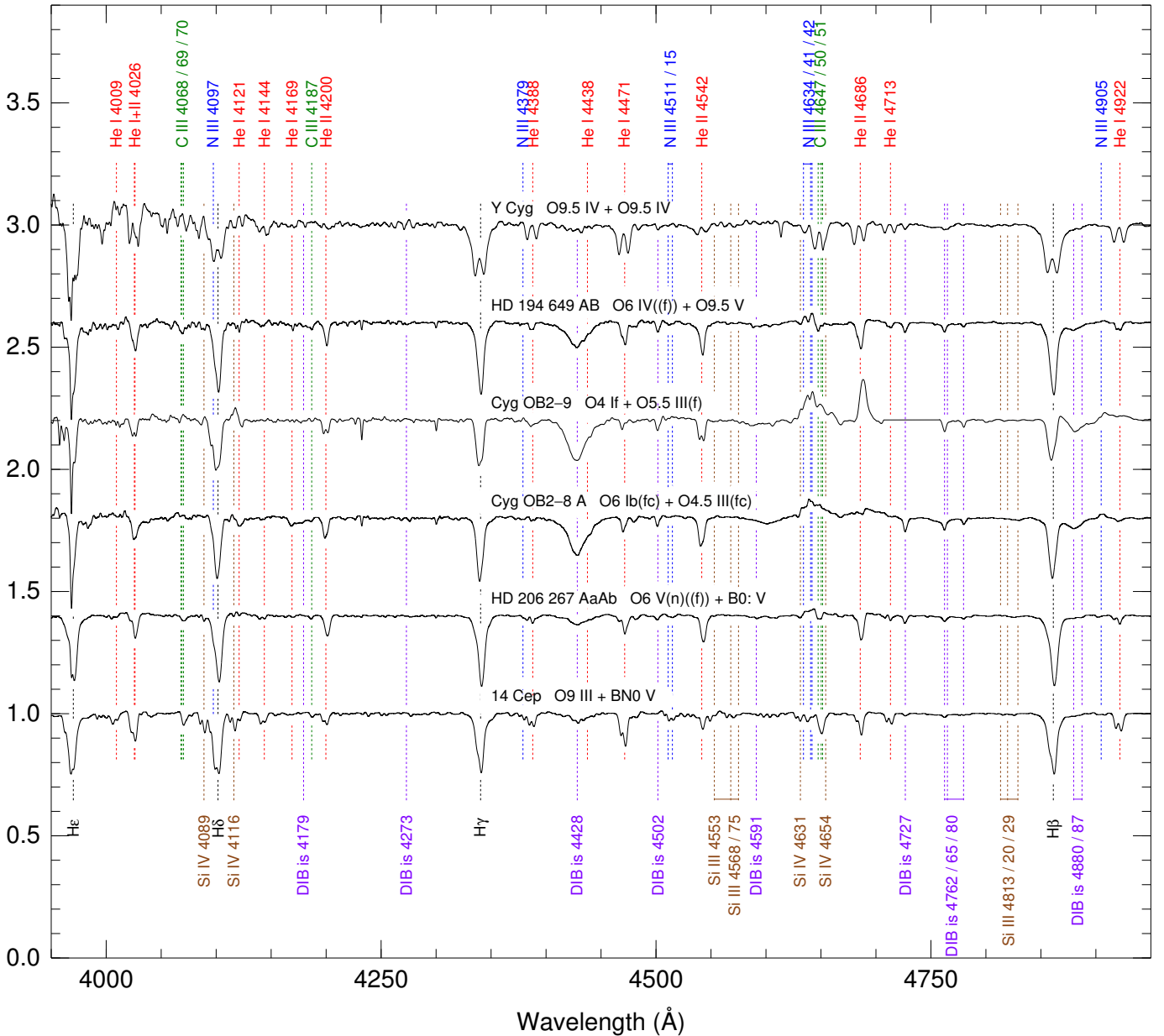


Fig. 2. (continued).

HD 175514 = V1182 Aql = BD +09 3928 = ALS 10048. **SB2E+C**. Mayer et al. (2005) studied this three-object system and gave spectral types of O5.5, O9.5, and O9, noting that the first two stars form an eclipsing system with a period of 1.621 861 d. The outer orbit has a period of at least 50 a. In GOSSS III we obtained a spectral classification of O7 V(n)((f))z + B, likely because we are seeing a blend of the two earliest stars (hence the O7 type, intermediate between O5.5 and O9.5) plus the third later-type star. In one of the LiLiMaRlin epochs we caught the system close to quadrature and derive spectral classifications of O5.5 V((f)) + B0.5: V + O7.5 IV((f)), where the two first types correspond to the eclipsing binary (extreme radial velocities) and the last one to the third object (central radial velocity). This target has no entry in the WDS catalog

and no significant companion is detected in our AstraLux images.

9 Sge = HD 188 001 = QZ Sge = BD +18 4276 = ALS 10596. **SB1?**. Underhill & Matthews (1995) calculated a SB1 orbit for this runaway star (Maíz Apellániz et al. 2018b). The orbit has not been confirmed and it is possible that the radial velocity variations are caused by pulsations. In GOSSS-I we classified it as O7.5 Iabf. 9 Sge has no entry in the WDS catalog and our AstraLux images show no companions.

3.2. Cygnus

Cyg X-1 = V1357 Cyg = HDE 226 868 = BD +34 3815 = ALS 10678. **SB1**. This is arguably the most famous O-type

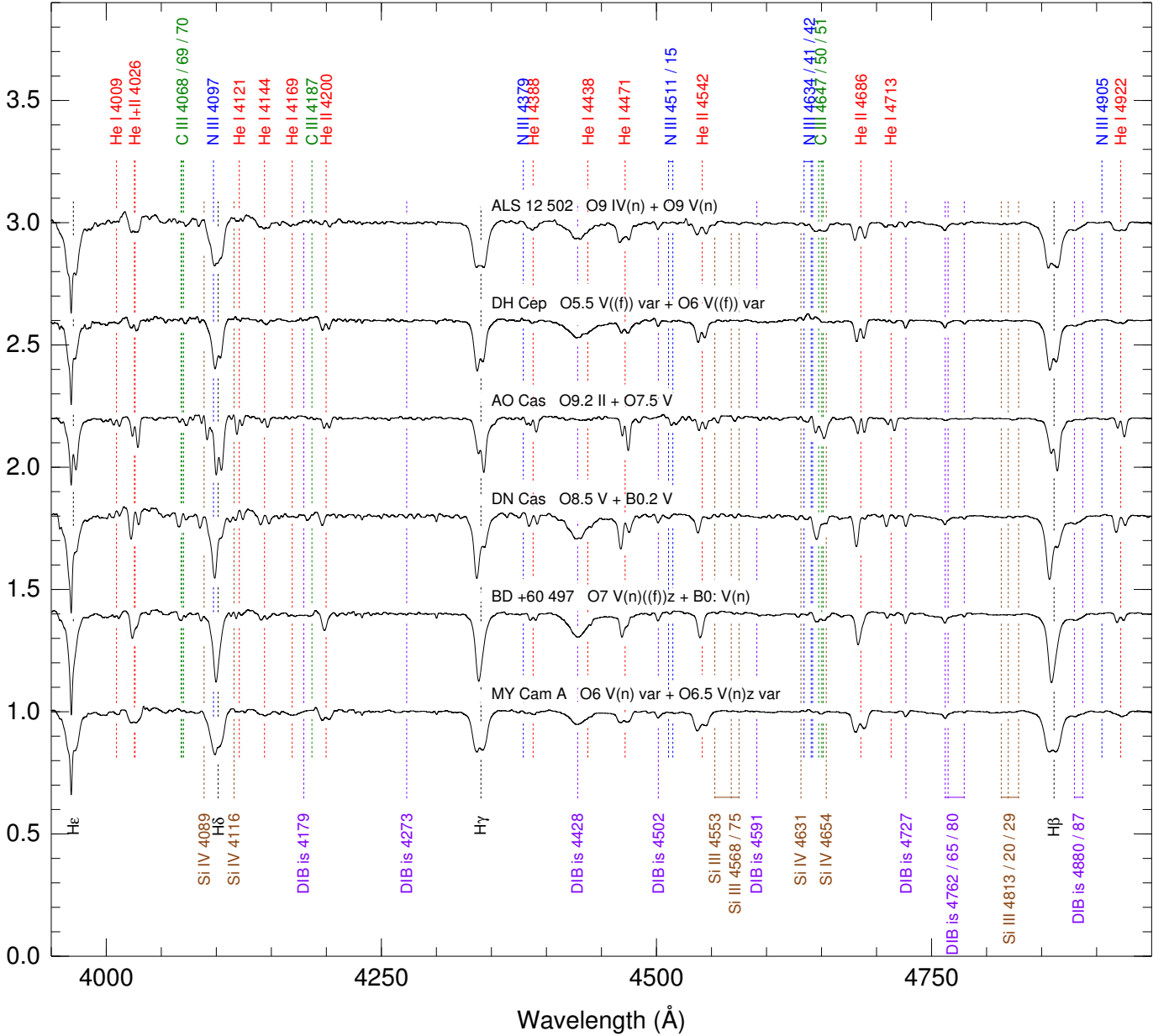


Fig. 2. (continued).

SB1 system, as it consists of an O supergiant orbiting the nearest known black hole. Orosz et al. (2011) is the last paper to give an orbital solution for it and also provides accurate values for the distance, masses, and inclination. GOSSS I gives a spectral classification of O9.7 Iabp var. Cyg X-1-a has no entry in the WDS catalog and our AstraLux images do not show any significant close companion.

HD 190967 = V448 Cyg = BD +34 3871 = ALS 10828. **SB2E.** Harries et al. (1997) give a spectral type of O9.5 V + B1 Ib-II for this binary but the origin of that classification is uncertain, as the work they cite (Morgan et al. 1955 though they incorrectly say that paper was published in 1965) only gives the classification for the B-type component. This system is quite peculiar, as it consists of an evolved B supergiant

mass donor (the brighter star) and an O main-sequence gainer surrounded by a thick accretion disk (Djurašević et al. 2009). This target had not been previously observed with GOSSS and the new spectral classification is O9.7: V + B1.5 Iab. With a LiLiMaRlin epoch we obtain O9.7: V + B1.5 II, that is, a lower luminosity class for the B-type component. The object has no entry in the WDS catalog. Our AstraLux images reveal a previously undetected B companion with a large Δm (Table 1 and Fig. 3). Note that the magnitude difference is significantly smaller in z than in i , indicating that the companion is redder. A comparison with isochrones with ages of 3 and 10 Ma indicates that the color difference is too large for the magnitude difference, so if the system is coeval and bound it is likely that the B visual companion has not reached the ZAMS. Alternatively, the color difference may be distorted by the existence of the thick ac-

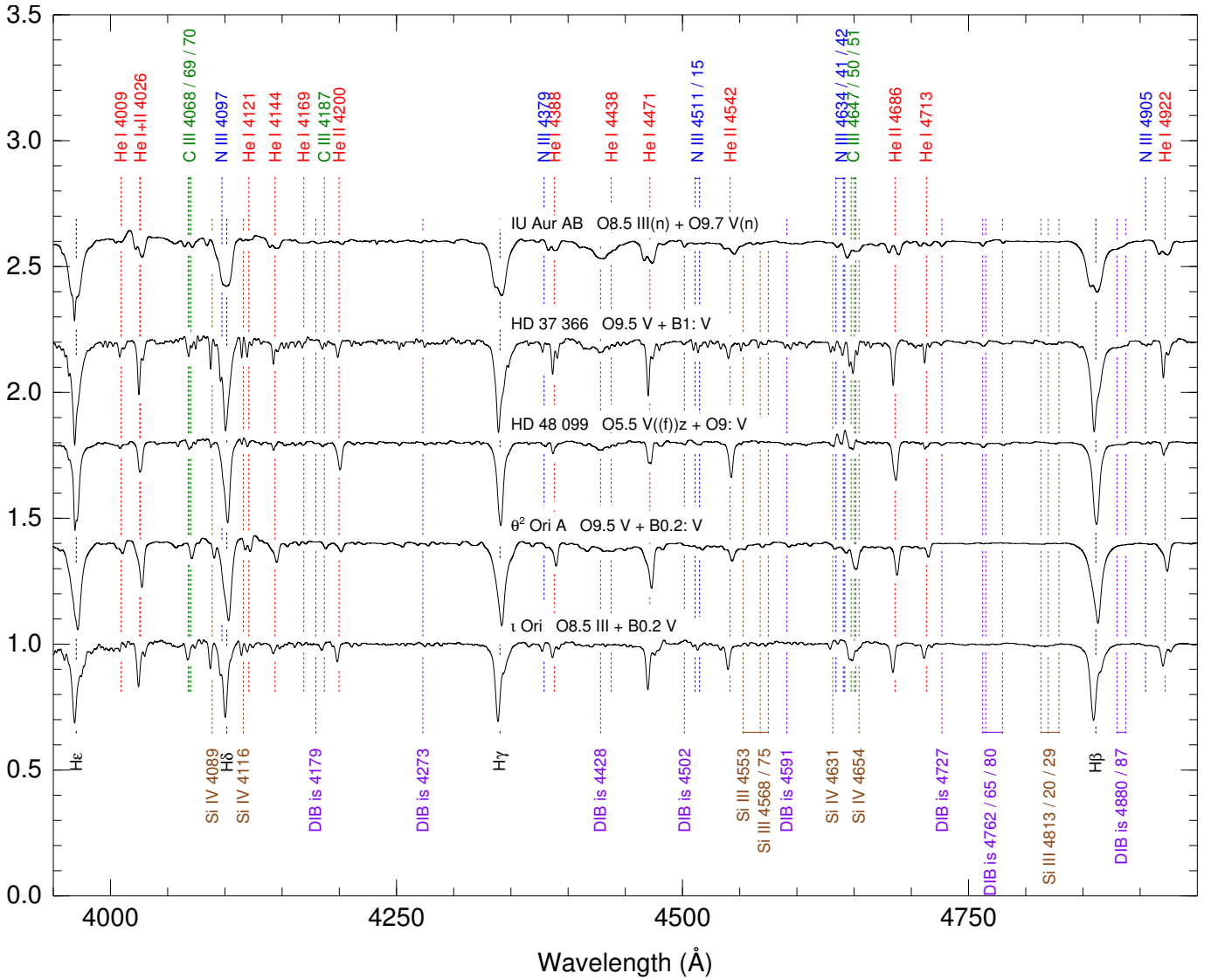


Fig. 2. (continued).

cretion disk around the O-type spectroscopic component in the A visual component. However, that additional extinction around the A component would change its color in the opposite direction and our high-resolution spectroscopy reveals no emission lines in the *i* band, so that alternative explanation does not work.

HD 191 201 A = BD +35 3970 A = ALS 10 843 A. **SB2+Cas.** This object is a hierarchical multiple system formed by an inner spectroscopic object (A) and an external B component at a distance of $1''.0$ and a Δm of 1.8 magnitudes (between the sum of the two stars in A and B, Fig. 3 and Table 1). The system was known to be an O-type SB2 as far back as Plaskett (1926) but it was not until GOSSS I that it was determined that the B component is also an O star with spectral type O9.7 III. The A component has a GOSSS classification of O9.5 III + B0 IV. As the system includes three objects of similar spectral type within a small aperture, special care has to be taken to ensure what light is entering the spectrograph. For example, Conti & Alschuler (1971) classified this system as O9 III + O9 V and is quite possible that their spectral classification for the secondary included the B compo-

nent as well as the lower luminosity star in A. In GOSSS we fit spatial profiles to the long-slit data to obtain separate spectrograms and spectral classifications, something not possible with the echelle data, and that spatial separation is indicated by the “s” in the SB2+Cas typing (Fig. 7). Our LiLiMaRlin data do not show significant radial velocity differences for the external component in a 14 a time span (from 2004 to 2018) and the WDS catalog shows little astrometric change in the relative position of the A-B system over 170 a (with many measurements in between but noisy ones), indicating that the period is measured in millennia. The AstraLux measurements in Table 1 are also consistent with a very long period.

HD 191 612 = BD +35 3995 = ALS 10 885. **SB2.** This is one of the five previously known Of?p stars in the Galaxy (Walborn et al. 2010 but see below for θ^1 Ori CaCb). Its magnetic field is the main source of its variability, tied to the 538 d rotational period (Donati et al. 2006). Superimposed on the strong line variations caused by the changes in the relative orientation of the magnetic field, Howarth et al. (2007) detected the signal of

Pair	Even. date (YYMMDD)	HJD-2.4 · 10 ⁶ (d)	ρ ($''$)	θ (deg)	Δi (mag)	Δz (mag)	Δzn (mag)	ΔY (mag)
HD 190 967 A,B	180920	58 382.3	1.124±0.006	145.14±0.21	5.20±0.01	4.80±0.01
HD 191 201 A,B	110915	55 819.9	0.984±0.001	83.32±0.01	...	1.78±0.03
	121001	56 201.9	0.983±0.001	83.36±0.03	...	1.81±0.01
	130916	56 551.9	0.980±0.001	83.51±0.01	1.78±0.02
HD 193 322 Aa,Ab	080614	54 632.1	0.065±0.001	113.45±2.21	...	0.16±0.01
	110913	55 817.9	0.067±0.001	129.82±3.18	...	0.23±0.03
	121001	56 201.9	0.074±0.003	134.55±1.89	...	0.14±0.01
	130915	56 550.9	0.066±0.002	136.12±2.31	0.32±0.06	0.19±0.02
	180920	58 381.8	0.067±0.001	150.55±1.00	...	0.22±0.03
HD 193 322 Aa,B	080614	54 632.1	2.719±0.003	245.22±0.08	...	1.63±0.01
	110913	55 817.9	2.728±0.003	245.01±0.08	...	1.65±0.01
	121001	56 201.9	2.744±0.003	244.80±0.08	...	1.61±0.01
	130915	56 550.9	2.735±0.003	245.00±0.08	1.72±0.02	1.64±0.02
	180920	58 381.8	2.758±0.003	244.89±0.08	...	1.65±0.02
HD 194 649 A,B	121002	56 202.9	0.399±0.004	212.12±0.04	...	0.91±0.05
	130916	56 552.0	0.399±0.001	212.53±0.13	0.99±0.06
	181128	58 450.8	0.400±0.002	213.11±0.27	0.96±0.01	0.93±0.02
ALS 15 133 A,B	181128	58 450.8	4.367±0.001	214.60±0.02	...	4.53±0.03
Cyg OB2-A11 A,B	181128	58 450.8	2.222±0.001	276.76±0.02	...	4.53±0.02
Cyg OB2-5 A,B	071113	54 418.3	0.931±0.008	54.92±0.12	2.75±0.07	2.96±0.08
	181128	58 451.3	0.932±0.008	55.28±0.03	3.00±0.03	3.06±0.04
Cyg OB2-22 A,Ba	110915	55 819.9	1.530±0.001	146.16±0.02	...	0.63±0.02
	130919	56 554.9	1.526±0.002	146.20±0.02	...	0.62±0.07
	180919	58 381.0	1.525±0.001	146.07±0.05	...	0.66±0.01
	181228	58 450.8	1.524±0.003	145.97±0.06	...	0.66±0.01
Cyg OB2-22 Ba,Bb	110915	55 819.9	0.217±0.003	180.28±1.00	...	2.50±0.14
	130919	56 554.9	0.206±0.019	178.96±1.94	...	2.53±0.38
	180919	58 381.0	0.191±0.024	174.15±5.44	...	2.16±0.13
	181228	58 450.8	0.215±0.009	181.73±3.18	...	2.33±0.08
Cyg OB2-1 A,B	130919	56 554.9	1.174±0.001	341.90±0.05	...	2.66±0.01
Cyg OB2-8 Aa,Ac	110915	55 820.3	3.110±0.050	339.85±0.10	...	5.65±0.10
	180920	58 832.3	3.106±0.050	339.89±0.10	...	5.83±0.10
HD 206 267 Aa,Ab	110913	55 818.4	0.091±0.006	220.64±6.27	...	1.63±0.30
	130916	56 552.6	0.112±0.007	203.58±1.59	1.95±0.30
	181227	58 450.3	0.105±0.007	196.18±9.00	2.02±0.06	...
HD 206 267 Aa,B	110913	55 818.4	1.803±0.010	319.30±0.20	...	5.72±0.13
	130916	56 552.6	1.778±0.010	319.74±0.20	5.73±0.25
	181227	58 450.3	1.787±0.010	319.43±0.20	5.55±0.07	...
ALS 12 502 A,B	130917	56 553.484	1.578±0.002	345.97±0.03	2.98±0.02	2.96±0.01
	181128	58 451.359	1.587±0.004	345.88±0.13	3.16±0.02	3.12±0.03

Table 1. Measurements for visual pairs using our AstraLux lucky images. The evening date, Heliocentric Julian Date (HJD), separation (ρ), position angle (θ), and magnitude difference is given in each case. Four different filters were used: SDSS i and z , zn (a narrow filter with a central wavelength similar to that of z), and Y .

a double-lined spectroscopic binary with small radial velocity amplitudes and a period of 1542 d (later updated to 1548 d by Wade et al. 2011). Those authors give a spectral type of O6.5-8f?p var + B0-2. Our similar GOSSS-I classification is O6-8 f?p var, as the combination of spectral resolution and S/N of the spectrogram there is not sufficient to reveal the weak lines that originate in the secondary component. This object has no entry in the WDS catalog and no apparent companion is seen in our AstraLux images.

HDE 228 854 = V382 Cyg = BD +35 4062 = ALS 11 132. **SB2E.** Pearce (1952) classified this short-period binary as O6.5 + O7.5. The GOSSS I spectral classification is O6 IVn var + O5 Vn var, with variations in the spectral type likely caused by different parts of the star being exposed or eclipsed during different orbital phases. The WDS catalog lists a companion at a distance of 11''.3 (with a single observation from 1896) but our AstraLux images show nothing at that position, so it is likely to be a spurious detection.

HDE 228 766 = BD +36 3991 = ALS 11 089. **SB2.** Walborn (1973) classified this system as O4 If + O8-9 In and in GOSSS I we refined the classification of the secondary to obtain O4 If + O8: II:. Rauw et al. (2014) claimed that the GOSSS-I classification was incorrect and that the early-type component should be an early Of/WN star (or “hot slash”, see GOSSS-II). However, that goes against the morphological criterion established by Crowther & Walborn (2011) based on the H β profile: if that line is in absorption, the object should be classified as an early Of star; if it has a P-Cygni profile, as an early Of/WN star; and if it is in emission as a WN star. The H β profile of HDE 228 766 is variable but it never shows a clear P-Cygni profile. Therefore, even though it is true that other emission lines are strong, the early type component should not be classified as an early Of/WN star. This object has no entry in the WDS catalog and no apparent companion is seen in our AstraLux images.

HD 193 443 AB = BD +37 3879 AB = ALS 11 137 AB. **SB2+Ca.** Mahy et al. (2013) classified this system as

Pair	Even. date (YYMMDD)	HJD-2.4 · 10 ⁶ (d)	ρ ($''$)	θ (deg)	Δi (mag)	Δz (mag)	Δz_n (mag)	ΔY (mag)
DN Cas A,B	181128	58 451.4	1.073±0.011	128.21±0.17	4.96±0.07	4.68±0.16
HD 16 429 Aa,Ab	080118	54 483.9	0.290±0.001	90.80±0.12	...	2.16±0.07
	110913	55 818.1	0.282±0.004	90.62±0.52	...	2.19±0.07
	130918	56 554.2	0.277±0.002	91.35±0.28	2.33±0.23
	181127	58 449.9	0.275±0.006	91.17±0.30	2.26±0.07	2.29±0.07
HD 16 429 Aa,B	080118	54 483.9	6.794±0.002	189.84±0.03	...	2.16±0.07
	110913	55 818.1	6.817±0.001	189.83±0.03	...	2.19±0.07
	130918	56 554.2	6.841±0.002	189.76±0.03	2.33±0.23
	181127	58 449.9	6.859±0.001	189.84±0.03	2.26±0.07	2.29±0.07
	080118	54 483.9	2.976±0.001	112.92±0.04	...	7.51±0.07
HD 16 429 Aa,D	110913	55 818.1	2.973±0.001	113.02±0.04	...	7.42±0.07
	130918	56 554.2	2.968±0.001	113.01±0.07	7.62±0.07
	181127	58 449.9	2.964±0.021	113.03±0.56	7.54±0.07	7.78±0.07
	110915	55 820.6	2.161±0.001	93.03±0.04	...	1.76±0.01
HD 17 505 A,B	180919	58 381.6	2.163±0.002	93.09±0.03	...	1.75±0.03
	130920	56 556.6	0.725±0.004	141.93±0.06	...	2.77±0.03
MY Cam A,B	180918	58 380.6	0.738±0.006	141.69±0.14	3.03±0.11	2.83±0.03
	110915	55 820.646	0.143±0.002	226.63±4.00	...	1.74±0.10
IU Aur A,B	121002	56 203.596	0.144±0.001	228.61±4.00	...	1.40±0.10
	181127	58 450.391	0.141±0.005	230.14±4.00	...	2.06±0.10
	181128	58 451.403	0.137±0.001	231.47±4.00	...	1.84±0.10
	181226	58 479.446	0.128±0.002	211.56±4.00	...	1.77±0.10
	181227	58 480.485	0.131±0.001	221.41±4.00	...	1.82±0.10
	181127	58 450.391	4.012±0.005	162.36±0.08	...	7.85±0.10
IU Aur A,C	181127	58 450.391	4.012±0.005	162.36±0.08	...	7.85±0.10
IU Aur A,D	181127	58 450.391	3.592±0.010	122.21±0.12	...	8.87±0.10
15 Mon Aa,Ab	080117	54 482.9	0.109±0.004	252.26±1.29	...	1.49±0.13
	121002	56 203.1	0.118±0.004	260.30±3.80	...	1.45±0.17	1.49±0.01	...
	130920	56 556.2	0.127±0.004	259.51±2.62	...	1.26±0.20
	180918	58 380.2	0.138±0.004	268.10±1.00	1.67±0.10	...
	181128	58 451.0	0.135±0.004	268.79±1.00	1.48±0.06	...
	080117	54 482.9	2.977±0.003	213.58±0.02	...	3.04±0.02
15 Mon Aa,B	121002	56 203.1	2.981±0.003	213.75±0.02	...	3.04±0.02	3.02±0.03	...
	130920	56 556.2	2.985±0.003	213.88±0.05	...	2.97±0.10
	180918	58 380.2	3.001±0.007	214.02±0.02	3.15±0.10	...
	181128	58 451.0	2.991±0.003	213.94±0.04	2.99±0.02	...
	081021	54 761.2	0.634±0.015	269.03±1.34	...	3.48±0.12
	081021	54 761.2	2.640±0.006	187.83±0.19	...	5.68±0.29
HD 52 533 Aa,Ab	081021	54 761.2	2.640±0.006	187.83±0.19	...	5.68±0.29
HD 52 533 Aa,B	081021	54 761.2	2.640±0.006	187.83±0.19	...	5.68±0.29
HD 52 533 Aa,G	081021	54 761.2	2.883±0.018	246.86±0.41	...	8.18±0.43

Table 1. (continued.)

O9 III/I + O9.5 V/III. In GOSSS I and II we were only able to obtain a combined spectral classification of O9 III. The WDS catalog reveals that the situation is complex, as there is a visual companion at a distance of $0''.1-0''.2$ with a Δm of 0.3 magnitudes (hence the designation AB, Fig. 3) and an appreciable motion in the last century. This visual companion is also detected in our AstraLux images. Therefore, there is a third body in the system contributing to the spectrum besides the two in the short-period binary, making HD 193 443 AB a hierarchical system with three late-O stars (one of them may be a B0 instead).

BD +36 4063 = ALS 11 334. **SB1.** Williams et al. (2009) measured the SB1 orbit of this interacting system and argued that the companion is invisible due to a thick and opaque disk around it. In GOSSS I we classified it as ON9.7 Ib. BD +36 4063 has no WDS entry and appears single in our AstraLux data.

HD 193 611 = V478 Cyg = BD +37 3890 = ALS 11 169. **SB2E.** Martins et al. (2017) classified this system as O9.5 V + O9.5 V. HD 193 611 had no previous GOSSS classification and here we derive O9.5 II + O9.5 III. With LiLiMaRlin we derive a similar classification of O9.5 III + O9.7 III. The

dwarf classification of Martins et al. (2017) is excluded on the basis of the low depth of He II $\lambda 4686$ for both components. The WDS catalog lists a dim component (also seen in our AstraLux images) $3''.7$ away that does not influence the classification.

HDE 228 989 = BD +38 4025 = ALS 11 185. **SB2E.** Mahy et al. (2013) determined an O8.5 + O9.7 spectral classification for this object and Laur et al. (2017) identified it as an eclipsing binary. HDE 228 989 was not previously included in GOSSS and here we derive a spectral classification of O9.5 V + B0.2 V. Using a LiLiMaRlin epoch we derive a similar classification of O9.5 V + B0 V. Both classifications are of later type for the two components than the Mahy et al. (2013) ones. More specifically, the secondary must be a B star because He II $\lambda 4542$ is very weak or absent and He II $\lambda 4686$ is weak. Also, the Si III $\lambda 4552$ /He II $\lambda 4542$ for the primary does not allow for a spectral classification as early as O8.5. The system has no entry in the WDS catalog and our AstraLux observations show no significant companion.

HDE 229 234 = BD +38 4069 = ALS 11 297. **SB1.** This system had not appeared in GOSSS before and here we obtain a single

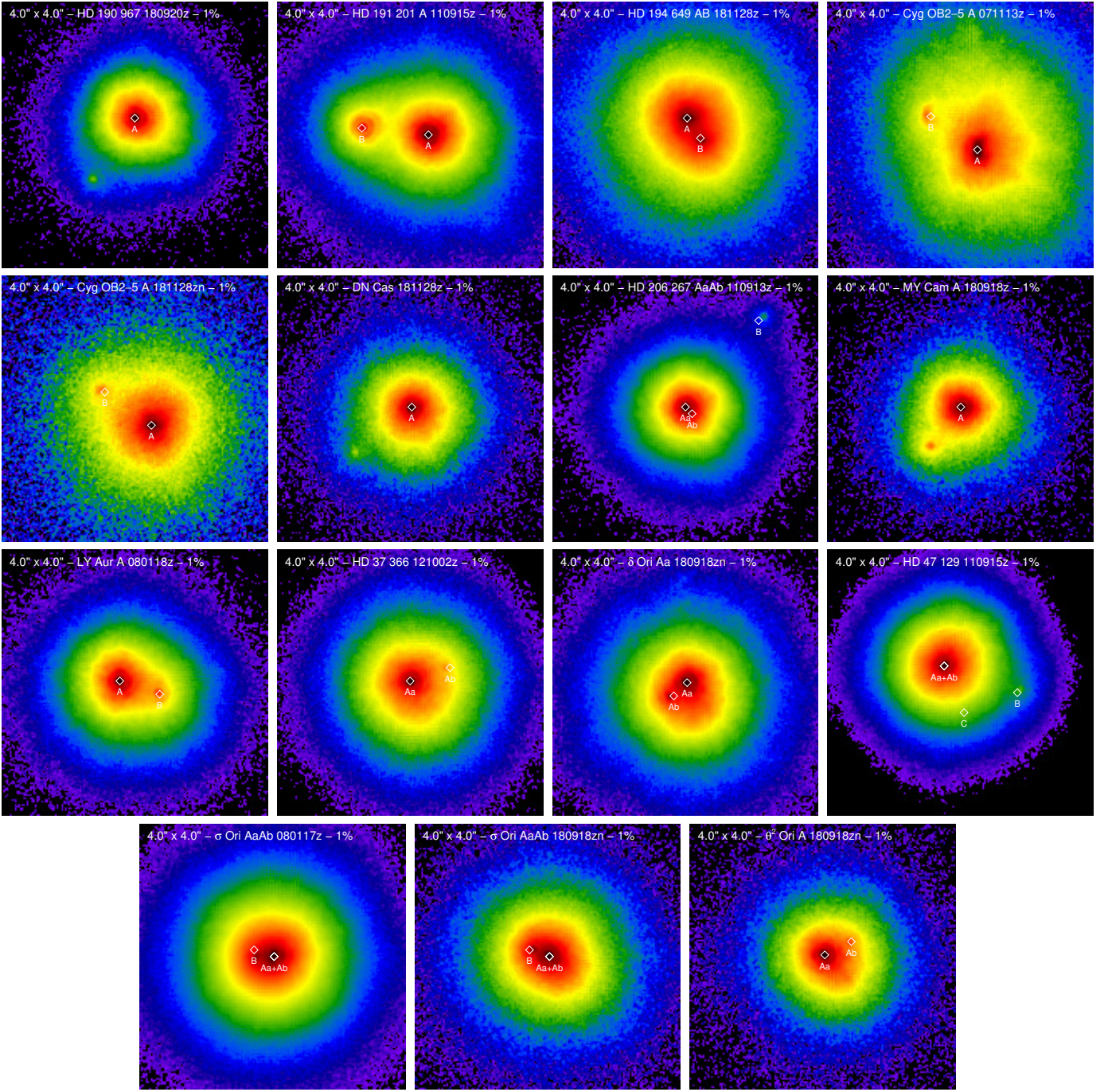


Fig. 3. Fragments of AstraLux fields for 13 of the targets in this paper (two of them with two epochs). The field size, target, evening date (YYMMDD), band, and lucky image frame selection fraction are given in each case (z stands for SDSS z , zn is a narrow-band filter with a similar central wavelength). The intensity scale is logarithmic to show both bright and faint sources. Diamonds are used to mark the last position of the known components in the WDS catalog (if no entry exists there, then an A is used to mark the brightest detected component). Each frame is $4'' \times 4''$ (160×160 pixels) with North up and East left.

spectral classification of O9 III with no sign of the secondary. The object has no entry in the WDS catalog and appears single in our AstraLux images.

HD 192 281 = V2011 Cyg = BD +39 4082 = ALS 10 943. **SB1.** Barannikov (1993) identified this object as a SB1 but its nature has not been confirmed afterwards. In GOSSS III we classified it as O4.5 IV(n)(f). It is a runaway star (Maíz Apellániz et al.

2018b). HD 192 281 has no WDS entry and no significant companion is seen in our AstraLux data.

Y Cyg = HD 198 846 = BD +34 4184 = ALS 11 594. **SB2E.** This eccentric short-period binary has a rapid apsidal motion (Harmanec et al. 2014) and was classified by Burkholder et al. (1997) as O9.5 V + O9.5 V. In GOSSS I we obtained a spectral classification of O9.5 IV + O9.5 IV, which we reproduce here using a LiLiMarlin epoch. The object has no entry in the

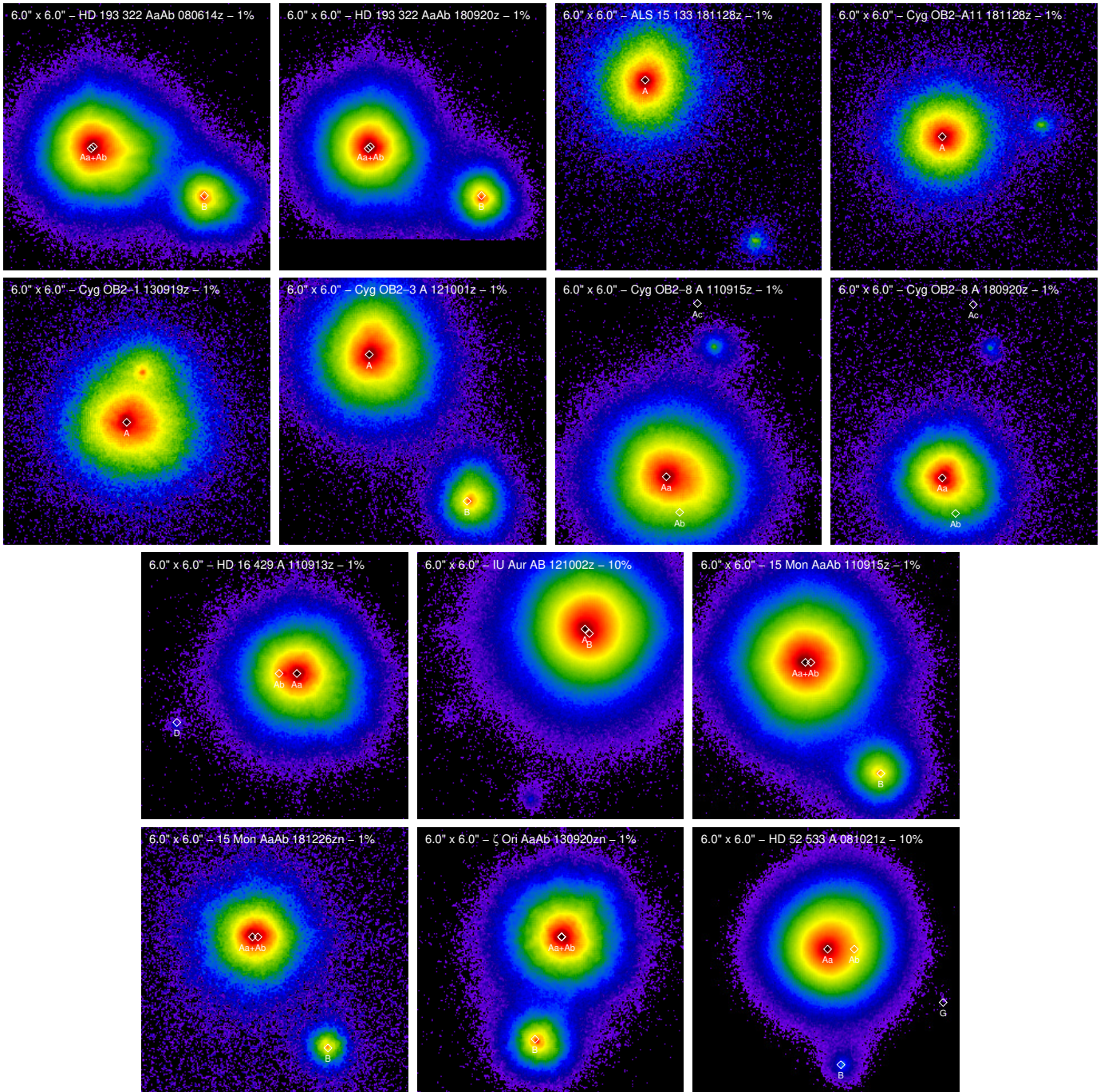


Fig. 4. Same as Fig. 3 for eleven additional targets (three with two epochs) with fields of view of $6'' \times 6''$ (240×240 pixels).

WDS catalog and appears single in our AstraLux images. It is a runaway star (Maíz Apellániz et al. 2018b).

HDE 229 232 AB = BD +38 4070 AB = ALS 11 296 AB. **SB1+Ca?**. This system has one low-amplitude SB1 orbit published (Williams et al. 2013). In GOSSS III we classified it as O4 V:n(f) and noted the anomalous profiles. The WDS catalog lists a bright nearby companion (hence the AB designation) but with only partial information. There is only one detection of B (Aldoretta et al. 2015) which seems robust (S. Caballero-Nieves, private communication) and with a maximum separation of 40 mas but a large uncertainty in the magnitude difference. No companion is seen in our AstraLux images but note that B is

too close to be resolved with that technique. It is a runaway star (Maíz Apellániz et al. 2018b).

HD 193 322 AaAb = BD +40 4103 AaAb = ALS 11 113 AaAb. **SB2a+Sa**. This hierarchical system is quite complex and its four inner components include two O stars and two B stars within $3''$, with two late-type B stars farther away (ten Brummelaar et al. 2011, from where some of the information in this paragraph comes from). An inner SB2 binary Ab1+Ab2 has a period of 312.4 d and is composed of an O8.5 III star (Ab1) with a dimmer B2.5 V: companion (Ab2, note that we do not design the system as AaAb1Ab2 because the contribution of Ab2 to the integrated spectrum is small). The Ab subsystem orbits around

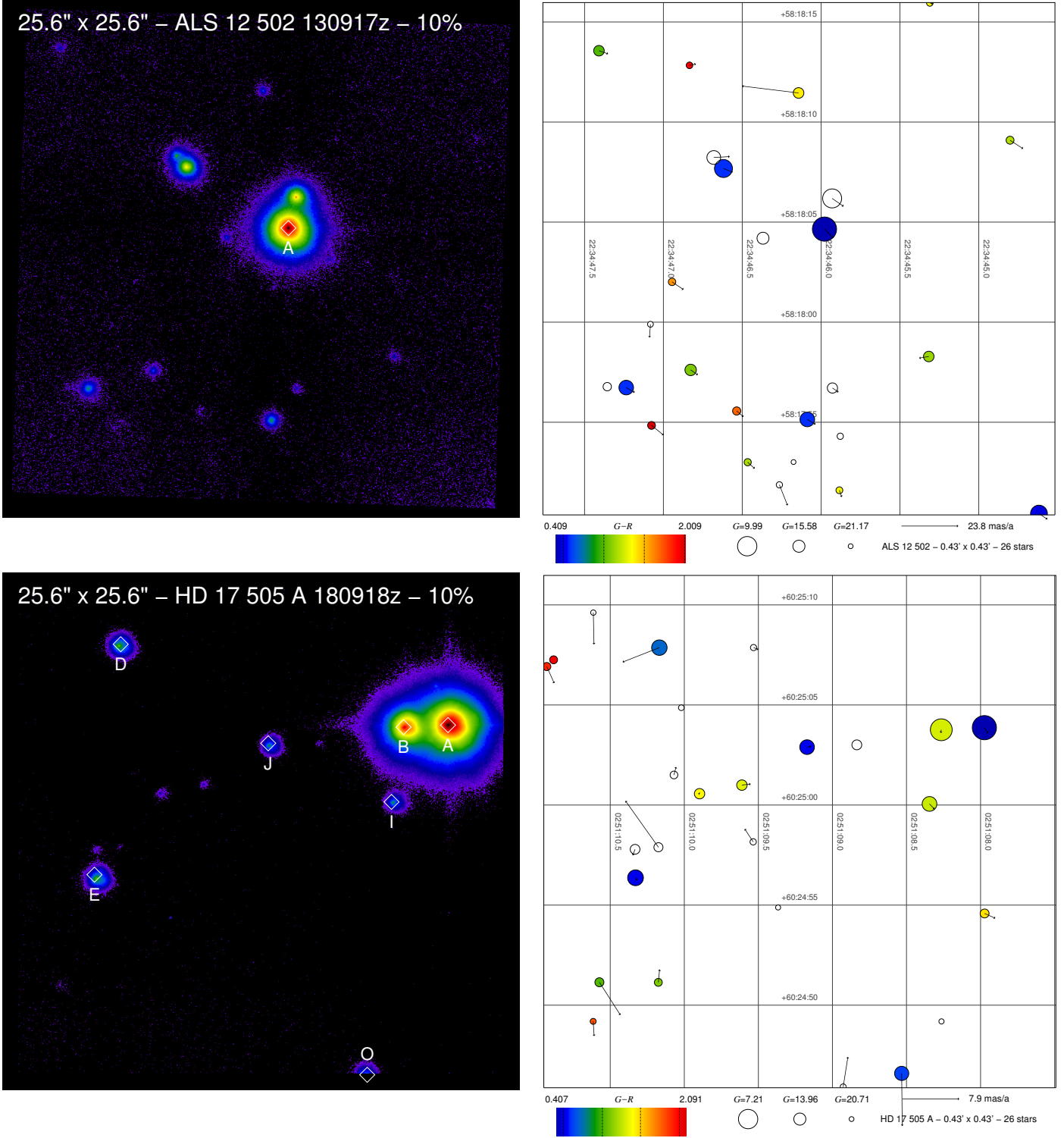


Fig. 5. (left column) Same as Fig. 3 for two additional targets with the full AstraLux field of view. (right column) Charts of the same fields built from Gaia DR2 sources with magnitude coded as size, $G - G_{RP}$ as color, and arrow size for total proper motion. Empty circles indicate no or bad-quality color information.

Aa, an O9 Vnn star, with a period of 35.2 a. In GOSSS-I we were unable to separate any of the three combined components and we were only able to give a combined O9 IV(n) classification. In Maíz Apellániz (2010) we measured (based on a single epoch) that Ab was brighter than Aa by 0.04 mag but the uncertainty was large enough to allow for the situation to be reversed. Our reanalysis of the original AstraLux epoch and of three new

ones with improved PSFs yields that Aa is brighter than Ab in the z band by 0.15–0.20 mag (Table 1 and Fig. 4), with a possible (but unconfirmed at this stage) small color term that would make the difference larger at shorter wavelengths. Note that Aa being slightly brighter than Ab1+Ab2 is incompatible with the first being of luminosity class V and Ab1 of luminosity class III (with both having similar spectral subtypes), leading us to think that

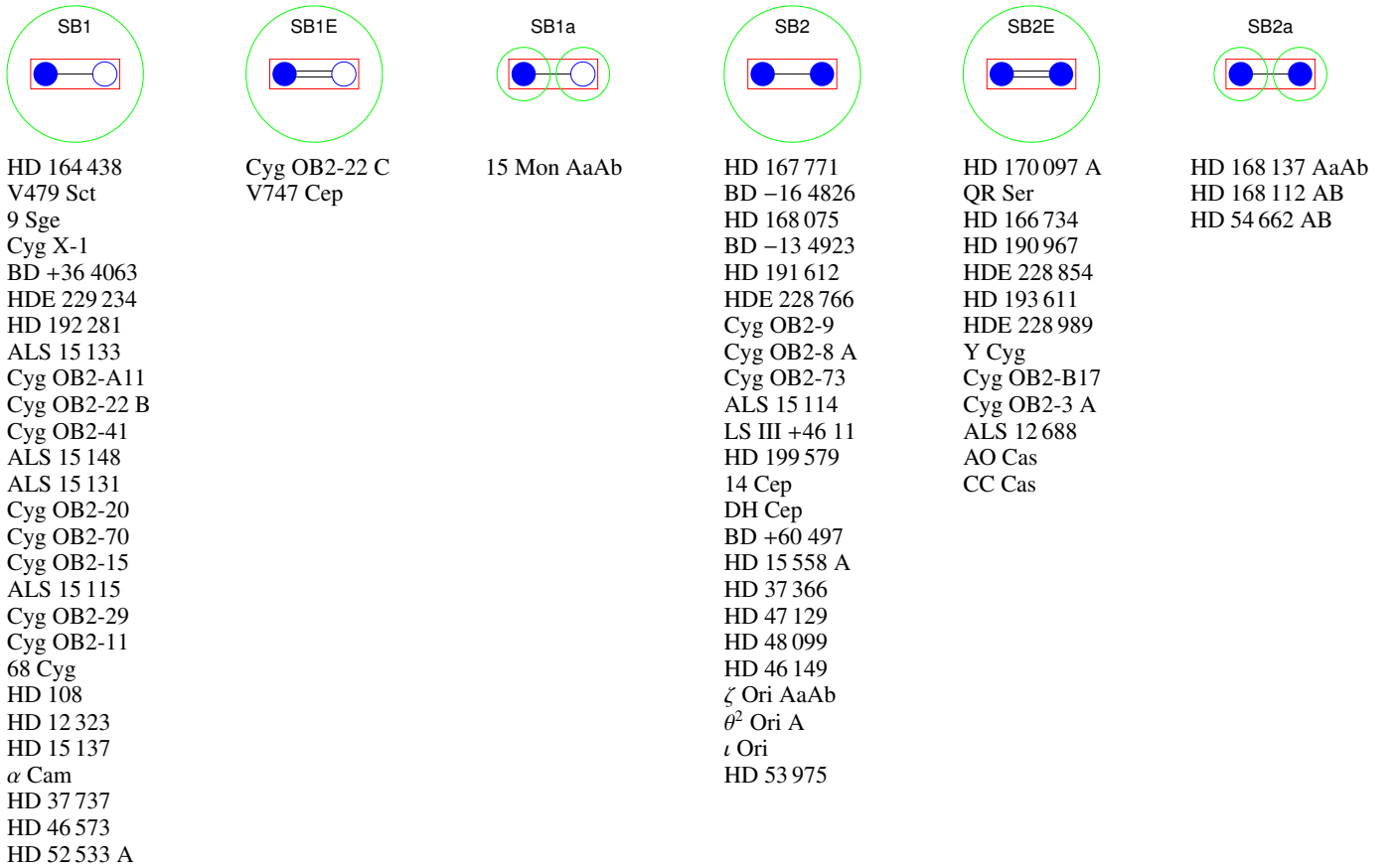


Fig. 6. Spectroscopic binary status (SBS) diagrams and systems that belong to each category. Blue circles are used to represent components: filled if they are significantly detected in the spectrum, empty otherwise. Lines connecting the components represent orbits: dashed if they do not induce detected radial velocity variations in the observed lines, single-solid if they do, and double-solid if they do and also produce eclipses. Empty green circles identify the observed astrometric components. Red rectangles identify the components included in the GOSSS long-slit spectra, note that if two red rectangles are shown in a diagram because GOSSS spatially separates components then the secondary spectrum is listed in parenthesis in the list below. Components outside the high-resolution aperture or low-mass components that do not induce detected radial velocity variations in the observed lines are not included. This subfigure shows systems with two components and the next subfigure those with three or four.

the luminosity classes of the two O stars may need to be revised. Our AstraLux observations cover a significant part of the 35.2 a orbit of Aa+Ab and indeed we detect a significant astrometric motion. HD 193 322 B is located $2''.7$ away with a Δz of 1.6 mag, far enough not to contaminate significantly observations with high-resolution spectrographs and normal seeing. Roberts et al. (2010) classified it as B1.5 V and the GOSSS spectrum shown here concurs with that classification but adding a (n)p suffix, as there is substantial broadening with respect to the standard and the He I lines are too deep, leading us to suspect a He enrichment that should be confirmed with further data. Finally, we note that we detect a significant outward motion (~ 39 mas in 10 years) for B with respect to Aa, something that is not seen in the historical WDS data or in the recent Gaia DR2 proper motions. However, those other measurements refer to the A,B separation, not to Aa,B. The detected outward motion is actually compatible with the effect of the Aa,Ab orbit in the position of Aa. This system and its cluster, Collinder 419, will be analyzed in a separate paper (Maíz Apellániz 2019, in preparation).

HD 194 649 AB = BD +39 4177 AB = ALS 11 324. **SB2+Ca.** Mahy et al. (2013) classified this system as O6 III(f) + O8 V.

Despite its short period there is no mention of eclipses in the literature. In GOSSS III we gave it an unresolved classification of O6.5 V((f)). Here we present a new GOSSS spectrogram from which we are able to derive a separate spectral classification of O6 V((f)) + O9.7: V. In one of the LiLiMaRlin epochs we caught the system close to quadrature and derive a similar separate spectral classification of O6 IV((f)) + O9.5 V((f)). Both the GOSSS and LiLiMaRlin results differ from the Mahy et al. (2013) one in that the primary has a lower luminosity class (He II $\lambda 4686$ is too strong to be a giant) and in that the secondary is of later spectral type. As a further complication, the WDS catalog lists a component $0''.4$ away with a Δm of 0.9 mag which is also seen in our AstraLux images (hence the AB designation). This implies that HD 194 649 AB is another example of a hierarchical triple system where three stars contribute to the spectrum. Our AstraLux data shows that B has moved 1 degree with respect to A in 6 years in a clockwise direction, which is consistent with the existing WDS information and yields a period of 2-3 ka.

Cyg OB2-B17 = V1827 Cyg = [CPR2002] B17. **SB2E.** This is the dimmest and one of the most extinguished targets in our sample. Stroud et al. (2010) found Cyg OB2-B17 to be an

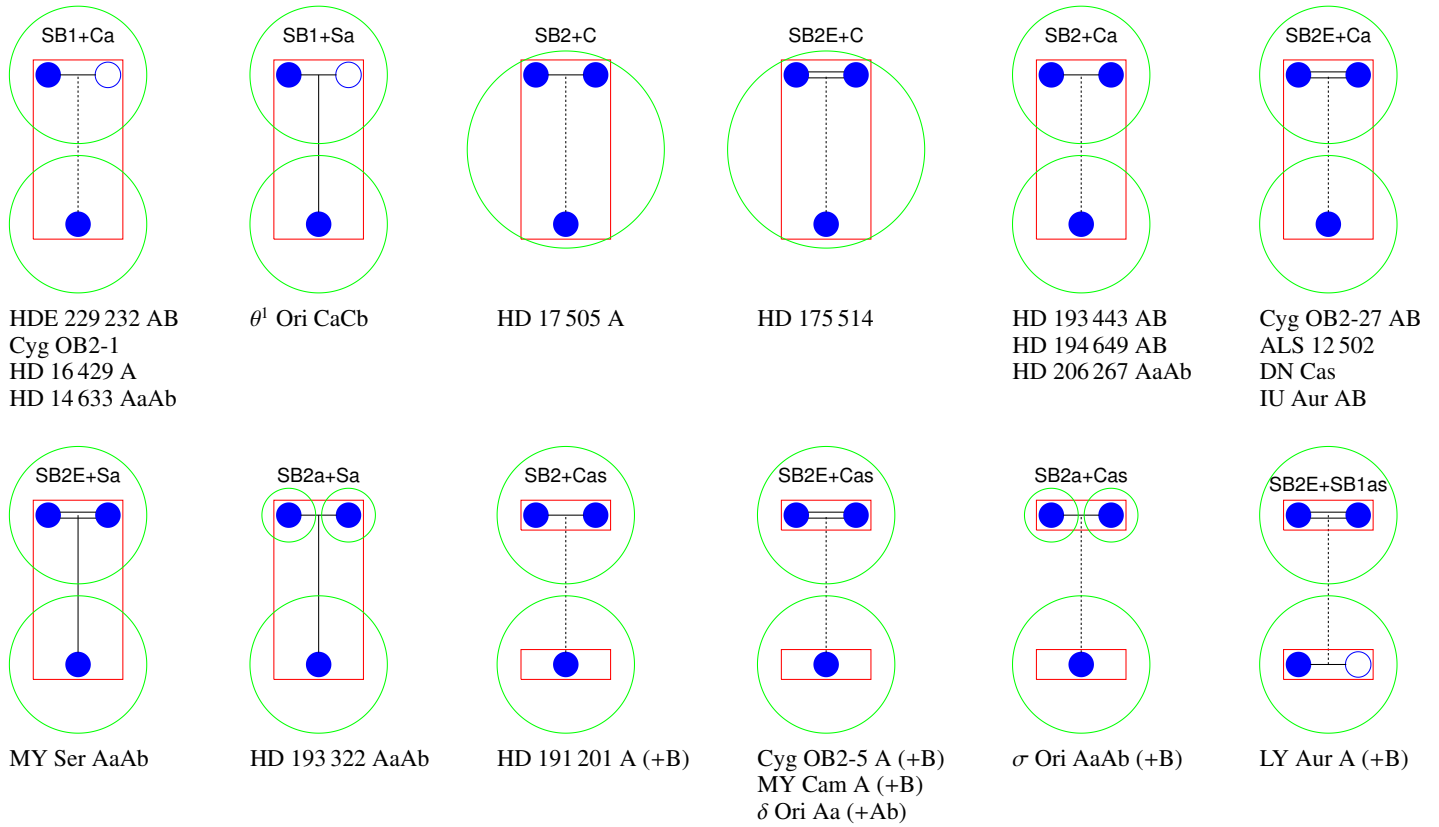


Fig. 6. (continued).

eclipsing SB2 composed by two supergiants with spectral types O7 Iaf + O9 Iaf. In GOSSS-III we derived an earlier classification for the primary, yielding O6 Iaf + O9: Ia:. It does not have an entry in the WDS catalog and our AstraLux image does not reveal any significant companion.

Cyg OB2-3 A = BD +40 4212 A = ALS 11 403 A = Schulte 3 A. **SB2E**. Kiminki et al. (2008) classified this system as O9 III + O6 IV: and Salas et al. (2015) identified it as an eclipsing binary. Cyg OB2-3 A was not previously included in GOSSS. Here we obtain a GOSSS spectral type of O8.5 Ib(f) + O6 III:. The WDS catalog gives a bright companion 4'0 away which also appears in our AstraLux images (Fig. 4). We aligned the GOSSS slit to obtain simultaneous spectra of the two targets and we derived a spectral type of B0 IV for Cyg OB2-3 B. Note that the B component is too far away to contribute to the LiLiMaRlin spectra.

ALS 15 133. **SB1**. This object was identified as a SB1 by Kobulnicky et al. (2012), who classified it as O9 III. ALS 15 133 had not appeared in any previous GOSSS papers and here we classify it as O9.5 IV. It has no entry in the WDS and here we identify a B component 4'4 away (Table 1 and Fig. 4) that also appears in Gaia DR2. Salas et al. (2015) identified it as having low-amplitude long-term photometric variability.

Cyg OB2-A11 = ALS 21 079 = [CPR2002] A11. **SB1**. Negueruela et al. (2008) classified Cyg OB2-A11 as O7 Ib-II and Kobulnicky et al. (2012) identified it as a SB1. In GOSSS III

we classified it as O7 Ib(f). This object has no entry in the WDS and here we detect a B companion 2'2 away (Table 1 and Fig. 4) that also appears in Gaia DR2.

Cyg OB2-5 A = V279 Cyg A = BD +40 4220 A = ALS 11 408 A. **SB2E+Cas**. In Rauw et al. (1999) they classified this SB2 supergiant as O5.5-6.5 + O6.5. In GOSSS I we gave a composite spectral classification of O7 Iafpe. In the new spectrogram presented here we separate the two components to give new spectral types of O6.5: Iafe + O7 Iafe. The emission lines associated with both components are quite strong, likely as a result of the interaction between the two winds. Note that there is a third lower-luminosity supergiant in the system, Cyg OB2-5 B, for which in GOSSS III we gave a spectral type of O6.5 Iabfp. It is located at an angular distance of 0'93 with a Δz of 3 magnitudes (Maíz Apellániz 2010), so its light falls at least partially in the aperture of the LiLiMaRlin spectrographs. However, given the large magnitude difference it contributes little to the combined spectra (Fig. 8). Here we have obtained a new spectrogram for Cyg OB2-5 B where the contamination noise due to the brighter A component is significantly lower. The classification is slightly revised to O7 Ib(f)p var? with the suffix indicating an anomalous He II λ 4686 profile and a possible variability (unclear whether it has a physical origin or is due to contamination from A). We have reanalyzed our previous AstraLux observations from 2007 and added a new epoch from 2018 (Table 1). We detect no motion along the line that joins the stars and only a slight one in position angle over a span of 11 years. This contrasts with a significant difference in separation (0'6) and position angle (11°) between the first (from 1967, Herbig 1967) and last (from 2007,

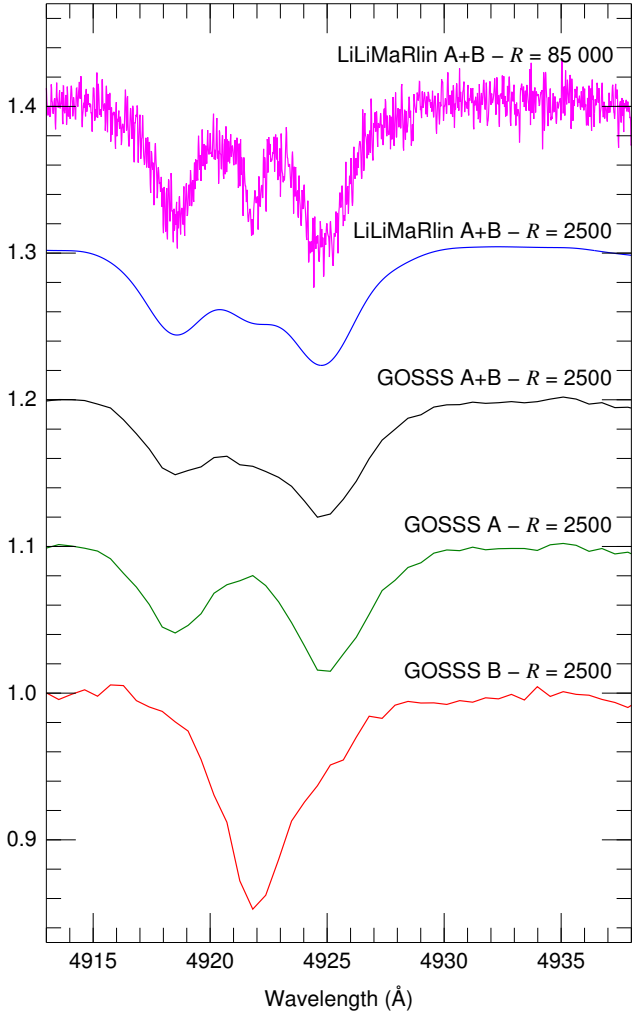


Fig. 7. Comparison of HD 191 201 spectra for the He I λ 4922 region that highlights the importance of combining spatially and spectrally resolved information to analyze multiple systems. The two bottom plots show the spatially resolved, rectified, and normalized GOSSS spectra of HD 191 201 A and B, respectively (all plots are offset by 0.1 continuum units with respect to the adjacent ones). The middle plot is a linear combination of the bottom two (using the measured Δm) to simulate the A+B spectrum, note how the B component leaves just a small imprint around $\lambda \approx 4922 \text{ \AA}$ due to its relative faintness. The top plot shows a LiLiMaRlin spectrum of A+B taken at a similar phase as the GOSSS spectra and the one below it is the same spectrum degraded to the GOSSS spectral resolution. Note the similarity between the two spectra of A+B at $R = 2500$ but the different paths taken to obtain them.

our previous data) epochs in the WDS, making us suspect that the 1967 measurement of the separation and position angle was incorrect. The consistency between our separation and position angle and those measured by Hipparcos point in the same direction. Another peculiarity of this visual pair is that the dimmer one (B) is bluer than the brighter one (A). As all stars involved have similar effective temperatures there should be no photospheric color differences. The difference could be caused by small-scale extinction differences (not surprising in a region with complex extinction such as Cyg OB2) or by wind-induced variability/emission lines in the A component.

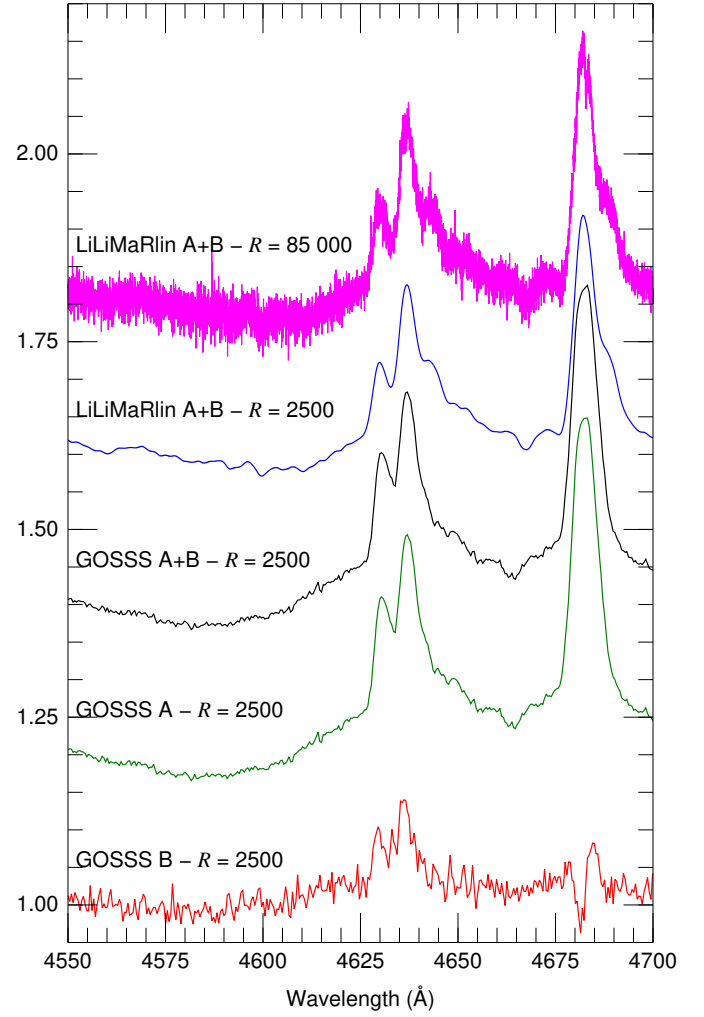


Fig. 8. Plot equivalent to Fig. 7 for Cyg OB2-5 and the 4550-4700 \AA region (all plots are offset by 0.2 continuum units with respect to the adjacent ones). Note that in this case there is a small phase difference between the GOSSS and LiLiMaRlin epochs for the A orbit. As the magnitude difference between A and B is larger than for HD 191 201 here the signature of the B component is much harder to detect in the spatially unresolved spectra.

Cyg OB2-22 C = V2185 Cyg = ALS 15 127. **SB1E?** Pigulski & Kołaczowski (1998) identified this object as an eclipsing binary (see also Salas et al. 2015) and Kiminki et al. (2012) as a potential SB1 (but without an orbit). In GOSSS-I we classified it as O9.5 III_n. It is a member of the Cyg OB2-22 cluster (in the Cygnus OB2 association) that includes at least five other O-type visual components (Maíz Apellániz 2010).

Cyg OB2-22 B = ALS 19 499 A. **SB1.** This object is the second brightest star in the Cyg OB2 cluster and is located $1''.5$ away from the brightest star in the cluster, Cyg OB2-22 A (Fig. 1 in Maíz Apellániz 2010 and Table 1), which was one of the first two O3 stars to be identified in the Northern hemisphere (Walborn et al. 2002). In GOSSS I we classified Cyg OB2-22 B as O6 V((f)). Kobulnicky et al. (2014) identified it as a SB1 but note that paper provides an incorrect position angle between A and B of 50 degrees: the correct value is 146 degrees (Table 1 and Table 2 in Maíz Apellániz 2010), with no appreciable mo-

tion over a time span of 13 years. Those values actually refer to the A,Ba pair, as there is a dim companion, Bb, that is included in the spectroscopic aperture but is too dim to significantly influence the spectral classification. The Ba,Bb pair shows no appreciable motion over the same time span but in that case the uncertainties in the individual measurements are larger (Table 1). All three components (plus others in the cluster) are included in the WDS.

Cyg OB2-41 = ALS 15 144. SB1. Cyg OB2-41 was classified as O9.7 III(n) in GOSSS III; previous papers misidentified it as a B star. It was identified as a SB1 by Kobulnicky et al. (2014). This object has no WDS entry.

ALS 15 148. SB1. Kobulnicky et al. (2014) identified this object as a SB1. It has not appeared in a GOSSS paper before and here we classify it as O6.5: V, noting that the spectrum has a S/N lower than most GOSSS spectra and needs to be repeated. Salas et al. (2015) found a quasi-sinusoidal photometric variation with a period of 3.170 d, which corresponds to the orbital period of Kobulnicky et al. (2014), so this object is likely an ellipsoidal variable. ALS 15 148 has no WDS entry and appears to be single in our AstraLux data.

Cyg OB2-9 = ALS 11 422. SB2. This target is a long-period highly eccentric SB2 system with strong non-thermal radio emission. Nazé et al. (2012) classified it as O5-5.5 I + O3-4 III. In GOSSS I we derived a composite spectral type of O4.5 If, as the high eccentricity yields double lines only during a small fraction of the orbit. With LiLiMaRlin we caught the system close to a periastron passage and derive a spectral classification of O4 If + O5.5 III(f), that is, the earlier-type component is the supergiant as opposed to the Nazé et al. (2012) result (note that our LiLiMaRlin spectrogram was obtained as part of NoMaDS, whose spectrograph does not include the 4710-4760 Å region). In other words, the He, N, and C emission lines do not take place at the radial velocity of the stronger He I absorption lines but at the radial velocity of the weaker ones. Cyg OB2-9 has only a distant and weak companion that is likely unbound (Maíz Apellániz 2010).

Cyg OB2-1 = ALS 11 401. SB1+Ca. This object was identified as a SB1 by Kiminki et al. (2008). It has not appeared in a GOSSS paper before and here we classify it as O8 IV(n)((f)). Cyg OB2-1 has no entry in the WDS but with AstraLux (Table 1 and Fig. 4) we detect a bright companion 1'2 away that also appears in Gaia DR2.

ALS 15 131. SB1. Kobulnicky et al. (2014) identified this target as a SB1. It has not appeared in a GOSSS paper before and here we classify it as O7.5 V((f)). ALS 15 131 has no WDS entry.

Cyg OB2-20 = ALS 11 404. SB1. This target was identified as a SB1 by Kiminki et al. (2009). It has not appeared in a GOSSS paper before and here we classify it as O9.7 IV. This object has no WDS entry and appears to be single in our AstraLux data.

Cyg OB2-8 A = BD +40 4227 A = ALS 11 423 A. SB2. Cyg OB2-8 is a cluster in the Cyg OB2 association with at least four O-type visual components (see GOSSS I+II). De Becker

et al. (2004)² classified Cyg OB2-8 A as O6 + O5.5 and in GOSSS-II we classified it as O6 Ib(fc) + O4.5: III:(fc). Here, we use a LiLiMaRlin epoch to derive the same classification but without the uncertainties in the secondary i.e. O6 Ib(fc) + O4.5 III(fc). The WDS catalog lists two dim nearby companions from Herbig (1967), Ab and Ac, but our AstraLux results (Table 1 and Fig. 4) do not agree with the data there. Ab is not seen so it is either dimmer than announced, has moved significantly (the single measurement in the WDS catalog is from 1961), or is a spurious detection. Ac is detected but it appears to have moved significantly since 1961, from a distance of 4'0 and a position angle of 350° to a distance of 3'1 and a position angle of 340° in 2018, with no significant motion in the seven previous years. Therefore, as with the Cyg OB2-5 A,B pair, we suspect an error in the separation and position angle of the first epoch.

Cyg OB2-70 = ALS 15 119. SB1. GOSSS III classified this object as an O star (O9.5 IV(n)) for the first time. Kobulnicky et al. (2014) identified it as a SB1. Cyg OB2-70 has no WDS entry.

Cyg OB2-15 = ALS 15 102. SB1. This target was identified as a SB1 by Kiminki et al. (2009). It has not appeared in a GOSSS paper before and here we classify it as O8 III. Cyg OB2-15 has no WDS entry and no significant companion appears in our AstraLux data.

ALS 15 115. SB1. Kobulnicky et al. (2014) identified this target as a SB1. In GOSSS III we classified it as O8 V. ALS 15 115 has no WDS entry.

Cyg OB2-27 AB = ALS 15 118 AB. SB2E+Ca. Ríos & DeGioia-Eastwood (2004) identified this object as a photometrically variable SB2. Salas et al. (2015) published a light curve that showed that it is an eclipsing variable with a period of 1.46917 ± 0.00002 d. In GOSSS III we classified it as O9.7 V(n) + O9.7 V:(n), that is, with the two stars more similar between them than the previous spectral classification of O9.5 V + B0 V of Kobulnicky et al. (2012). The WDS lists a close companion with a small Δm (Caballero-Nieves et al. 2014), hence the AB designation, that is not resolved in our AstraLux data.

Cyg OB2-73. SB2. Kiminki et al. (2009) identified Cyg OB2-73 as an O+O SB2 system and gave it the spectral classification O8 III + O8 III. In GOSSS III we give a classification of O8 Vz + O8 Vz, as the He II $\lambda 4686$ line is too deep to be a giant star in either case. This object has no WDS entry and appears to be single in our AstraLux data.

ALS 15 114. SB2. This object was identified as a SB2 by Kiminki et al. (2012), who classified it as O7 V + O9 V. It was included in GOSSS III but at that time we could not resolve the two components as the spectrum was obtained at an unfavorable epoch. A new GOSSS spectrum obtained since then allows us to derive a new classification of O7 V((f)) + O7 IV((f)), where the secondary is significantly earlier than the previous classification. Salas et al. (2015) identified a quasi-sinusoidal photometric

² Those authors published the only SB2 orbit available for this system but their paper does not give a value for ω .

variation with a 1.4316 ± 0.0006 d period, which corresponds to one half of the orbital period of Kiminki et al. (2012), making it a likely ellipsoidal variable. This object has no WDS entry.

Cyg OB2-29 = ALS 15 110. **SB1**. Kobulnicky et al. (2014) identified this object as a SB1. In GOSSS III we classified it as O7.5 V(n)((f))z. Cyg OB2-29 has no WDS entry and no significant companion appears in our AstraLux data.

Cyg OB2-11 = BD +41 3807 = ALS 11 438. **SB1**. This object was identified as a SB1 by Kobulnicky et al. (2012). In GOSSS I we classified it as O5.5 Ifc. Cyg OB2-11 has no WDS entry and appears to be single in our AstraLux data.

LS III +46 11 = ALS 11 448. **SB2**. This target is a very massive eccentric SB2 binary composed of two near-twin stars, both O3.5 If*, whose nature was discovered with GOSSS observations (Maíz Apellániz et al. 2015c). It is located at the center of the Berkeley 90 cluster and has several dim companions (see Fig. 1 in Maíz Apellániz et al. 2015b).

HD 199 579 = BD +44 3639 = ALS 11 633. **SB2**. Williams et al. (2001) published a SB1 orbit for this O star and used a Doppler tomography algorithm to search for the weak signal of the secondary, suggesting a B1-2 V spectral type for it and a mass ratio of 4 ± 1 for the system (effectively making it a SB2 orbit with a large K_2 uncertainty). In GOSSS I we gave a spectral type of O6.5 V((f))z for the primary. The WDS catalog lists a very dim companion 3'8 away.

68 Cyg = HD 203 064 = V1809 Cyg = BD +43 3877 = ALS 11 807. **SB1?**. Alduseva et al. (1982) identified this object as a SB1 and Gies & Bolton (1986) provided ephemerides for the radial velocity variations but warned that their origin is likely to be pulsational rather than orbital. In GOSSS I we give a spectral classification of O7.5 III(n)((f)). The WDS lists a dim companion 3'8 away but we do not see it in our AstraLux data and it does not appear in Gaia DR2 either. 68 Cyg is a runaway star (Maíz Apellániz et al. 2018b).

3.3. Cepheus-Camelopardalis

HD 206 267 AaAb = BD +56 2617 AaAb = ALS 11 937 AaAb. **SB2+Ca**. This system was classified as O6.5 V((f)) + O9.5: V by Burkholder et al. (1997). In GOSSS I we derived the similar classification of O6.5 V((f)) + O9/B0 V that here we modify with a new analysis of our GOSSS data to O6 V(n)((f)) + B0: V. A LiLiMaRlin spectrum yields the same spectral classification. HD 206 267 AaAb is the central object of a high-order multiple system. The two closest components (Aa and Ab) have a small Δm and are separated by just 0'1 according to the WDS. Our AstraLux data (Table 1 and Fig. 3) confirms that and detects a significant clockwise motion at near constant separation consistent with the previous WDS results that yields a combined preliminary orbital period of 153 ± 10 a. A third, dim, object, B, is located 1'7 away and should not contribute significantly to the LiLiMaRlin spectra. The seven-year span between our first and last epochs does not yield a significant relative motion for the Aa,B pair. Finally, two bright companions, C and D, are found within 25'' of the primary. Therefore, three components are likely to contribute to the spectral classifications here: the

two spectroscopic ones in Aa and the quasi-stationary in Ab (Raucq et al. 2018), implying that one of the spectral types is a composite. Raucq et al. (2018) also note that there are no apparent eclipses caused by the inner binary despite its short period.

14 Cep = LZ Cep = HD 209 481 = BD +57 2441 = ALS 12 096. **SB2**. Mahy et al. (2011) classified this system as O9 III + ON9.7 V. In GOSSS I we derived a classification of O9 IV(n) var + B1: V: that is revised here with a new analysis to O8.5 III + BN0 V. A LiLiMaRlin epoch yields the similar spectral types O9 III + BN0 V. Despite its short period, the system is not eclipsing. In the WDS catalog a very dim component is located 2'8 away but we do not see it in our AstraLux images.

ALS 12 502. **SB2E+Ca (previously SB2E)**. This eclipsing binary system (Maciejewski et al. 2004) was identified as a SB2 by Negueruela et al. (2004), who classified it as O8: + O9:. In GOSSS data we clearly see double lines and assign it the spectral classification O9 III:(n) + O9.2 IV:(n). Using a LiLiMaRlin we derive the classification O9 IV(n) + O9 V(n). In both the GOSSS and LiLiMaRlin we see evidence for the presence of a third light contaminating the spectrum. ALS 12 502 has no entry in the WDS catalog but our AstraLux images (Fig. 5) show a complex system, quite possibly a previously poorly studied cluster (Solin et al. 2012). One component is located 1'6 away (Table 1) and is the possible third light (note that we did not align the slit to separate that component as our GOSSS spectrum was obtained before our AstraLux data), hence the SBS typing as SB2E+Ca. Note that there is a significant magnitude difference between the two AstraLux epochs, likely caused by the primary being in different eclipse phases.

DH Cep = HD 215 835 = BD +57 2607 = ALS 12 597. **SB2**. Despite its short period, DH Cep is not an eclipsing binary but appears to be an ellipsoidal variable. Burkholder et al. (1997) classified this system as O5.5 III(f) + O6 III(f) and in GOSSS II we classified it as O5.5 V((f)) + O6 V((f)). Here we find the same spectral classification using a LiLiMaRlin epoch and we note that there are small differences in spectral classifications between epochs, prompting us to add var suffixes. The WDS catalog lists only two distant companions.

ALS 12 688. **SB2E**. This eclipsing binary system (Lewandowski et al. 2009) was identified as a spectroscopic binary in GOSSS III, where a classification of O5.5 V(n)((fc)) + B was given. No spectroscopic orbit has been published. This target has no entry in the WDS catalog.

AO Cas = HD 1337 = BD +50 46 = ALS 14 758. **SB2E**. Bagnuolo & Gies (1991) classified this system as O9.5 III + O8 V. In GOSSS II we obtained O9.2 II + O8 V((f)). Here we use a LiLiMaRlin epoch to obtain a similar classification of O9.2 II + O7.5 V. The WDS catalog lists only three dim companions, the closest one 2'8 away.

HD 108 = BD +62 2363 = ALS 6036. **SB1?**. Hutchings (1975) reported this object to be a SB1 but Nazé et al. (2008) pointed out that the spectroscopic variations are instead caused by magnetic effects. Indeed, HD 108 is an Of?p star (Walborn et al. 2010) classified as O8 fp in GOSSS I. Its magnetic/rotational cycle is

~50 a long and its variations are very slow so when GOSSS I was published we had not been collecting data for enough time to see the star in both of its two extreme states but now we have. We show in Fig. 1 a 2009 observation when HD 108 was in its O8.5 fp state (He I $\lambda 4471$ unfilled, no C III $\lambda 4650$ emission, H β in absorption) and a 2017 observation in its O6.5 f?p state (He I $\lambda 4471$ partially filled, C III $\lambda 4650$ in emission, H β in emission with absorption wings), leading to a combined classification of O6.5-8.5 f?p var. The WDS lists a dim companion 3''.2 away but we do not see it in our AstraLux data and it does not appear in Gaia DR2 either.

V747 Cep = BD +66 1673 = ALS 13375. **SB1E (previously E)**. Majaess et al. (2008) identified this system as an eclipsing binary but no spectroscopic orbits or separate spectral classifications have ever been published to our knowledge. In GOSSS III we derived a combined spectral type of O5.5 V(n)((f)) and our LiLiMaRlin data show a clear line motion between epochs, allowing us to identify it as a SB1 system. V747 Cep has no entry in the WDS catalog and our AstraLux images reveal no significant companion.

HD 12323 = BD +54 441 = ALS 6886. **SB1**. HD 12323 was identified as a SB1 by Bolton & Rogers (1978). In GOSSS II we classified it as ON9.2 V. This object has no WDS entry. It is a runaway star (Maíz Apellániz et al. 2018b).

DN Cas = BD +60 470 = ALS 7142. **SB2E+Ca (previously SB2E+C)**. Hillwig et al. (2006) classified this system as O8 V + B0.2 V. DN Cas had not appeared in GOSSS before and here we classify it as O8.5 V + B0.2 V. A LiLiMaRlin epoch yields the same spectral classification. Bakış et al. (2016) used precise eclipse timings to deduce the existence of a low-mass third body with a ~42 a orbit, which at the ~2 kpc distance to the system from Gaia DR2 yields a semi-major axis of ~20 mas. This target has no entry in the WDS catalog but our AstraLux data (Table 1 and Fig. 3) reveals a previously unknown visual component (which we label B) at a distance of 1''.07, indicating that DN Cas has at least four components. However, as the third and fourth bodies do not contribute significantly to the integrated spectrum or to the radial velocity of the other two components, we type DN Cas simply as SB2E+Ca³. DN Cas B is slightly redder than A in $z-i$, as expected from a coeval, young companion. Note, however, that we do not have multiple AstraLux epochs, so we do not know if the measured magnitude differences are affected by eclipses or not (see below for the similar IU Aur AB case).

BD +60 497 = ALS 7266. **SB2**. Rauw & De Becker (2004) gave a classification of O6.5 V((f)) + O8.5-O9.5 V for this system, which does not show eclipses despite its short period. In GOSSS I we classified it as O6.5 V((f)) + O8/B0 V and here we reclassify it as O6.5 V(n)((f))z + O9.5: V based on better data. Using LiLiMaRlin data instead of GOSSS we derive slightly later spectral types, O7 V(n)((f))z + B0: V(n). BD +60 497 has no entry in the WDS catalog and no significant companion is seen in our AstraLux images.

³ Properly speaking, we should classify the system as SB2e+C+Ca, but we do not because the third body is likely a low-mass star instead of an intermediate-mass one.

HD 15558 A = BD +60 502 A = ALS 7283. **SB2**. This long-period eccentric SB2 system was classified as O5.5 III(f) + O7 V by De Becker et al. (2006). In GOSSS II we classified the composite spectrum as O4.5 III(f), i.e., with a significantly earlier primary. With a new GOSSS spectrogram we obtain here O4.5 III(fc)p + O8:, where the secondary is quite weak and, hence, its spectral type is rather uncertain. As an anomaly in the spectrum, the primary appears to have not only the significant C III $\lambda 4650$ emission characteristic of the Ofc stars (Walborn et al. 2010) but also C IV $\lambda 4658$ in emission, hence the p suffix. HD 15558 is a high-order multiple system with 13 components in the WDS catalog. The only bright component within 15'' is HD 15558 B, located 9''.9 away. We aligned the GOSSS slit to acquire spectra of both components simultaneously and we obtained a classification of B0 V for B.

HD 16429 A = BD +60 541 A = ALS 7374. **SB1+Ca**. This system was classified by McSwain (2003) as O9.5 II + O8 III-V + B0 V?, with the primary corresponding to the visual Aa component and the other two spectroscopic components to the Ab component, located 0''.28 away. What makes this target special is that the Δm between Aa and Ab is larger than two magnitudes (Fig. 4 and Table 1, note that we have reanalyzed the data in Maíz Apellániz 2010), making the signal of the spectroscopic binary very weak in the integrated spectrum. McSwain (2003) actually underestimated the magnitude difference between Aa and Ab and was only able to compute a SB1 orbit for Ab after subtracting the constant-radial-velocity A component, leading us to suspect that the spectroscopic components may be in Aa instead of in Ab. In GOSSS II we were only able to give a composite O9 II-III(n) Nwk spectral classification. We attempted to separate Aa and Ab using lucky spectroscopy but we were unable to do so. HD 16429 is a high-order multiple with three additional components listed in the WDS catalog. HD 16429 B is an F star (McSwain 2003, GOSSS I, and Fig. 1) and the recent Gaia DR2 results give a large relative proper motion between A and B, indicating that it is a foreground object, something that our measurements (Table 1) confirm. We aligned the GOSSS slit with the other bright component, HD 16429 C, located 53'' away and we determined that its spectral type is B0.7 V(n).

HD 17505 A = BD +59 552 A = ALS 7499 A. **SB2+C**. This target is a system with spectral types O6.5 III((f)) + O7.5 V((f)) + O7.5 V((f)) according to Hillwig et al. (2006), with the secondary and tertiary forming a near identical pair with a short 8.5710 d period and the primary being stationary in their data (Rauq et al. 2018 does not detect a radial velocity change in the tertiary either and the inner binary does not produce eclipses, hence the SB2+C status for HD 17505 A). In GOSSS II we gave a composite spectral classification of O6.5 III(n)(f). We have obtained a new GOSSS spectrum using lucky spectroscopy to which we assign a classification of O6.5 IV((f)) + O7 V((f)), but one of the two spectral types should be a composite. The HD 17505 system is a high-order multiple, with the WDS catalog listing 20 components (Fig. 5). Some of those are likely to be not bound to the central stars but instead be part of the IC 4848 cluster where this system is located. HD 17505 B is close enough to A (Table 1) to be likely bound but too distant to contribute significantly to the flux in the echelle aperture (unless seeing is poor or the guiding system is not set up to properly follow A). In GOSSS I we gave HD 17505 B a spectral classification of O8 V, raising the number of O stars in the system to four, a classification we confirm

here with the new lucky spectroscopy data. The WDS lists a first epoch 1830 separation of the A,B pair larger than the current one by $1''$, which would imply a relative proper motion of ~ 5 mas/a or a change of ~ 35 mas in the 7 years between our two AstraLux observations, an effect we do not observe in our data, where the two relative positions are essentially coincident. The recent Gaia DR2 proper motions also yield a relative proper motion for A,B of less than 1 mas/a, indicating that the separation for the first epoch in the WDS is likely incorrect.

HD 15 137 = BD +51 579 = ALS 7218. **SB1**. This system is a low-amplitude single-lined spectroscopic binary (McSwain et al. 2007). In GOSSS I we classified it as O9.5 II-III_n. HD 15 137 has no entry in the WDS catalog and our AstraLux images show no significant companion.

CC Cas = HD 19 820 = BD +59 609 = ALS 7664. **SB2E**. Hill et al. (1994) derived spectral types of O8.5 III + B0 V for this system. In GOSSS I we obtained a composite spectral type of O8.5 III(n)((f)). Here we publish a GOSSS spectrogram where the companion leaves a weak signal that allows us to classify CC Cas as O8.5 III(n)((f)) + B. The WDS catalog lists only a very weak component $2''.8$ away that is undetected in our AstraLux images.

HD 14 633 AaAb = BD +40 501 = ALS 14 760. **SB1+Ca?**. This system is a low-amplitude single-lined spectroscopic binary (McSwain et al. 2007). In GOSSS I we classified it as ON8.5 V. The AaAb nomenclature is used because Aldoretta et al. (2015) detected a possible companion a short distance away but with a large Δm uncertainty, a case similar to that of HDE 229 232 AB above. Our AstraLux images show no apparent companion but the Ab companion should be too close for detection. Note that HD 14 633 AaAb is WDS 02228+4124 CaCb, as WDS 02228+4124 A corresponds to the brighter late-type HD 14 622. This target is a runaway star (Maíz Apellániz et al. 2018b).

α Cam = HD 30 614 = BD +66 358 = ALS 14 768. **SB1?**. This target has a single SB1 orbit published (Zeinalov & Musaeu 1986) which we deem suspicious as it is eccentric ($e = 0.45$), with a short period (3.6784 d), and a primary that is a late-O supergiant (in GOSSS I we classified it as O9 Ia), making it difficult for the orbit not to be quickly circularized or even for the companion to stay outside the primary. Furthermore, there are no detected eclipses, making it likely that the radial velocity variations are caused by pulsations. This object has no entry in the WDS catalog and no significant companions are seen in our AstraLux images. α Cam is a runaway star (Maíz Apellániz et al. 2018b).

MY Cam A = BD +56 864 A = ALS 7836 A. **SB2E+Cas (previously SB2E)**. Lorenzo et al. (2014) classified this extremely fast and short-period eclipsing binary as O5.5 V + O7 V. In GOSSS III we obtained a similar classification of O5.5 V(n) + O6.5 V(n) which we refine here to O5.5 Vnz + O6.5 Vnz with a lucky spectroscopy observation. Using a LiLiMaRlin epoch we classify the system as O6 V(n) + O6.5 V(n)z. We add the var suffix in all cases, as the spectral types appear to change as a function of the orbital phase. MY Cam A has no entry in the WDS catalog and with our

AstraLux images we detect a previously unknown B component $0''.73$ away (Table 1 and Fig. 3) for which a possible slight motion is detected, but it needs to be confirmed with future observations. Our lucky spectroscopy observation allowed us to spatially separate the spectrum of MY Cam B and give it a classification of B1.5: V (Fig. 1). The B component is slightly redder than A in $z - i$, as expected from the spectral type difference.

3.4. Auriga

LY Aur A = HD 35 921 A = BD +35 1137 A = ALS 8401 A. **SB2E+SB1as**. Mayer et al. (2013) classified this system as O9 II + O9 III. In GOSSS II we classified it as O9.5 II + O9 III. Here we present a new spectrogram obtained through lucky spectroscopy which we use to slightly revise the classification to O9.2 II(n) + O9.2 II(n). The visual B component is located $0''.6$ away with a Δm of 1.87 mag (Maíz Apellániz 2010 and Fig. 3). Using lucky spectroscopy we aligned the slit to obtain spatially separated spectra for each component and derived a GOSSS spectral type of B0.2 IV for LY Aur B (Fig. 9, note that as A and B are separated in GOSSS, B is not included in the star name), not far from the B0.5 prediction of Mayer et al. (2013). According to those authors, the B component is a SB1, so LY Aur AB contains four stars, making it the only system in this paper with four objects within the high-resolution aperture that induce detectable radial velocity variations (the second component of LY Aur B is not seen in the spectra but if it were its radial velocity shifts should be larger than those of B itself).

IU Aur AB = HD 35 652 AB = BD +34 1051 AB = ALS 8369 AB. **SB2E+Ca**. Özdemiř et al. (2003) classified this system as O9.5 V + B0.5 IV-V. IU Aur AB had not appeared in GOSSS papers before and here we classify it as O9.5 IV(n) + O9.7 IV(n). Using LiLiMaRlin we obtain a different spectral classification of O8.5 III(n) + O9.7 V(n). We believe the discrepancies between those spectral classifications are caused by [a] the known presence of a third light that is being added to the primary or the secondary depending on the phase of this very fast binary and [b] eclipse effects. Therefore, those spectral classifications should be taken as provisional until a more in-depth multi-epoch study is performed. Nevertheless, we can already point out that it is already clear that the secondary must be O9.7 or earlier based on the Si III $\lambda 4552$ /He II $\lambda 4542$ seen in different phases. For the third object Özdemiř et al. (2003) measured an orbit with a period of 293.3 d through light-time effects and estimated that the third light contributes a 24% of the total light (which corresponds to a Δm of 1.25). On the other hand, the WDS catalog lists a B companion $0''.1$ away with a Δm of 1.36 ± 1.01 mag discovered by Hipparcos. However, that component should have an orbit measured in centuries, implying there are two different companions. The question is which one of them is the main contributor to the third light, the outer B or the intermediate unnamed one with the 293.3 d period? Özdemiř et al. (2003) favor the inner one based on the large Δm uncertainty measured by Hipparcos for the outer one. Our AstraLux data (Table 1 and Fig. 4) shows that the A,B pair has a variable Δz between 1.40 and 2.06 magnitudes, where the variability fits the known eclipses of the A component. Taking the upper value as the one that corresponds to the uneclipsed A yields a contribution of B to the total light of $13 \pm 1\%$. Therefore, the outer (B) component appears to be the dominant contribution to the third light but further analyses are needed to determine whether the intermediate unnamed component also has a significant con-

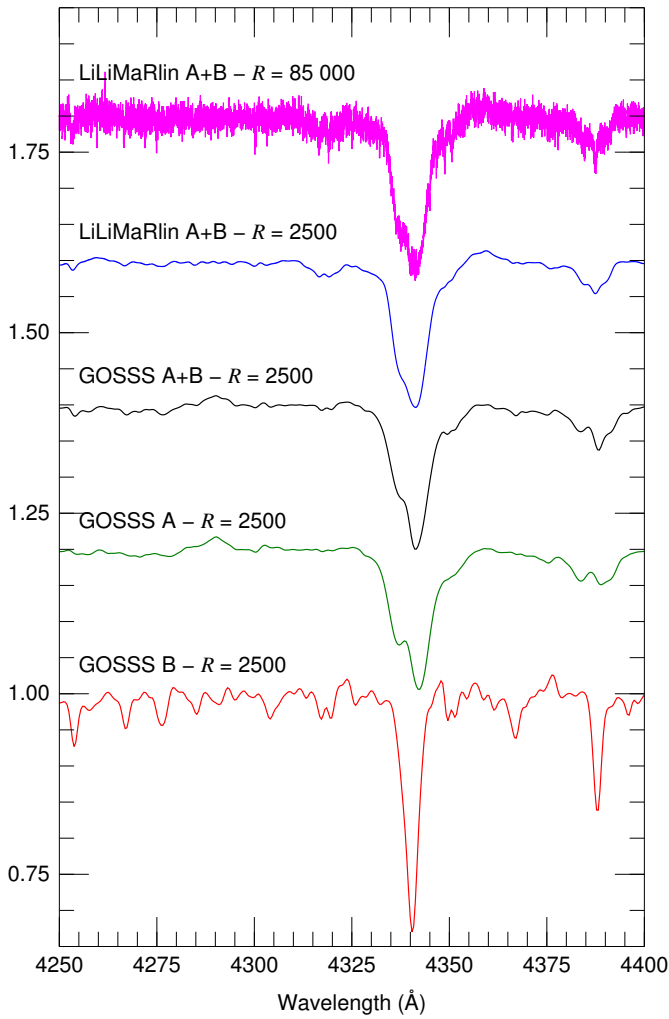


Fig. 9. Plot equivalent to Fig. 7 for LY Aur and the H γ region (all plots are offset by 0.2 continuum units with respect to the adjacent ones). Note that in this case there is a small phase difference between the GOSSS and LiLiMaRlin epochs for the A orbit.

tribution. Our AstraLux images reveal the existence of two dim previously undetected companions $3''.6$ and $4''.0$ away (lower left quadrant of the IU Aur AB panel in Fig. 4), to which we assign the respective component classifications of C and D. Note that if future observations using e.g. interferometry resolve the intermediate component it should be identified as Ab, leaving Aa for the SB2E primary. Finally, we note that the four inner components of IU Aur have the same configuration as DN Cas (but with a smaller Δm between A and B), so the same comment about classifying it as SB2E+Ca or SB2E+C+Ca applies here.

HD 37 737 = BD +36 1233 = ALS 8496. **SB1.** This target is a single-lined spectroscopic binary (McSwain et al. 2007) that was classified as O9.5 II-III(n) in GOSSS I. It has no entry in the WDS catalog and our AstraLux images show no significant nearby companion.

HD 37 366 = BD +30 968 = ALS 8472. **SB2.** Boyajian et al. (2007) classified this star as O9.5 V + B0-1 V. In GOSSS I we gave a composite classification of O9.5 IV but with a new spectrogram we are able to give it a new classification as

O9.5 V + B1: V, which we also reproduce with a LiLiMaRlin spectrogram. The WDS catalog lists a dim companion $0''.6$ away that we also see in our AstraLux data (Fig. 3).

3.5. Orion-Monoceros

15 Mon AaAb = S Mon AaAb = HD 47 839 AaAb = BD +10 1220 AaAb = ALS 9090 AaAb. **SB1a.** 15 Mon AaAb is a visual + SB1 binary whose orbit has been studied in different papers (Gies et al. 1993, 1997; Cvetković et al. 2009, 2010; ?) with diverging results. The discrepancies arise because only a partial orbit has been observed (with a periastron around 1996), the radial velocity amplitude of the spectroscopic orbit is small (with historical measurements having a relatively large scatter), and the orbit has a large eccentricity. A third component, B, is located $3''$ away from the Aa+Ab pair. In Maíz Apellániz et al. (2018a) we used lucky spectroscopy to separate AaAb (O7 V((f)z var) from B (B2: Vn). Our AstraLux data resolves the three components and shows a significant orbital motion of Ab with respect to Aa in the lapse of ten years. Also, in a manner similar to what we see for the HD 193 322 Aa+Ab+B triple system, there is a significant change in the relative position of B with respect to Aa, in this case more easily seen in position angle (Table 1 and Fig. 4). The detected motion is compatible with the effect of the Aa,Ab orbit in the position of Aa. This system and its cluster, NGC 2264, will be analyzed in a separate paper (Maíz Apellániz 2019, in preparation).

δ Ori Aa = Mintaka Aa = HD 36 486 A = BD -00 983 A = ALS 14 779 A. **SB2E+Cas.** Harvin et al. (2002) classified this object as O9.5 II + B0.5 III and noted the complexity of the system. It is composed of an inner eclipsing binary (Aa1+Aa2) with a 5.7 d period (to whose components belong their spectral types) with a visual companion (Ab) located $0''.3$ away (Fig. 3). All three stars are bright enough to contribute to the spectrum, though Aa1 is the brightest (Pablo et al. 2015; Shenar et al. 2015). In Maíz Apellániz et al. (2018a) we applied the novel lucky spectroscopy technique to spatially separate Aa from Ab and obtain a GOSSS spectral classification of O9.5 IINwk for Aa and one of O9.7 III:(n) for Ab (as Aa and Ab are separated in GOSSS, Ab is not included in the star name). We were unable to separate the spectroscopic components in Aa because the two epochs we obtained were not close to quadrature but we did observe some small variations between the two spectrograms that were indicative of orbit-induced radial velocity changes. Also, there were differences between the Aa spectra and the AaAb one we presented in GOSSS I. Most notably, some lines were narrower, as Ab is a moderately fast rotator. Note that there is some confusion with the component nomenclature for this system. For example, Simbad currently calls “*del Ori B” what we call δ Ori Ab here (following the WDS catalog). There are two distant components of the system, one relatively bright (C) and one very faint (B). δ Ori C has its own Henry Draper designation (HD 36 485).

HD 47 129 = Plaskett star = V640 Mon = BD +06 1309 = ALS 9054. **SB2.** The binarity of this object was discovered by Plaskett (1922). Linder et al. (2008) classified it as O8 III/I + O7.5 V/III and noted the variability and complexity of the spectra (see also Struve et al. 1958). Some of the variability of the spectrum was assigned to the magnetic field of the secondary by Grunhut et al. (2013). In GOSSS I we classified

the composite spectrum as O8 fp var. Here we present a new GOSSS spectrogram that yields O8 Iabf + O8.5:fp, where we do not assign a luminosity class to the secondary due to the peculiarity of the spectrum. The WDS catalog lists three faint components within 1''2, of which the most distant one appears in our AstraLux images (Fig. 3)

HD 48 099 = BD +06 1351 = ALS 9098. **SB2**. Mahy et al. (2010) classified this system as O5.5 V((f)) + O9 V. It shows no eclipses despite its short period. In GOSSS III we found the same spectral classification with the only addition of a z suffix to the primary. We also have a LiLiMaRlin spectrum at the correct phase and found the same spectral classification as GOSSS but with an added uncertainty to the spectral subtype of the secondary. HD 48 099 has no entry in the WDS catalog and appears single in our AstraLux data.

HD 46 149 = BD +05 1282 = ALS 8983. **SB2**. Mahy et al. (2009) classified this system as O8 V + B0-1 V. In GOSSS I we obtained a composite classification of O8.5 V. The target has no entry in the WDS catalog and we see no obvious companion in our AstraLux data.

ζ Ori AaAb = Alnitak AaAb = HD 37 742 AB = BD -02 1338 AaAb = ALS 14 793 AB. **SB2**. Hummel et al. (2013) give spectral types of O9.5 Ib + B0.5 IV for this object but it should be noted that their spectral type for the secondary is estimated, not directly measured, as the Δm between the two components is large (2 magnitudes) and the radial velocity differences are small. Another important point is that their spectroscopic secondary is the visual Ab, as ζ Ori AaAb is one of the few spectroscopic systems with a full interferometric orbit, with a seven-year period. ζ Ori B is another bright component 2''.4 away (Fig. 4), too far to significantly contribute to the LiLiMaRlin spectra. In Maíz Apellániz et al. (2018a) we applied lucky spectroscopy to obtain separate spectra for AaAb and B. Both are of O-type, with the composite AaAb classified as O9.2 IbNwk var (slightly earlier than the Hummel et al. 2013 classification for Aa) and B as O9.7 III_n.

σ Ori AaAb = HD 37 468 AaAb = BD -02 1326 AaAb = ALS 8473 AaAb. **SB2a+Cas**. Simón-Díaz et al. (2011) classified this system as O9.5 V + B0.5 V, where the interferometric visual pair Aa,Ab (Schaefer et al. 2016) is also a SB2 with a 143.198±0.005 d period (Simón-Díaz et al. 2015a). The aperture used by Simón-Díaz et al. (2011) included the other bright visual companion, B, currently located 0''.26 away and with a 159.9 a period, for which they provided a spectral classification of B0/1 V. Figure 3 shows two AstraLux observations of σ Ori where the clockwise motion of B with respect to AaAb is apparent over the ten years spanned. In Maíz Apellániz et al. (2018a) we applied lucky spectroscopy to obtain spatially separated spectra for AaAb and B for the first time (as AaAb and B are separated in GOSSS, B is not included in the star name). Here we present a new lucky spectroscopy observation with a crucial difference with the previous one: it was obtained near the Aa,Ab periastron. This allows to spatially+kinematically separate the three components (Fig. 1) and derive three spectral classifications with a single observation for the first time. Aa is O9.5 V, Ab is B0.2 V, and B is B0.2 V(n). σ Ori is a high-order multiple system with many entries in the WDS catalog and is lo-

cated at the center of the cluster with the same name (Caballero 2014).

HD 46 573 = BD +02 1295 = ALS 9029. **SB1**. Mahy et al. (2009) identified it as a SB1. In GOSSS I we classified it as O7 V((f))z. HD 46 573 has no WDS entry and appears single in our AstraLux data.

θ^1 Ori CaCb = HD 37 022 AB = BD -05 1315 CaCb = ALS 14 788 AB. **SB1?+Sa**. As the main ionizing source of the Orion nebula, θ^1 Ori CaCb is one of the most studied O stars. It is also one of the most complicated ones in terms of variability, with different periods from 15 d to 120 a having been proposed in the last two decades. Nowadays we understand that the shortest 15.422±0.002 d period (Stahl et al. 1996) is rotational and its associated variations are caused by magnetic effects (Donati et al. 2002). Weigelt et al. (1999) discovered a close companion (θ^1 Ori Cb) for which an eccentric astrometric+SB1 orbit with a period of ~11 a was computed later on by Kraus et al. (2009). As a further complication, Lehmann et al. (2010) proposed that the primary (Ca) is itself a SB1 with a 61.5 d period but this has not been confirmed and the 4:1 relationship between the rotation period of the primary and the alleged inner period could be a real resonance or a data artifact. Hence the SB1?+Sa typing. Note that the Ca+Cb pair is too close to be resolved with AstraLux. θ^1 Ori CaCb was classified in GOSSS I as O7 V_p. In Fig. 1 we show two GOSSS spectra taken with the same setup eight days apart to illustrate the variations associated with its magnetic cycle. The most obvious one is the transformation of He II λ 4686 from an absorption profile to an inverse P-Cygni one but others are also visible, such as a change in the H β profile caused by the similar apparition of an emission component that is not strong enough to emerge from the photospheric absorption but is sufficient to significantly change the shape and equivalent width of the line. Note also that C III λ 4650 is in emission with an intensity similar to that of N III λ 4634 and variable, the most prominent defining characteristic of the Of?p phenomenon. Therefore, here we add θ^1 Ori CaCb to the group of Galactic Of?p stars (becoming the sixth member of the club) and give it a spectral classification of O7 f?p var.

θ^2 Ori A = HD 37 041 = BD -05 1319 A = ALS 14 789. **SB2 (previously SB1)**. Stickland & Lloyd (2001) gave spectral types of O9 V + B0.5 V for this system but we should note that they only calculated a SB1 orbit and the secondary spectral type is an estimation, not a real measurement. In GOSSS I we derived a composite spectral type of O9.5 IV_p and here we present a new spectrogram where we obtain a separate classification of O9.2 V + B0.5: V(n), which we believe to be the first time a spectral type is measured for the secondary. A LiLiMaRlin spectrogram at a different orbital phase than the GOSSS one yields a similar classification of O9.5 V + B0.2: V. There is a faint visual Ab component listed in the WDS catalog with a Δm of 3.2 mag and a separation of 0''.4 which we also detect in our AstraLux images (Fig. 3).

ι Ori = Hatysa = HD 37 043 = BD -06 1241 = ALS 14 790. **SB2**. Stickland et al. (1987) classified this eccentric SB2 system with apsidal motion as O9 III + B1 III. In GOSSS I we derived a composite spectral classification of O9 IIIvar. Here we present a new spectrogram with separate spectral types of

O8.5 III + B0.2: V. With a LiLiMaRlin spectrogram we achieve a slightly better separation and we obtain a classification of O8.5 III + B0.2 V (the same as GOSSS without the uncertainty in the spectral subtype of the secondary). The WDS catalog lists a weak visual companion 0'.1 away but it should not influence the spectral classification.

HD 52533 A = BD -02 1885 A = ALS 9251 A. **SB1.** In GOSSS I we classified this single-lined spectroscopic binary (McSwain et al. 2007) as O8.5 IVn. HD 52533 has nine components listed in the WDS catalog, including three nearby dim ones (Ab, B, and G) visible in Fig. 4 (see also Table 1). The second brightest component listed is C (= BD -02 1886), 22'' to the north, which is a late-type star with a Gaia DR2 proper motion very different from that of A, so it is likely a foreground object.

HD 54662 AB = BD -10 1892 AB = ALS 197 AB. **SB2a.** Boyajian et al. (2007) classified this SB2 system as O6.5 V + O7-9.5 V. In GOSSS II we give a composite spectral type of O7 Vz var?. Le Bouquin et al. (2017) have resolved this spectroscopic binary into their visual orbit and have been able to compute an orbit with a period of 2103.3 d, a value that agrees well with the previous value quoted in GOSSS II based on OWN data (2119 d) and with the more recent determination by Mossoux et al. (2018) of 2103.4 d. According to Tetzlaff et al. (2011) it is a runaway star based on its radial velocity (we did not detect it in Maíz Apellániz et al. 2018b because its proper motion does not deviate significantly from the average values for O stars in that direction of the Galaxy). It has no entry in the WDS catalog and appears single in our AstraLux images.

HD 53975 = BD -12 1788 = ALS 166. **SB2.** Gies et al. (1994) classified this object as O7.5 V + B2-3 V with a extreme magnitude difference between primary and secondary that only allowed an estimate for the secondary spectral type but not an orbital measurement. In GOSSS I we classified it as O7.5 Vz. The WDS catalog has no entry for this star and our AstraLux image does not reveal any significant companion.

4. Analysis

In this final section we summarize our results and present our first conclusions. In future papers we will present a more thorough analysis once we include the southern systems and additional northern stars.

In this first MONOS paper we have presented updated spectroscopic classifications and visual multiplicity information for 92 multiple systems with $\delta > -20^\circ$ that include at least one O+OBcc spectroscopic binary. The last similar analysis was that of M98, which had a different scope as it concentrated more on the astrometric than on the spectroscopic systems (as opposed to this paper), covered both hemispheres, its sample selection was different, and no new spectral classifications were presented. Nevertheless, it is interesting to compare the information in common between both works. M98 identified 24 O+OBcc systems with $\delta > -20^\circ$ and published SB1 or SB2 orbits⁴. We correct that number by including IU Aur AB (classified as B0.5 + B0.5 in M98) and excluding SZ Cam AB and RY Sct (which we classify as B stars) to yield 23 systems. The sample in

this paper quadruples that number, a reflection of the important progress made in the study of spectroscopic binaries in the last two decades. Furthermore, if we look at those 23 systems and compare the number of astrometric companions within 6'' of the central source detected by M98 and compare it with the current number (including objects from the WDS catalog, Gaia DR2, and companions detected in this paper, see below) the number has grown from 12 to 28, an equally impressive advancement. As we will show in future papers, there is still room for significant improvements in the case of new spectroscopic orbits. The same should be true for the discovery of new astrometric companions, not only using lucky imaging but also more sophisticated techniques such as the ones used in the southern hemisphere by the SMASH+ survey (Sana et al. 2014).

The value of our results lies mostly in the updated detailed information, such as the homogeneous revision of the spectral classification of the sample applying the criteria we have developed for GOSSS, that can be used for future global analyses of the multiplicity in O stars. We indeed plan to do such analyses in future papers ourselves but it is also worthy to point out some results for individual systems in this work. We present first-time O-type GOSSS spectral classifications for 17 objects: HD 170097 A, QR Ser, BD -13 4923, HD 190967, HD 193611, HDE 228989, HDE 229234, Cyg OB2-3 A, ALS 15133, ALS 15148, Cyg OB2-1, ALS 15131, Cyg OB2-20, Cyg OB2-15, ALS 12502, DN Cas, and IU Aur AB. For another six objects we present their first-time B-type GOSSS spectral classifications: HD 193322 B, Cyg OB2-3 B, HD 15558 B, HD 16429 C, MY Cam B, and LY Aur B.

We have identified one eclipsing system as SB2 for the first time, HD 170097 A, and derived its separate spectral classifications. To that one we can add a second eclipsing system in the sample, ALS 12688, that was identified as having double absorption lines for the first time in GOSSS III. For another eclipsing binary, V747 Cep, we detect moving lines (SB1) for the first time using our LiLiMaRlin spectra. For two systems that have published SB1 orbits, BD -16 4826 and θ^2 Ori A, we publish the first spectrograms with double lines (SB2) and derive their first true separate spectral classifications. For HD 168112 AB we also publish the first SB2 spectrograms and separate spectral classification. We have also detected nine new astrometric components, one each around HD 190967, ALS 15133, Cyg OB2-A11, Cyg OB2-1, ALS 12502, DN Cas, and MY Cam A and two around IU Aur AB.

The results of this paper will be added to GOSC at the time of publication, which will reach version 4.2. With them, GOSC will contain a total of 655 objects: 611 in the main catalog (Galactic O stars), 32 in supplement 2 (Galactic early-type stars), and 12 in supplement 3 (Galactic late-type stars).

It is not possible to do a full multiplicity analysis based on our 92 stars for two reasons: the sample is too small and is biased. The most obvious bias is that we selected our stars from systems that had spectroscopic orbits previously published, so no single targets are included. Note, however, that several SB1? targets are likely to be removed from the list once we check they are not really spectroscopic binaries. Another bias is that objects with spectroscopic orbits tend to be bright (and, therefore, close to us), as multi-epoch high-resolution spectroscopy is expensive in observing time. Indeed, our 92 stars have an average B magnitude of 9.4 with a range between 1.9 and 15.9. The other 428 O stars with GOSSS spectral classifications and $\delta > -20^\circ$ have an average B magnitude of 10.5 with a range between 2.6 and 17.2. Nevertheless, we can still study the different proportions of double, triple, and higher-order systems in a relatively unbi-

⁴ We select systems with an O in the spectroscopic status given in Table 1 of M98.

Table 2. Multiplicity statistics for the sample of 92 objects in this paper. The last row and column give the percentages for the total.

m_1	m_2						%
	2	3	4	5	6	7	
2	36	25	4	3	1	1	76.1
3	...	6	12	2	1	...	22.8
4	1	1.1
%	39.1	33.7	18.5	5.4	2.2	1.1	

ased way (other than the fact that many companions are likely to remain undetected, see above). To do such a study we have compiled the statistics on: [1] m_1 , the multiplicity as derived from the SBS, as defined above, which is the number of objects shown in the diagrams in Fig. 6 and [2] m_2 , the multiplicity derived from the number of objects within 6'' from the SBS, the WDS catalog, Gaia DR2, low-mass objects detected through eclipse timings, and the new astrometric companions discovered here (being careful not to incur into double accounting). m_1 reflects the number of massive and nearby (known) companions while m_2 adds more distant and less massive companions. m_1 should be relatively robust and, barring technological advances (e.g. an extreme version of lucky spectroscopy), we expect it not to change for most stars in the sample in the coming years, especially for objects with extensive previous coverage. m_2 , on the other hand, should increase as new astrometric components are added or decrease as some of them are shown to be unbound to the central object. The statistics for m_1 and m_2 are shown in Table 2.

Table 2 shows that most (~3/4) O-type spectroscopic multiple systems have just one massive nearby companion. On the other hand, only a minority of them have just one companion once we take into account distant and low-mass objects: about two fifths are double systems, another third are triple systems, and the rest are of a higher order. Massive stars prefer high-order multiplicity over simple binarity.

Acknowledgements. We would like to thank Joel Sánchez Bermúdez, Michelangelo Pantaleoni González, and the Calar Alto staff for their help with the AstraLux campaigns and Miguel Penadés Ordaz for his help with the data compilation. We also thank Saída Caballero-Nieves for revising the data from Aldoretta et al. (2015) for some targets and Brian Mason for providing us with the WDS detailed data and for his efforts maintaining the catalog. Several authors acknowledge support from the Spanish Government Ministerio de Ciencia, Innovación y Universidades through different grants: AYA2016-75931-C2-1/2-P (J.M.A., E.T.P., A.S., and E.J.A.), AYA2015-68012-C2-1/2-P (E.T.P., I.N., S.S.-D., J.L., and A.M.), AYA2016-79425-C3-2-P (J.A.C.), and SEV2015-0548 (S.S.-D.). R.H.B. acknowledges support from the ESAC Faculty Council Visitor Program. R.H.B. and J.I.A. were also supported by the Dirección de Investigación y Desarrollo de la Universidad de La Serena through projects PR18 143 and PR16 142, respectively. S.S.-D. acknowledges support from the Gobierno de Canarias grant ProID2017010115. This research has made extensive use of the SIMBAD database (indeed, we would not have attempted if it did not exist), operated at CDS, Strasbourg, France.

References

Aldoretta, E. J., Caballero-Nieves, S. M., Gies, D. R., et al. 2015, *AJ*, 149, 26
Alduseva, V. I., Aslanov, A. A., Kolotilov, E. A., & Cherepashchuk, A. M. 1982, *Soviet Astronomy Letters*, 8, 386
Bagnuolo, Jr., W. G. & Gies, D. R. 1991, *ApJ*, 376, 266
Bakış, V., Bakış, H., Bilir, S., & Eker, Z. 2016, *PASA*, 33, e046
Barannikov, A. A. 1993, *Astronomy Letters*, 19, 420
Barbá, R. H., Gamén, R., Arias, J. I., & Morrell, N. I. 2017, in *IAU Symposium*, Vol. 329, *The Lives and Death-Throes of Massive Stars*, ed. J. J. Eldridge, J. C. Bray, L. A. S. McClelland, & L. Xiao, 89–96
Barbá, R. H., Gamén, R. C., Arias, J. I., et al. 2010, in *RMxAC*, Vol. 38, 30–32
Bolton, C. T. & Rogers, G. L. 1978, *ApJ*, 222, 234
Boyajian, T. S., Gies, D. R., Dunn, J. P., et al. 2007, *ApJ*, 664, 1121

Burkholder, V., Massey, P., & Morrell, N. I. 1997, *ApJ*, 490, 328
Caballero, J. A. 2014, *The Observatory*, 134, 273
Caballero-Nieves, S. M., Nelan, E. P., Gies, D. R., et al. 2014, *AJ*, 147, 40
Conti, P. S. & Alschuler, W. R. 1971, *ApJ*, 170, 325
Crowther, P. A. & Walborn, N. R. 2011, *MNRAS*, 416, 1311
Cvetković, Z., Vince, I., & Ninković, S. 2009, *Publications of the Astronomical Observatory of Belgrade*, 86, 331
Cvetković, Z., Vince, I., & Ninković, S. 2010, *New Astronomy*, 15, 302
De Becker, M., Rauw, G., & Manfroid, J. 2004, *A&A*, 424, L39
De Becker, M., Rauw, G., Manfroid, J., & Eenens, P. 2006, *A&A*, 456, 1121
Djurašević, G., Vince, I., Khruzina, T. S., & Rovithis-Livaniou, E. 2009, *MNRAS*, 396, 1553
Donati, J., Howarth, I. D., Bouret, J., et al. 2006, *MNRAS*, 365, L6
Donati, J.-F., Babel, J., Harries, T. J., et al. 2002, *MNRAS*, 333, 55
Duchêne, G. & Kraus, A. 2013, *ARA&A*, 51, 269
Dvorak, S. W. 2004, *Information Bulletin on Variable Stars*, 5542, 1
Gies, D. R. & Bolton, C. T. 1986, *ApJS*, 61, 419
Gies, D. R., Fullerton, A. W., Bolton, C. T., et al. 1994, *ApJ*, 422, 823
Gies, D. R., Mason, B. D., Bagnuolo, Jr., W. G., et al. 1997, *ApJL*, 475, L49
Gies, D. R., Mason, B. D., Hartkopf, W. I., et al. 1993, *AJ*, 106, 2072
González, J. F. & Levato, H. 2006, *A&A*, 448, 283
Grunhut, J. H., Wade, G. A., Leutenegger, M., et al. 2013, *MNRAS*, 428, 1686
Harmanc, P., Holmgren, D. E., Wolf, M., et al. 2014, *A&A*, 563, A120
Harries, T. J., Hilditch, R. W., & Hill, G. 1997, *MNRAS*, 285, 277
Harvin, J. A., Gies, D. R., Bagnuolo, Jr., W. G., Penny, L. R., & Thaller, M. L. 2002, *ApJ*, 565, 1216
Herbig, G. H. 1967, *PASP*, 79, 502
Hill, G., Hilditch, R. W., Aikman, G. C. L., & Khalessheh, B. 1994, *A&A*, 282, 455
Hillwig, T. C., Gies, D. R., Bagnuolo, Jr., W. G., et al. 2006, *ApJ*, 639, 1069
Howarth, I. D., Walborn, N. R., Lennon, D. J., et al. 2007, *MNRAS*, 381, 433
Hummel, C. A., Rivinius, T., Nieva, M.-F., et al. 2013, *A&A*, 554, A52
Hutchings, J. B. 1975, *ApJ*, 200, 122
Ibanoglu, C., Çakırlı, Ö., & Sipahi, E. 2013, *MNRAS*, 436, 750
Kiminki, D. C., Kobulnicky, H. A., Ewing, I., et al. 2012, *ApJ*, 747, 41
Kiminki, D. C., Kobulnicky, H. A., Gilbert, I., Bird, S., & Chunev, G. 2009, *AJ*, 137, 4608
Kiminki, D. C., McSwain, M. V., & Kobulnicky, H. A. 2008, *ApJ*, 679, 1478
Kobulnicky, H. A., Kiminki, D. C., Lundquist, M. J., et al. 2014, *ApJS*, 213, 34
Kobulnicky, H. A., Smullen, R. A., Kiminki, D. C., et al. 2012, *ApJ*, 756, 50
Kraus, S., Weigelt, G., Balega, Y. Y., et al. 2009, *A&A*, 497, 195
Langer, N., Cantello, M., Yoon, S.-C., et al. 2008, in *IAUS*, Vol. 250, 167–178
Laur, J., Kolka, I., Eenmäe, T., Tuvikene, T., & Leedjärv, L. 2017, *A&A*, 598, A108
Le Bouquin, J.-B., Sana, H., Gosset, E., et al. 2017, *A&A*, 601, A34
Lehmann, H., Vitrichenko, E., Bychkov, V., Bychkova, L., & Klochkova, V. 2010, *A&A*, 514, A34
Leitherer, C., Forbes, D., Gilmore, A. C., et al. 1987, *A&A*, 185, 121
Lewandowski, M., Gorecka, M., Maciejewski, G., & Niedzielski, A. 2009, *OAJ*, 104, 1
Linder, N., Rauw, G., Martins, F., et al. 2008, *A&A*, 489, 713
Lorenzo, J., Negueruela, I., Baker, A. K. F. V., et al. 2014, *A&A*, 572, A110
Maciejewski, G., Czart, K., & Niedzielski, A. 2004, *Information Bulletin on Variable Stars*, 5518
Mahy, L., Martins, F., Machado, C., Donati, J.-F., & Bouret, J.-C. 2011, *A&A*, 533, A9
Mahy, L., Nazé, Y., Rauw, G., et al. 2009, *A&A*, 502, 937
Mahy, L., Rauw, G., De Becker, M., Eenens, P., & Flores, C. A. 2013, *A&A*, 550, A27
Mahy, L., Rauw, G., Martins, F., et al. 2010, *ApJ*, 708, 1537
Maíz Apellániz, J. 2010, *A&A*, 518, A1
Maíz Apellániz, J., Alfaro, E. J., Arias, J. I., et al. 2015a, in *HSA8*, 603–603
Maíz Apellániz, J., Alonso Moragón, A., Ortiz de Zárate Alcarazo, L., & The GOSSS Team. 2017a, in *HSA9*, 509–509
Maíz Apellániz, J., Barbá, R. H., Simón-Díaz, S., et al. 2018a, *A&A*, 615, A161
Maíz Apellániz, J., Barbá, R. H., Sota, A., & Simón-Díaz, S. 2015b, *A&A*, 583, A132
Maíz Apellániz, J., Negueruela, I., Barbá, R. H., et al. 2015c, *A&A*, 579, A108
Maíz Apellániz, J., Pantaleoni González, M., Barbá, R. H., et al. 2018b, *A&A*, 616, A149
Maíz Apellániz, J., Pellerin, A., Barbá, R. H., et al. 2012, in *Astronomical Society of the Pacific Conference Series*, ed. L. Drissen, C. Robert, N. St-Louis, & A. F. J. Moffat, Vol. 465, 484
Maíz Apellániz, J., Sana, H., Barbá, R. H., Le Bouquin, J.-B., & Gamén, R. C. 2017b, *MNRAS*, 464, 3561
Maíz Apellániz, J., Sota, A., Arias, J. I., et al. 2016, *ApJS*, 224, 4
Maíz Apellániz, J., Sota, A., Walborn, N. R., et al. 2011, in *HSA6*, 467–472

- Maíz Apellániz, J., Trigueros Páez, E., Jiménez Martínez, I., et al. 2019, in HSA X, 420
- Maíz Apellániz, J., Walborn, N. R., Galué, H. Á., & Wei, L. H. 2004, *ApJS*, 151, 103
- Majaess, D. J., Turner, D. G., Lane, D. J., & Moncrieff, K. E. 2008, *JAVSO*, 36, 90
- Martins, F., Mahy, L., & Hervé, A. 2017, *A&A*, 607, A82
- Mason, B. D., Gies, D. R., Hartkopf, W. I., et al. 1998, *AJ*, 115, 821
- Mason, B. D., Hartkopf, W. I., Gies, D. R., Henry, T. J., & Helsel, J. W. 2009, *AJ*, 137, 3358
- Mason, B. D., Wycoff, G. L., Hartkopf, W. I., Douglass, G. G., & Worley, C. E. 2001, *AJ*, 122, 3466
- Mayer, P., Drechsel, H., Harmanec, P., Yang, S., & Šlechta, M. 2013, *A&A*, 559, A22
- Mayer, P., Drechsel, H., & Lorenz, R. 2005, *ApJS*, 161, 171
- Mayer, P., Harmanec, P., Chini, R., et al. 2017, *A&A*, 600, A33
- McSwain, M. V. 2003, *ApJ*, 595, 1124
- McSwain, M. V., Boyajian, T. S., Grundstrom, E. D., & Gies, D. R. 2007, *ApJ*, 655, 473
- McSwain, M. V., Gies, D. R., Huang, W., et al. 2004, *ApJ*, 600, 927
- Morgan, W. W., Code, A. D., & Whitford, A. E. 1955, *ApJS*, 2, 41
- Morrison, N. D. & Conti, P. S. 1978, *ApJ*, 224, 558
- Mossoux, E., Mahy, L., & Rauw, G. 2018, *A&A*, 615, A19
- Nazé, Y., Mahy, L., Damerdjji, Y., et al. 2012, *A&A*, 546, A37
- Nazé, Y., Walborn, N. R., & Martins, F. 2008, *RMxAA*, 44, 331
- Negueruela, I., Maíz Apellániz, J., Simón-Díaz, S., et al. 2015, in *HSA8*, 524–529
- Negueruela, I., Marco, A., Herrero, A., & Clark, J. S. 2008, *A&A*, 487, 575
- Negueruela, I., Steele, I. A., & Bernabeu, G. 2004, *AN*, 325, 749
- Orosz, J. A., McClintock, J. E., Aufdenberg, J. P., et al. 2011, *ApJ*, 742, 84
- Özdemir, S., Mayer, P., Drechsel, H., Demircan, O., & Ak, H. 2003, *A&A*, 403, 675
- Pablo, H., Richardson, N. D., Moffat, A. F. J., et al. 2015, *ApJ*, 809, 134
- Pearce, J. A. 1952, *PASP*, 64, 219
- Pigulski, A. & Kołaczowski, Z. 1998, *MNRAS*, 298, 753
- Plaskett, J. 1922, *Publications of the Dominion Astrophysical Observatory Victoria*, 2, 147
- Plaskett, J. S. 1926, *Publications of the Dominion Astrophysical Observatory Victoria*, 3, 247
- Porter, J. M. & Rivinius, T. 2003, *PASP*, 115, 1153
- Pourbaix, D., Tokovinin, A. A., Batten, A. H., et al. 2004, *A&A*, 424, 727
- Raucq, F., Rauw, G., Mahy, L., & Simón-Díaz, S. 2018, *A&A*, 614, A60
- Rauw, G. & De Becker, M. 2004, *A&A*, 421, 693
- Rauw, G., Mahy, L., Nazé, Y., et al. 2014, *A&A*, 566, A107
- Rauw, G., Vreux, J.-M., & Bohannan, B. 1999, *ApJ*, 517, 416
- Ríos, L. Y. & DeGioia-Eastwood, K. 2004, in *Bulletin of the American Astronomical Society*, Vol. 205, American Astronomical Society Meeting Abstracts, 1348
- Roberts, L. C., Gies, D. R., Parks, J. R., et al. 2010, *AJ*, 140, 744
- Salas, J., Maíz Apellániz, J., & Barbá, R. H. 2015, in *HSA8*, 615–615
- Sana, H., de Mink, S. E., de Koter, A., et al. 2012, *Science*, 337, 444
- Sana, H. & Evans, C. J. 2011, in *IAUS*, Vol. 272, 474–485
- Sana, H., Gosset, E., & Evans, C. J. 2009, *MNRAS*, 400, 1479
- Sana, H., Le Bouquin, J.-B., Lacour, S., et al. 2014, *ApJS*, 215, 15
- Schaefer, G. H., Hummel, C. A., Gies, D. R., et al. 2016, *AJ*, 152, 213
- Shenar, T., Oskinova, L., Hamann, W.-R., et al. 2015, *ApJ*, 809, 135
- Simón-Díaz, S., Caballero, J. A., & Lorenzo, J. 2011, *ApJ*, 742, 55
- Simón-Díaz, S., Caballero, J. A., Lorenzo, J., et al. 2015a, *ApJ*, 799, 169
- Simón-Díaz, S., Godart, M., Castro, N., et al. 2017, *A&A*, 597, A22
- Simón-Díaz, S., Negueruela, I., Maíz Apellániz, J., et al. 2015b, in *HSA8*, 576–581
- Solin, O., Ukkonen, E., & Haikala, L. 2012, *A&A*, 542, A3
- Sota, A., Maíz Apellániz, J., Morrell, N. I., et al. 2014, *ApJS*, 211, 10
- Sota, A., Maíz Apellániz, J., Walborn, N. R., et al. 2011, *ApJS*, 193, 24
- Sota, A., Maíz Apellániz, J., Walborn, N. R., & Shida, R. Y. 2008, in *RMxAC*, Vol. 33, 56
- Stahl, O., Kaufer, A., Rivinius, T., et al. 1996, *A&A*, 312, 539
- Stickland, D. J. & Lloyd, C. 2001, *The Observatory*, 121, 1
- Stickland, D. J., Pike, C. D., Lloyd, C., & Howarth, I. D. 1987, *A&A*, 184, 185
- Stroud, V. E., Clark, J. S., Negueruela, I., et al. 2010, *A&A*, 511, A84
- Struve, O., Sahade, J., & Huang, S.-S. 1958, *ApJ*, 127, 148
- ten Brummelaar, T. A., O'Brien, D. P., Mason, B. D., et al. 2011, *AJ*, 142, 21
- Tetzlaff, N., Neuhäuser, R., & Hohle, M. M. 2011, *MNRAS*, 410, 190
- Turner, N. H., ten Brummelaar, T. A., Roberts, L. C., et al. 2008, *AJ*, 136, 554
- Underhill, A. B. & Matthews, J. M. 1995, *PASP*, 107, 513
- Wade, G. A., Howarth, I. D., Townsend, R. H. D., et al. 2011, *MNRAS*, 416, 3160
- Walborn, N. R. 1973, *AJ*, 78, 1067
- Walborn, N. R., Gamen, R. C., Morrell, N. I., et al. 2017, *AJ*, 154, 15
- Walborn, N. R., Howarth, I. D., Lennon, D. J., et al. 2002, *AJ*, 123, 2754
- Walborn, N. R., Sota, A., Maíz Apellániz, J., et al. 2010, *ApJL*, 711, L143
- Weigelt, G., Balega, Y., Preibisch, T., et al. 1999, *A&A*, 347, L15
- Williams, A. M., Gies, D. R., Bagnuolo, Jr., W. G., et al. 2001, *ApJ*, 548, 425
- Williams, S. J., Gies, D. R., Hillwig, T. C., McSwain, M. V., & Huang, W. 2013, *AJ*, 145, 29
- Williams, S. J., Gies, D. R., Matson, R. A., & Huang, W. 2009, *ApJL*, 696, L137
- Zeinalov, S. K. & Musaev, F. A. 1986, *Soviet Astronomy Letters*, 12, 125
- Zinnecker, H. & Yorke, H. W. 2007, *ARA&A*, 45, 481

Table 3. Coordinates and spectral classifications for the sample in this paper sorted by GOSC ID. For the GOSSS spectral classifications we indicate which ones are **modified**, **new**, or correspond to **visual companions**. For the alternate spectral classifications we give the reference. The information in this table is also available in electronic form at the GOSC web site (<http://gosc.cab.inta-csic.es>) and at the CDS via anonymous ftp to cdsarc.u-strasbg.fr (130.79.128.5) or via <http://cdsweb.u-strasbg.fr/cgi-bin/qcat?J/A+A/>.

Name	GOSC ID		R.A. (J2000)	Declination (J2000)	SBS	GOSSS classification			Alternate classification			Ref.		
	1	2				ST	LC	Qualifier	Secondary (+tertiary)	Ref.	ST		LC	Qualifier
HD 164438	010.35+01.79.01	18:01:52.279	-19:06:22.07	SB1	O9.2	IV	S14
HD 167771	012.70-01.13.01	18:17:28.556	-18:27:48.43	SB2	O7	III	(f)	O8 III	S14	O8 III	new
BD -16.4826	015.26-00.73.01	18:21:02.231	-16:01:00.94	SB2	O5.5	V	(f)z	M16	O9/B0 V	new
HD 170097 A	015.48-02.61.01	18:28:25.109	-16:42:04.44	SB2E	O9.5	V	...	B1: V	new	B1: V	new
QR Ser	016.81+00.67.01	18:18:58.690	-13:59:28.45	SB2E	O9.7	III	new	B	S09
V479 Ser	016.88-01.29.01	18:26:15.045	-14:50:54.33	SB1	ON6	V	(f)z	M16
HD 168075	016.94+00.84.01	18:18:36.043	-13:47:36.46	SB2	O6.5	V	(f)	M16	B0-1 V	S09
HD 168137 AaAb	016.97+00.76.01	18:18:56.189	-13:48:31.08	SB2a	O8	V	z	M16	O8.5 V	new
BD -13.4923	016.97+00.87.01	18:18:32.732	-13:45:11.88	SB2	O4	V	(f)	O7.5 V	new	O7.5 V	new
MY Ser AaAb	018.25+01.68.01	18:18:05.895	-12:14:33.29	SB2E+Sa	O8	la	f	O4/5 If + O4/5 V-III	mod	O4.5 If + O4: V-III	new
HD 168112 AB	018.44+01.62.01	18:18:40.868	-12:06:23.39	SB2a	O5	IV	(f)	O6: IV;	mod	O5.5 IV(f)	new
HD 166734	018.92+03.63.01	18:12:24.656	-10:43:53.04	SB2E	O7.5	la	f	O9 lab	mod	O8.5 Ib(f)	new
HD 175514	041.71+03.38.01	18:55:23.124	+09:20:48.07	SB2E+C	O7	V	(n)(f)z	B	M16	B0.5: V + O7.5 IV(f)	new
9 Sge	056.48-04.33.01	19:52:21.765	+18:40:18.75	SB1?	O7.5	lab	f	S11a
Cyg X-1	071.34+03.07.01	19:58:21.677	+35:12:05.81	SB1	O9.7	lab	p var	S11a
HD 190967	072.33+01.81.01	20:06:09.949	+35:23:09.61	SB2E	O9.7:	lab	...	B1.5 lab	new	B1.5 II	new
HD 191201 A	072.75+01.78.01	20:07:23.684	+35:43:05.91	SB2+Cas	O9.5	III	...	B0.5 V	S11a	O9	C71
HD 191612	072.99+01.43.01	20:09:28.608	+35:44:01.31	SB2	O6-8	...	f?p var	S11a	B0-2	H07
HDE 228854	074.54+00.20.01	20:18:47.219	+36:20:26.08	SB2E	O6	IV	n var	O5 Vn var	M16	O7.5	P52
HDE 228766	075.19+00.96.01	20:17:29.703	+37:18:31.13	SB2	O4	I	f	O8: II;	S11a	O8-9 In	W73
HD 193443 AB	076.15+01.28.01	20:18:51.707	+38:16:46.50	SB2+Ca	O9	III	S11a	O9.5 V/III	M13a
BD +36.4063	076.17-00.34.01	20:25:40.608	+37:22:27.07	SB1	ON9.7	lb	S11a
HD 193611	076.28+01.19.01	20:19:38.748	+38:20:09.18	SB2E	O9.5	V	...	O9.5 III	new	B0 V	new
HDE 228989	076.66+01.28.01	20:20:21.394	+38:41:59.71	SB2E	O9.5	V	...	B0.2 V	new	...	new
HDE 229234	076.92+00.59.01	20:24:01.298	+38:30:49.55	SB1	O9	III	M16
HD 192281	077.12+03.40.01	20:12:33.121	+40:16:05.45	SB1	O4.5	IV	(n)(f)	M16
Y Cyg	077.25-06.23.01	20:52:03.577	+34:39:27.51	SB2E	O9.5	IV	...	O9.5 IV	S11a	...	new
HDE 229232 AB	077.40+00.93.01	20:23:59.183	+39:06:15.27	SB1+Ca?	O4	V:	nt(f)	M16
HD 193322 B	078.10+02.78.02	20:18:06.770	+40:43:54.35	...	B1.5	V:	(n)p	vis
HD 193322 AaAb	078.10+02.78.01	20:18:06.990	+40:43:55.46	SB2a+Sa	O9	IV	(n)	S11a	O8.5 III + B2.5: V;	T11
HD 194649 AB	078.46+01.35.01	20:25:22.124	+40:13:01.07	SB2+Ca	O6	IV	(f)	O9.7: V	mod	O9.5 V	new
Cyg OB2-B17	079.84+01.16.01	20:30:27.302	+41:13:25.31	SB2E	O6	la	f	O9: Ia;	M16	O9 laf	S10
Cyg OB2-3 B	079.97+00.98.02	20:31:37.326	+41:13:18.04	...	B0	IV	vis
Cyg OB2-3 A	079.97+00.98.01	20:31:37.509	+41:13:21.01	SB2E	O8.5	lb	(f)	O6 III;	new	O6 IV;	K08
ALS 15 133	080.04+01.11.01	20:31:18.330	+41:21:21.66	SB1	O9.5	IV	new
Cyg OB2-A11	080.08+00.85.01	20:32:31.543	+41:14:08.21	SB1	O7	lb	(f)	M16
Cyg OB2-5 B	080.12+00.91.02	20:32:22.489	+41:18:19.45	...	O7	lb	(f)p var?	vis
Cyg OB2-5 A	080.12+00.91.01	20:32:22.422	+41:18:19.91	SB2E+Sa	O6.5:	lb	fe	O7 lafe	mod
Cyg OB2-22 C	080.14+00.74.01	20:33:09.598	+41:13:00.54	SB1E?	O9.5	III	n	S11a
Cyg OB2-22 B	080.14+00.75.02	20:33:08.835	+41:13:17.36	SB1	O6	V	(f)	S11a
Cyg OB2-41	080.15+00.79.01	20:32:59.643	+41:15:14.67	SB1	O9.7	III	(n)	M16
ALS 15 148	080.15+00.74.01	20:33:13.265	+41:13:28.74	SB1	O6.5:	V	new
Cyg OB2-9	080.17+00.76.01	20:33:10.733	+41:15:08.21	SB2	O4.5	I	f	S14	O5.5 III(f)	new
Cyg OB2-1	080.17+01.23.01	20:31:10.543	+41:31:53.47	SB1+Ca	O8	IV	(n)(f)	new
ALS 15 131	080.19+00.81.01	20:33:02.922	+41:17:43.13	SB1	O7.5	V	(f)	new
Cyg OB2-20	080.19+01.10.01	20:31:49.665	+41:28:26.51	SB1	O9.7	IV	new
Cyg OB2-8 A	080.22+00.79.01	20:33:15.078	+41:18:50.51	SB2	O6	lb	(fc)	O4.5: III:(fc)	S14	O4.5 III(fc)	new
Cyg OB2-70	080.23+00.71.01	20:33:37.001	+41:16:11.30	SB1	O9.5	IV	(n)	M16
Cyg OB2-15	080.24+00.98.01	20:32:27.666	+41:26:22.08	SB1	O8	III	new
ALS 15 115	080.27+00.81.01	20:33:18.046	+41:21:36.90	SB1	O8	V	M16
Cyg OB2-27 AB	080.29+00.66.01	20:33:59.528	+41:17:35.48	SB2E+Ca	O9.7	V	(n)	O9.7 V:(n)	M16	B0 V	K12

Table 3. (Continued).

Name	GOSC ID	R.A. (J2000)	Declination (J2000)	SBS	ST	LC	GOSSS classification			Ref.	ST	LC	Qualifier	Alternate classification		Ref.
							Qualifier	Secondary (+tertiary)	Tertiary					Qualifier	Secondary (+tertiary)	
Cyg OB2-73	080.32+00.60.01	20:34:21.930	+41:17:01.60	SB2	O8	V	O8 Vz	M16	O8 III	M16	III	...	O8 III	K09		
ALS 15 114	080.54+00.73.01	20:34:29.601	+41:31:45.42	SB2	O7	V	O7 IV(ff)	mod	O9 V	mod	V	...	O9 V	K12		
Cyg OB2-29	080.55+00.80.01	20:34:13.505	+41:35:03.01	SB1	O7.5	V	(n)(ff)z	M16	...	M16		
Cyg OB2-11	080.57+00.83.01	20:34:08.513	+41:36:59.42	SB1	O5.5	I	fc	S11a	...	S11a		
LS III +46 11	084.88+03.81.01	20:35:12.642	+46:51:12.12	SB2	O3.5	I	f*	O3.5 If*	...	M16		
HD 199 579	085.70+00.30.01	20:56:34.779	+44:55:29.01	SB2	O6.5	V	(ff)z	S11a	B1-2 V	S11a	V	(ff)	B1-2 V	W01		
68 Cyg	087.61+03.84.01	21:18:27.187	+43:56:45.40	SB1?	O7.5	III	n(ff)	S11a	...	S11a		
HD 206 267 AaAb	099.29+03.74.01	21:38:57.618	+57:29:20.55	SB2+Ca	O6	V	(n)(ff)	mod	B0: V	mod	V	(n)(ff)	B0: V	new		
14 Cep	102.01+02.18.01	22:02:04.576	+58:00:01.33	SB2	O8.5	III	...	BN0 V	BN0 V	mod	III	...	BN0 V	new		
ALS 12 502	105.77+00.06.01	22:34:45.972	+58:18:04.64	SB2E+Ca	O9	III	(n)	O9.2 IV(n)	O9 V(n)	mod	IV	(n)	O9 V(n)	new		
DH Cep	107.07+00.90.01	22:46:54.111	+58:05:03.55	SB2	O5.5	V	(f) var	O6 V(ff) var	O6 V(ff) var	mod	V	(ff) var	O6 V(ff) var	new		
ALS 12 688	107.42+02.87.01	22:55:44.944	+56:28:36.70	SB2E	O5.5	V	(n)(ff)	B	...	M16		
AO Cas	117.59+11.09.01	00:17:43.059	+51:25:59.12	SB2E	O9.2	II	(ff) var	O8 V(ff)	...	S14	O7.5 V	new		
HD 108	117.93+01.25.01	00:06:03.386	+63:40:46.75	SB1?	O6.5-8	...	f* p var	mod		
V747 Cep	118.20+05.09.01	00:01:46.870	+67:30:25.13	SB1E	O5.5	...	(n)(ff)	M16		
HD 12 323	132.91+05.87.01	02:02:30.126	+55:37:26.38	SB1	ON9.2	V	...	S14	...	S14		
DN Cas	133.88+00.08.01	02:23:11.536	+60:49:50.18	SB2E+Ca	O8.5	V	new	V	...	B0.2 V	new		
BD +60 497	134.58+01.04.01	02:31:57.087	+61:36:43.95	SB2	O6.5	V	(n)(ff)z	O9.5: V	B0.2 V	mod	V	(n)(ff)z	B0: V(n)	new		
HD 15 558 A	134.72+00.92.01	02:32:42.536	+61:27:21.56	SB2	O4.5	III	(fc)p	O8:	O8:	mod	III	(f)	O7 V	D06		
HD 15 558 B	134.73+00.93.01	02:32:43.895	+61:27:20.33	...	B0	V	(n)	vis		
HD 16 429 C	135.67+01.16.01	02:40:46.149	+61:17:48.54	...	B0.7	V	(n)	vis		
HD 16 429 A	135.68+01.15.01	02:40:44.951	+61:16:56.04	SB1+Ca	O9	II-III	(n) Nwk	S14	O8 III-V + B0 V?	M03		
HD 16 429 B	135.68+01.14.01	02:40:44.805	+61:16:49.43	...	F	vis		
HD 17 505 A	137.19+00.90.01	02:51:07.971	+60:25:03.88	SB2+C	O6.5	IV	(ff)	O7 V(ff)	...	mod	III	(ff)	O7.5 V(ff) + O7.5 V(ff)	H06		
HD 17 505 B	137.19+00.90.02	02:51:08.262	+60:25:03.78	...	O8	V	vis		
HD 15 137	137.46+07.58.01	02:27:59.811	+52:32:57.60	SB1	O9.5	II-III	n	S11a	B0 V	H94		
CC Cas	140.12+01.54.01	03:14:05.333	+59:33:48.50	SB2E	O8.5	III	(n)(ff)	B	...	S11a		
HD 14 633 AaAb	140.78+18.20.01	02:22:54.293	+41:28:47.72	SB1+Ca?	ON8.5	V	S11a		
α Cam	144.07+14.04.01	04:54:03.011	+66:20:33.58	SB1?	O9	Ia	S11a		
MY Cam A	146.27+03.14.01	03:59:18.290	+57:14:13.72	SB2E+Cas	O5.5	V	nz var	O6.5 Vnz var	...	vis	V	(n) var	O6.5 V(n)z var	new		
MY Cam B	146.27+03.14.02	03:59:18.345	+57:14:13.15	...	B1.5:	IV	vis		
LY Aur B	172.76+00.61.02	05:29:42.600	+35:22:29.90	...	B0.2	V	vis		
LY Aur A	172.76+00.61.01	05:29:42.647	+35:22:30.07	SB2E+SB1as	O9.2	II	(n)	O9.7 II	...	mod	II	...	O9 III	M13b		
IU Aur AB	173.05+00.03.01	05:27:52.398	+34:46:58.23	SB2E+Ca	O9.5	IV	(n)	O9.7 IV(n)	...	new	III	(n)	O9.7 V(n)	new		
HD 37 737	173.46+03.24.01	05:42:31.160	+36:12:00.51	SB1	O9.5	II-III	(n)	S11a		
HD 37 366	177.63+00.11.01	05:39:24.799	+30:53:26.75	SB2	O9.5	V	...	B1: V	...	mod	V	...	B1: V	new		
15 Mon AaAb	202.94+02.20.01	06:40:58.656	+09:53:44.71	SB1a	O7	V	(ff)z var	M18		
δ Ori Aa	203.86+17.74.01	05:32:00.398	+00:17:56.69	SB2E+Cas	O9.5	II	Nwk	M18	B0.5 III	H02		
HD 47 129	205.87+00.31.01	06:37:24.042	+06:08:07.38	SB2	O8	Iab	f	O8.5:fp	...	mod	III/I	...	O7.5 V/III	L08		
HD 48 099	206.21+00.80.01	06:41:59.231	+06:20:43.54	SB2	O5.5	V	(ff)z	O9 V	...	M16	...	(ff)z	O9: V	new		
HD 46 149	206.22+02.04.01	06:31:52.533	+05:01:59.19	SB2	O8.5	V	S11a	B0-1 V	M09		
ζ Ori AaAb	206.45+16.59.01	05:40:45.527	+01:56:33.26	SB2	O9.2	Ib	Nwk var	M18	B0.5 IV	H13		
σ Ori AaAb	206.82+17.34.01	05:38:44.765	+02:36:00.25	SB2a+Cas	O9.5	V	...	B0.2 V	...	mod	V	...	B0.5 V	S11b		
σ Ori B	206.82+17.34.02	05:38:44.782	+02:36:00.27	...	B0.2	V	(n)	vis		
HD 46 573	208.73+02.63.01	06:34:23.568	+02:32:02.94	SB1	O7	V	(ff)z	S11a		
θ^1 Ori CaCb	209.01+19.38.01	05:35:16.463	+05:23:23.18	SB1?+Sa	O7	...	f* p var	mod	B0.2: V	...		
ζ Ori	209.05+19.37.01	05:35:22.900	+05:24:57.80	SB2	O9.2	V	...	B0.5: V(n)	...	mod	V	...	B0.2: V	new		
HD 52 533 A	216.85+00.80.01	07:01:27.048	+03:07:03.28	SB1	O8.5	IV	n	mod	III		
HD 54 662 AB	224.17+00.78.01	07:09:20.249	+10:20:47.64	SB2a	O7	V	z var?	S11a	O7-9.5 V	B07		
HD 53 975	225.68+02.32.01	07:06:35.964	+12:23:38.23	SB2	O7.5	V	z	S11a	B2-3 V	G94		

References: B07: Boyajian et al. (2007), C71: Conti & Alschuler (1971), D06: De Becker et al. (2006), G94: Gies et al. (1994), H02: Harvin et al. (2002), H06: Hillwig et al. (2006), H07: Howarth et al. (2007), H13: Hummel et al. (2013), H94: Hill et al. (1994), K08: Kiminki et al. (2008), K09: Kiminki et al. (2009), K12: Kobulnicky et al. (2012), L08: Linder et al. (2008), M03: McSwain (2003), M09: Mahy et al. (2009), M13a: Mahy et al. (2013), M13b: Mayer et al. (2013), M16: Maíz Apellániz et al. (2016), M18: Maíz Apellániz et al. (2018a), P52: Pearce (1952), R99: Rauw et al. (1999), S09: Sana et al. (2009), S10: Stroud et al. (2010), S11a: Sota et al. (2011), S11b: Simón-Díaz et al. (2011), S14: Sota et al. (2014), T11: ten Brummelaar et al. (2011), W01: Williams et al. (2001), W73: Walborn (1973).